CHALMERS
UNIVERSITY OF TECHNOLOGY

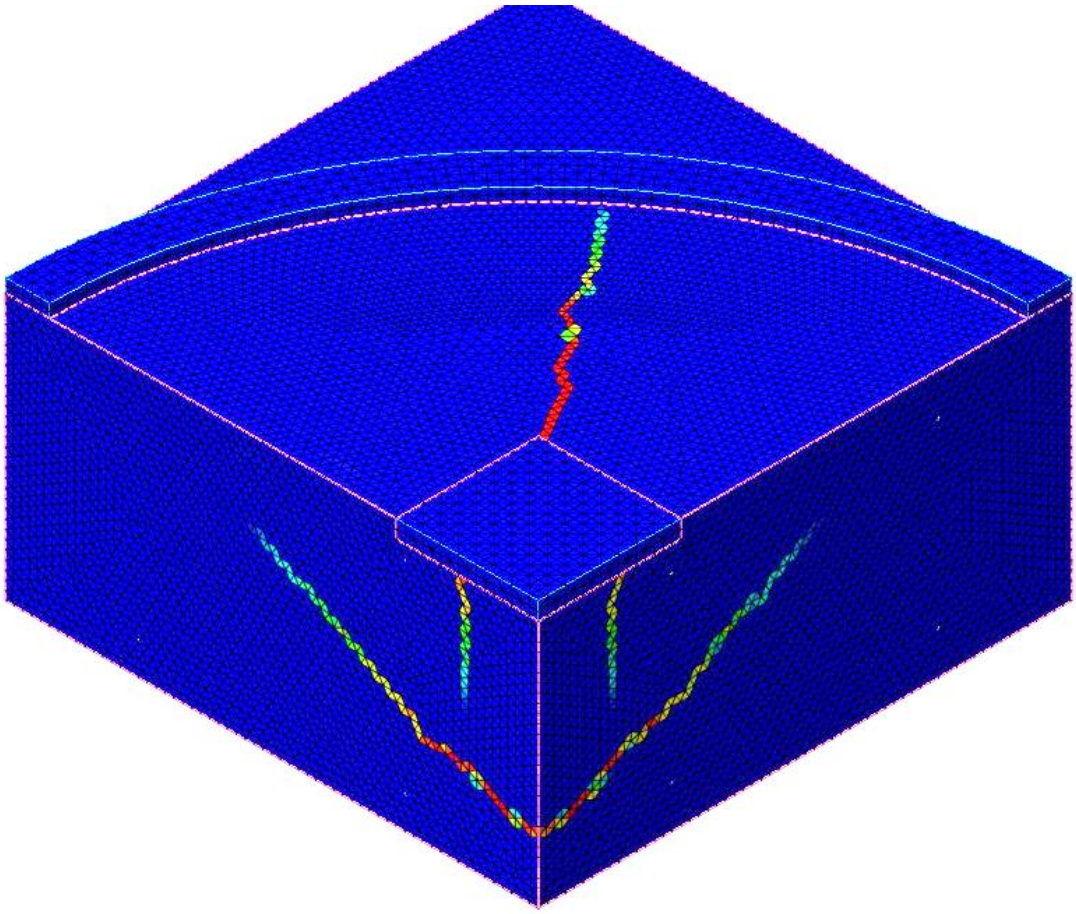

Numerical analyses of surface reinforcement's impact on anchorage in concrete

Master's Thesis in the Master's Programme Structural engineering

Emil Axelsson

Filip Božić

Department of Civil and Environmental Engineering

Division of Structural Engineering

Concrete Structures

CHALMERS UNIVERSITY OF TECHNOLOGY

Gothenburg, Sweden 2016

Master's Thesis BOMX02-16-58

MASTER'S THESIS BOMX02-16-58

Numerical analyses of surface reinforcement's impact on anchorage in concrete

Master's Thesis in the Master's Programme Structural engineering

Emil Axelsson

Filip Božić

Department of Civil and Environmental Engineering

Division of Structural Engineering

CONCRETE STRUCTURES

CHALMERS UNIVERSITY OF TECHNOLOGY

Göteborg, Sweden 2016

Numerical analyses of surface reinforcement's impact on anchorage in concrete
Master's Thesis in the Master's Programme Structural engineering

Emil Axelsson

Filip Božić

Examensarbete BOMX02-16-58/ Institutionen för bygg- och miljöteknik,
Chalmers tekniska högskola 2016

Department of Civil and Environmental Engineering
Division of Structural Engineering
Concrete Structures

Chalmers University of Technology

SE-412 96 Göteborg
Sweden
Telephone: + 46 (0)31-772 1000

Cover:
Contour plot of first principle strain for concrete slab with thickness 300 mm and reinforcement amount of Φ12 S300.
Department of Civil and Environmental Engineering. Göteborg, Sweden, 2016

Numerical analyses of surface reinforcement's impact on anchorage in concrete

Master's thesis in the Master's Programme Structural Engineering

EMIL AXELSSON

FILIP BOŽIĆ

Department of Civil and Environmental Engineering

Division of Structural Engineering

CONCRETE STRUCTURES

Chalmers University of Technology

ABSTRACT

For concrete anchorage of pipe support and frame structures in industrial facilities it is common to use expander bolts or cast-in anchors. Calculations to determine the design strength of such details are done using the European pre-standard CEN/TS. Concrete cone failure is often decisive when cast-in anchors are loaded in tension and codes of praxis do not consider the influence of surface reinforcement for this type of failure. In industry it usually exist large amount of surface reinforcement which can be favorable for the capacity. Performed tests at Luleå University indicate that higher capacity was gained when surface reinforcement was present.

The aim of the thesis was to investigate how the surface reinforcement contributes to the capacity for cast-in anchors when the concrete cone failure is the decisive case. This included both single anchors and group of four anchors with the comparison between the impacts on both sets and with the design codes from CEN/TS.

A literature study was carried out where previous numerical evaluations on the subject, design methods and earlier performed tests on slabs were studied. The finite element (FE) software DIANA and ABAQUS were used to establish a model that could describe the crack pattern and capacity. The DIANA model was verified against physical tests of a single anchor and then used for a group of anchors and replicated in ABAQUS with the same parameters and assumptions.

Load versus Displacement graphs were obtained from the analyses in both DIANA and ABAQUS. The calibration against the physical tests was accurate with respect to capacity but less accurate in displacement.

The surface reinforcement had influence on the capacity for single anchors. It could be seen that the increase was larger in percentage for the thinner slabs than for the thicker. The thinner slabs that were loaded by the group of anchors had also a big influence from the surface reinforcement. However it had no or small influence for the thicker slabs that was loaded by the group of anchors.

Key words: Concrete cone failure, Surface reinforcement, FE, DIANA, ABAQUS, anchors, CEN/TS

Numeriska analyser av ytarmerings inverkan på förankring i betong

Examensarbete inom masterprogrammet Structural Engineering

EMIL AXELSSON

FILIP BOŽIĆ

Institutionen för bygg- och miljöteknik

Avdelningen för Konstruktionsteknik

Betongkonstruktioner

Chalmers Tekniska Högskola

SAMMANFATTNING

För betongförankring av rör-stöd och ramkonstruktioner i industrianläggningar är det vanligt att använda expanderförankringar eller ingjutna förankringar. Beräkningar för att bestämma dimensionerande hållfasthet för sådana detaljer görs med hjälp av den europeiska standarden CEN/TS. Konbrott i betong är ofta avgörande när ingjutna förankringar lastas i drag. Dimensioneringsnormen tar inte hänsyn till ytarmeringens påverkan för denna typ av brott. Inom industrin finns det oftast stora mängder ytarmering som kan vara gynnsamt för kapaciteten. Utförda tester vid Luleås tekniska högskola visar att högre kapacitet erhölls när ytarmering användes.

Syftet med avhandlingen var att undersöka hur ytarmeringen bidrog till kapaciteten för ingjutna förankringar när konbrott i betong var den dimensionerande brottmoden. Detta inkluderade både ensamma förankringar och grupp av fyra förankringar med jämförelser mellan dessa uppsättningar och med CEN/TS.

En litteraturstudie genomfördes för tidigare numeriska utvärderingar i ämnet, dagens dimensioneringsmetoder och tidigare utförda tester på plattor studerades. Finita element (FE) programvarorna DIANA och ABAQUS har använts för att skapa en modell som kan beskriva sprickmönster och kapacitet. DIANA-modellen verifieras mot fysiska tester av en ensam förankring och används sedan för en grupp av förankringar och implementerades till ABAQUS med samma parametrar och antaganden.

Last-deformationskurvor erhölls från analyserna i både DIANA och ABAQUS. Kalibreringen mot de fysiska testerna var korrekta i förhållande till kapacitet, men överensstämmer inte så bra mot deformation.

Ytarmering hade inflytande på kapaciteten för ensamma förankringar. Det kunde observeras att ökningen var högre i procent för de tunnare plattorna än för de tjockare. De tunnare plattorna som var lastade av en grupp av förankringar hade också ett stort inflytande från ytarmeringen, men ingen eller liten påverkan för de tjockare plattorna.

Nyckelord: Konbrott i betong, ytarmering, FE, DIANA, ABAQUS, förankringar, CEN/TS

Contents

Preface

The work on this thesis was carried out between February 2016 and June 2016 at the Department of Civil and Environmental Engineering, Division of Structural Engineering, Concrete Structures at Chalmers University of Technology. The Master thesis was carried out in collaboration between Chalmers and FS Dynamics to investigate if surface reinforcement could increase the capacity in CEN/TS regarding the Concrete cone failure for headed anchors. The project was based on performed tests on headed single anchors with surface reinforcement from Luleås university of Technology.

We want to thank our supervisor MSc Johan Mattsson for helpful guidance throughout the whole project and FS Dynamics for letting us use their computers and facilities, Associate professor Mario Plos for excellent suggestions and supervisor/examiner Assistant professor Filip Nilenius for great guidance through the report. Further, we would like to express our gratitude to PhD Rasoul Nilfourash for providing us with literature and previous knowledge from similar simulations and to PhD student Jiangpeng Shu, MSc Simon Vikström and MSc Armin Halilovic for their valuable comments and discussions regarding FE-modelling.

Göteborg, June 2016

Emil Axelsson and Filip Božić

Notations

Roman upper case letters

$A^0_{\mathrm{c,N}}$	Reference projected area, $(S_{\mathrm{cr,N}} \times S_{\mathrm{cr,N}})$, [m]
$A_{\mathrm{c,N}}$	Actual projected area limited by edges of the concrete and overlapping cones $(S \leq S_{cr,N})$ [m]
$A^{'}_{\mathrm{S}}$	Amount of bottom reinforcement, [m^2]
$C_{\mathrm{cr,N}}$	Half of $S_{\mathrm{cr,N}}$, [m]
E_{cm}	Young's modulus for concrete, [Pa]
E_{S}	Young's modulus for reinforcement, [Pa]
F_{C}	Cross-section force from compressed concrete, [N]
$F^{'}_{\mathrm{S}}$	Cross-section force from bottom reinforcement, [N]
G_f	Fracture energy, [Nm/m^2]
H	Thickness of slab, [m]
K	Linear relation between applied point load and bending moment
L	Width of slab, [m]
M	Bending moment, [Nm]
M_{Rd}	Bending moment capacity for reinforced slabs, [Nm]
M_{Rdu}	Bending moment capacity for un-reinforced slabs, [Nm]
N_{Analysis}	Capacity given from analysis, [kN]
$N_{\mathrm{Test,average}}$	Average capacity for slabs given by performed tests, [kN]
$N_{\mathrm{CEN/TS}}$	Capacity given from code of praxis, [kN]
N_{Ed}	Twice the amplitude of the tensile action for anchors, [N]
N_{group}	Capacity given from performed simulations on group of anchors, [kN]
$N_{\mathrm{Rk,c}}$	Characteristic capacity, [N]
$N_{\mathrm{Simulation}}$	Capacity given from performed simulations on single anchor, [kN]
N_{single}	Capacity given from performed simulations on single anchor, [kN]
$N_{\mathrm{Test,range}}$	Capacity range given from performed tests, [kN]
P	Applied point load, [N]
P_{Rd}	Bending capacity, [N]
P_{Test}	Average capacity for slabs given by performed tests, [kN]
R	Reaction force at anchor, [N]
$S_{\mathrm{cr,N}}$	Distance without impact from other anchors or edges, for headed anchor according to current experience, $S_{cr,N} = 3 * h_{ef}$, [m]
V	Volume of element, [m^3]

Roman lower case letters

b	Width of cross-section, [m]
c	Smallest distance to edge, [m]
c_1	Constant
c_2	Constant
d	Effective height for top reinforcement, [m]
$d^{´}$	Effective height for bottom reinforcement, [m]
e_{n}	Eccentricity of the resulting tensile load, [m]
f	Compressive stress in concrete, [Pa]
$\mathrm{f_c}$	Compressive capacity for concrete, [Pa]
f_{ck}	Characteristic cylinder strength for concrete, [MPa]
f_{cm}	Mean compressive cylinder strength for concrete, [MPa]
$f_{\mathrm{ck,cube}}$	Characteristic cube strength for concrete, [MPa]
$f_{\mathrm{cm,cube}}$	Mean compressive cube strength for concrete, [MPa]
f_{ctm}	Mean tensile strength for concrete, [MPa]
f_t	Tensile capacity for concrete, [Pa]
f_{ub}	Ultimate capacity for anchor steel, [Pa]
f_{y}	Yield stress for steel, [Pa]
h	Crack band width, [m]
h_{ef}	Effective length of anchor, [$\mathrm{mm^2}$]
k	Factor used for stress-strain relation in compression for concrete, [-]
k_{ucr}	Factor to take into account the influence of load transfer different values for un-cracked concrete, [$\mathrm{N^{0.5}/mm^{0.5}}$]
l	Scaling factor in FE- software DIANA for compressive behaviour of concrete, [m]
n	Factor used for stress-strain relation in compression for concrete, [-]
x	Compressed cross-section height, [m]

Greek upper case letters

ΔN_{Ek}	Twice the amplitude of the tensile action for anchors, [N]
$\Delta N_{\mathrm{Rk,c}}$	Fatigue resistance, tension, concrete, [N]

Greek lower case letters

α	Factor for effective compressive capacity for concrete, [-]

α_{cr}	Crack angle between the crack and the concrete for a concrete cone failure, [°]
β	Factor for compressed cross-section height, [-]
ε	Concrete strain, [-]
$\varepsilon_{\mathrm{cr}}$	Concrete crack strain, [-]
ε_{ult}^{cr}	Ultimate concrete crack strain, where the crack is fully open, [-]
ε_{p}	Strain corresponding to when the stress is at its peak value in compression for concrete, [-]
$\varepsilon^{'}{}_{\mathrm{S}}$	Strain in bottom reinforcement, [-]
δ	Applied displacement, [m]
γ_{c}	Partial factor for concrete under compression, [-]
$\gamma_{\mathrm{F,fat}}$	Partial factor for fatigue actions, [-]
γ_{inst}	Partial factor taking into account installation safety of the fastening system, [-]
γ_{Mc}	Partial factor covering concrete break out failure modes (cone failure, blow out failure, pry out failure and edge failure), [-]
$\gamma_{\mathrm{Mc,fat}}$	Partial factor for concrete cone failure, [-]
υ	Poisson's ratio, [-]
σ^{cr}	Crack stress, [Pa]
$\psi_{\mathrm{ec,N}}$	Factor taking group effect into account, [-]
$\psi_{re,N}$	Shell spalling factor, [-]
$\psi_{s,N}$	Factor taking disturbance of the distribution of stresses in the concrete due to edges into account, [-]
ψ_{sr}	Factor for increased capacity due to surface reinforcement

1 Introduction

1.1 Background

For concrete anchorage of pipe support and frame structures in industrial facilities it is common to use expander bolts or cast in anchors. Calculations for determining the design strength of such details are done by using the European pre-standard (CEN/TS 1992-4-1, 2009), which is about to be included in Eurocode 2. In the code of praxis the approach for determining the strength is similar for expander bolts and cast in anchors. The method is based on review of many failure modes and the strength is then governed by the mode with lowest capacity. One of these failure modes that many times are decisive for the strength is the cone failure, meaning that the concrete is pulled out as a cone together with the anchor, see Figure 1.1. The influence of the surface reinforcement in the concrete is however not taken into account in the code of praxis. In industry there usually exists large amount of surface reinforcement which can be favourable for the capacity since the code of praxis is conservative.

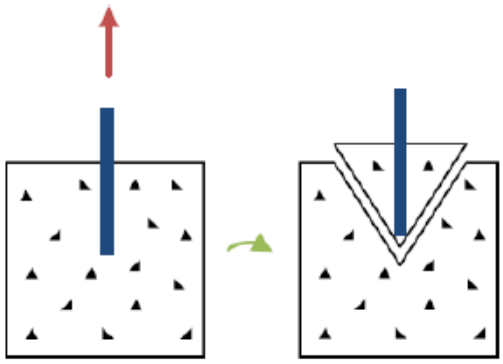

Figure 1.1- Concrete cone failure.

According to (Elfgren & Nilsson, 2009) the surface reinforcement in the concrete does give some increased capacity to the concrete cone failure. 66 tests were performed that considered different sized slabs and different amount of reinforcement. From these results the conclusion was drawn that the increase of capacity depends on the geometry, amount and placement of the surface reinforcement. It was also stated that further work is needed such as numerical modelling of the failure process to be able to generalise the test results.

Based on these tests some numerical evaluations were made on single anchors by (Nilforoush, 2015) that took surface reinforcement into account. The conclusion was that the surface reinforcement had impact on the capacity if the cross-sectional height of the member was not too large compared to the effective length of the anchor. Further numerical evaluations were also made by (Segle, et al., 2013) where group of anchors also were investigated and these analyses also showed an increase in the capacity.

There are still more to be analysed for the tension strength of concrete and what impact the surface reinforcement has on the capacity. The code of praxis consider many parameters for the concrete cone failure that needs to be considered when determining the influence on the capacity from the surface reinforcement.

1.2 Aim and objectives

The aim of this master thesis is to study how the surface reinforcement is affecting the anchor strength for the concrete cone failure in tension.

The specific objectives for this thesis are:

- To do a literature study about failure modes of anchors in concrete, where focus is on the cone failure. The study will include both performed tests, numerical evaluations and todays design methods.
- To establish a modelling method for finite element (FE) analysis of the concrete cone failure in FE software DIANA and ABAQUS.
- To verify the modelling method by comparing with tests found in literature for a single anchor with surface reinforcement.
- To use verified modelling method to investigate what impact the surface reinforcement has on single anchors and group of anchors.

1.3 Limitation

There are several failure modes that can occur for anchors in concrete but this thesis focused on the cone failure. The height of the slab has an impact on the cone failure but in this thesis only two heights were studied. One height should however be relatively thin so that the concrete itself did not have too much stiffness and one with double the height and thereby also greater stiffness. The size of the anchor's head is also shown to have an effect on the capacity but was set to one size in the thesis. The size of the anchor was not too small so that the anchorage itself failed and the size of the anchor head was also not too small so that pull out failure was the decisive failure mode. Studies can be performed on un-cracked or pre-cracked concrete and this thesis chose to study un-cracked concrete.

1.4 Method

A literature study was carried out on anchorage failure of anchors in concrete with main focus on concrete cone failure. Previous tests and numerical evaluation performed were studied to establish a basis for a FE modelling method of concrete cone failure in DIANA.

When the FE-modelling method was established it was verified against three tests performed by (Elfgren & Nilsson, 2009). The verification was done for a single anchor with the same parameters and geometry as in the performed tests. The amount of surface reinforcement, size of slab, size of anchor etc. was the same for the FE-model as in the performed tests. When similar results were achieved from the calibration it was possible to move on to investigate the impact of the surface reinforcement for single anchors and to model and investigate group of anchors. An FE-model was also created in ABAQUS based on the model created in DIANA. The ABAQUS model was first verified with the results given by DIANA on single anchors and then used to compare results for group of anchors between the two FE-models. The analyses were made for non-linear behaviour where cracking in the concrete and yielding of the reinforcement were considered and the loading of the model was of static nature.

The results from the FE-analyses of single anchors and group of anchors were then compared to the design capacity for the cone failure given by (CEN/TS 1992-4-2, 2009). This was done to determine how much more capacity that could be accounted for in these cases if surface reinforcement would be included in the calculations in the code of praxis. The results for single anchor and group of anchors were also compared with each other to see if the surface reinforcement had similar impact.

2 Anchors in Concrete

2.1 General about concrete

Concrete is the most common building material in civil structures, since it has high flexibility in shaping of structures and is of low cost. Concrete is known to be strong in compression and weak in tension. In compression the load is carried in the aggregates within the concrete while in tension the cement holding the aggregates together will crack. Because of its low tensile strength, concrete is often combined with steel reinforcement, which carries the tensile stresses in the structure (Engström, 2013).

The stiffness of a reinforced concrete section during loading varies non-linearly. Before the applied load reaches the concrete tensile strength the stiffness of the section can be seen to be linear depending mainly on the elasticity of the concrete. As cracking start the reinforcement will be "activated" and start to contribute to the stiffness while the concrete in the tensile part of the cross-section is seen to have little effect on the stiffness and is therefore neglected. As more cracks develop under increasing load the stiffness will keep changing until the section is fully cracked. The stiffness can also change due to yielding of the reinforcement but for a simple supported beam this would mean that failure is reached (Engström, 2013).

The concrete is classified in different strength classes, where the classes represent the characteristic 5% fractile compressive cylinder strength (f_{ck}) and cube strength ($f_{ck.cube}$) at the age of 28 days (Engström, 2013).

2.2 Anchors

Anchors act to carry an applied load from a component and into the concrete. Anchors loaded in tension mainly transfers load through mechanical interlock, friction or chemical interlock (bond). For most anchors resistance to tension load is done by one or more of this type of load transfer mechanisms (Eligehausen, et al., 2006). Mechanical interlock means that the load is transferred through bearing interlock between the anchor and the concrete see Figure 2.1. This type of load transfer can be carried out by headed anchors, anchor channels, screw anchors etc. (Eligehausen, et al., 2006).

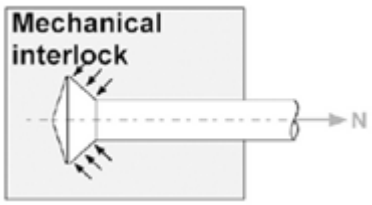

Figure 2.1- Load transfer through mechanical interlocking, (Eligehausen, et al., 2006).

Friction forces are possible to obtain if expansion anchors are used. During installation an expansion force will be generated which will give friction force between the anchor and the sides of the drilled hole see Figure 2.2. This friction force will then be in equilibrium with the applied tension load (Eligehausen, et al., 2006).

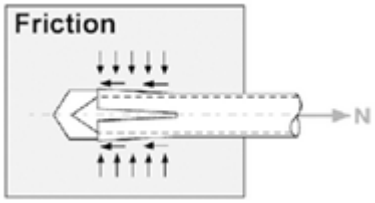

Figure 2.2- Load transfer through friction, (Eligehausen, et al., 2006).

For chemical interlocking the applied tension load is transferred from the anchor to the concrete trough bond meaning usually some kind of adhesion is used see Figure 2.3. This load transfer is employed for all anchors where bond is used (Eligehausen, et al., 2006).

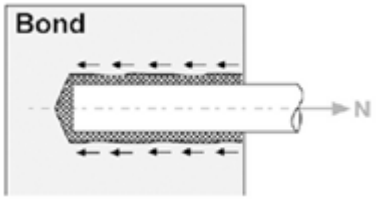

Figure 2.3- Load transfer through bond, (Eligehausen, et al., 2006).

Type of tension load transfer used can be described by which type of anchor used or how it is installed. For the installation procedure there are three main categories, cast in place anchors, drilled in anchors and direct installed anchors (Eligehausen, et al., 2006).

In the following section cast in place system and one common anchor for the cast in place system will be further explained.

2.2.1 Cast in place anchor

Anchors that are cast in place are commonly used in industrial facilities such as nuclear power plants to anchor pipe support and frame structures. Cast in place anchors transfers tension load to the concrete mainly through mechanical interlock. When reinforced concrete is used the anchor must be coordinated with the reinforcement layout. One of the advantages with cast in place anchors is that the location of the external load is known and therefore the reinforcement layout can be design accordingly. The disadvantages is that coordinating the reinforcement layout can be more time consuming than for other anchor systems (Eligehausen, et al., 2006).

One of the most common anchor types used for cast in place systems is headed studs. Headed stud anchors consist of headed studs that are butt welded on to a steel plate, see Figure 2.4. The welding of the studs to the steel plate is seldom performed at site but more commonly at factory. The fixture that is to be a connected to the anchor is usually welded to the cast in steel plate and the headed studs then transfers the tension load through mechanical interlock to the concrete (Eligehausen, et al., 2006).

Figure 2.4- Headed stud anchors.

2.3 Modes of failure

There are different kinds of failure modes for anchors in concrete when loaded in tension. The concrete is weaker in tension compared to compression as explained in Section 2.1. Depending on embedment length, size and steel strength, concrete strength and placement of the anchors different modes are occurring. These five are the normally failure modes occurring:

a) Pull-out and Pull-through

b) Concrete cone failure

c) Splitting failure

d) Steel failure

In Figure 2.5 the load-displacement curves can be seen for different failure modes and which modes that are ductile respectively brittle.

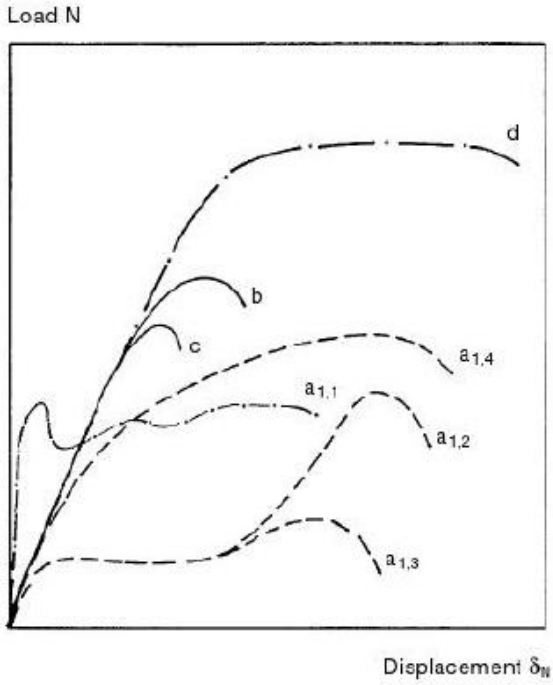

Figure 2.5-Load versus Displacement curves for the different failure modes, (Eligehausen, et al., 2006).

2.3.1 Pull-out and pull through failure

Pull-out failure mode is as the name indicates, the anchor is "pulled out" from the drilled hole see Figure 2.6a. The concrete at the surface may be damaged as well (Eligehausen, et al., 2006). This failure mode can occur if the expansion force for a displacement-controlled expansion anchor is inadequate to hold the anchor at the installed embedment depth the load corresponding to concrete cone failure. It can also occur for undercut or headed anchors if the mechanical interlock (bearing surface) is insufficient. For the expansion anchors a proportional expansion force can be used (Eligehausen, et al., 2006).

Pull through failure is similar to pull out failure but it is a unique failure only occurring when torque controlled expansion anchors are used, see Figure 2.6b. The load- displacement for this failure is similar to pull out failure for undercut and headed anchors (Eligehausen, et al., 2006).

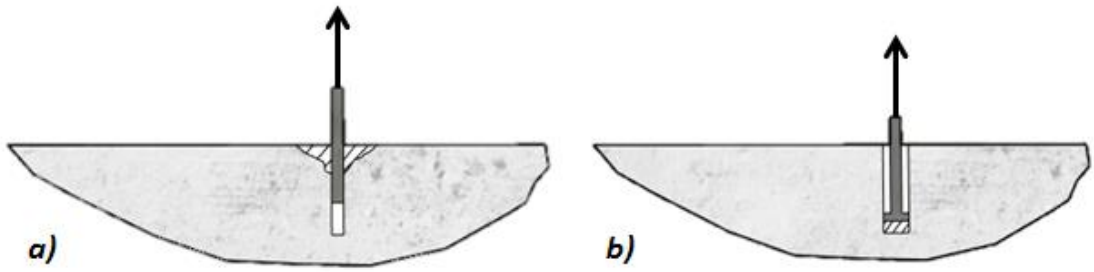

Figure 2.6- a) Pull-out and b) Pull-through failure.

2.3.2 Concrete cone failure

This failure mode is the most common and will occur if the anchor has sufficient capacity for pull-out and pull-through and if the steel capacity is not exceeded. The shape of the brake out is formed like a cone with normally an angle of 30-40 degrees see Figure 2.7a. The load-displacement behaviour for the concrete cone failure is relatively non-ductile and is also largely dependent on the anchor type (Eligehausen, et al., 2006).

There are some reductions in capacity that need to be considered if the anchors are too close to each other or if they are placed too close to an edge, see Figure 2.7b. If the anchors are too close to each other it will lead to an overlap of each projected cone and one aggregated cone will appear. The projected cone and the capacity will decrease when the anchor is too close to an edge (Eligehausen, et al., 2006). This is considered in the code of praxis (CEN/TS 1992-4-2, 2009) with factors that decreases the capacity.

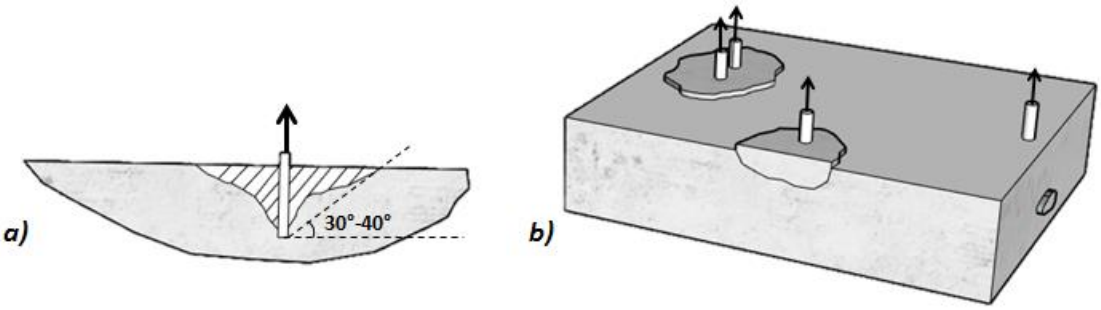

Figure 2.7- a) Concrete cone failure and b) variations of the mode.

2.3.3 Splitting failure

When the dimensions of the concrete member is small compared to the anchor then a splitting failure can occur, see Figure 2.8 a. It can also happen when the anchor is placed too close to an edge or in line with other anchors see Figure 2.8b. The capacity of this mode can be less than for concrete cone failure because of the undeveloped impact area (Eligehausen, et al., 2006).

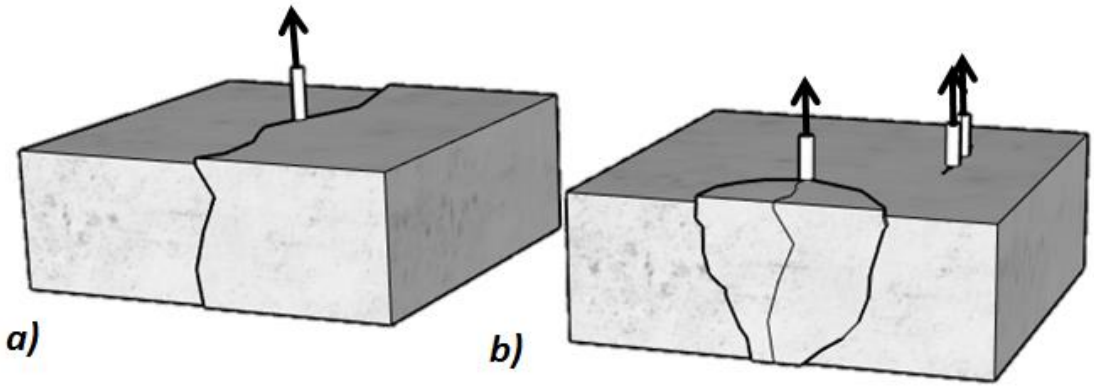

Figure 2.8- a) Splitting failure and b) variations of the mode

2.3.4 Steel failure

The ultimate load is the product of the steel area times the tensile steel strength and fails in rupture of the steel see Figure 2.9. Of all the previous mentioned failure modes, this is the one that often gives the highest capacity and it gives a ductile failure see Figure 2.5. This mode happens when the anchor has sufficient embedment depth and the concrete has high strength (Eligehausen, et al., 2006).

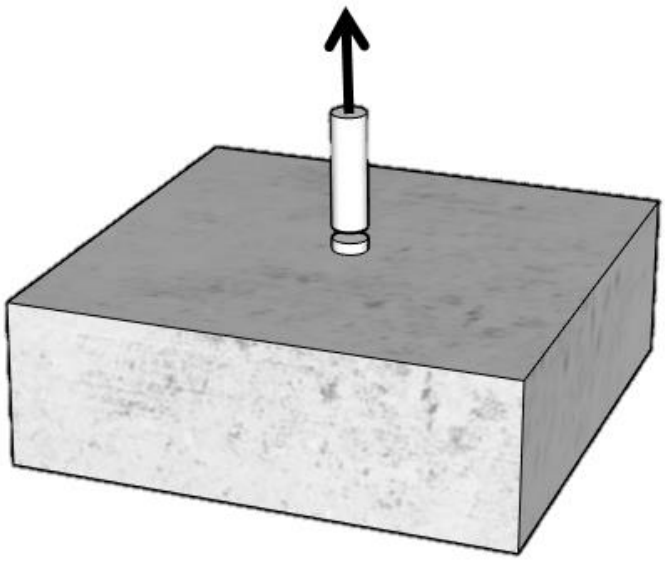

Figure 2.9- Steel failure

3 Concrete Cone Failure in Design Code

There are standardization and codes of praxis for design of anchors for instance in (CEN/TS 1992-4-1, 2009). This thesis aims to improve the code of praxis for the concrete cone failure in tension so that more capacity can be accounted for both when designing anchorage and when trying to verify capacity in already existing structures. This chapter will explain the concrete cone failure and what parameters that are included in today's code of praxis.

The resistance given by the code of praxis for concrete cone failure in tension is verified with Equation (3.1), (CEN/TS 1992-4-1, 2009).

$$\gamma_{F,fat} \times \Delta N_{Ek} \leq \frac{\Delta N_{Rk,c}}{\gamma_{Mc,fat}} \tag{3.1}$$

With $\gamma_{\mathrm{F,fat}} = 1{,}0$
$\gamma_{\mathrm{Mc,fat}} = 1{,}15$

This report does however only consider headed anchors even though it looks similar for the expander bolts. The resistance in tension loading for these anchors are verified by using Equation (3.2), (CEN/TS 1992-4-2, 2009).

$$N_{Ed} \leq N_{Rd,c} = \frac{N_{Rk,c}}{\gamma_{Mc}} \tag{3.2}$$

With $\gamma_{\mathrm{Mc}} = \gamma_{\mathrm{c}} \cdot \gamma_{\mathrm{inst}}$
$\gamma_{\mathrm{c}} = 1.5$
$\gamma_{\mathrm{inst}} = 1.0$

The characteristic resistance for a single anchor or group of anchors in case of concrete cone failure for a headed anchor can be calculated by Equation (3.3) given by (CEN/TS 1992-4-2, 2009).

$$N_{Rk,c} = N^{o}_{Rk,c} \times \frac{A_{c,N}}{A^{0}_{c,N}} \times \psi_{s,N} \times \psi_{re,N} \times \psi_{ec,N} \tag{3.3}$$

The factors given in Equation (3.3) are explained further in the sections below.

3.1 Single anchor

In Equation (3.4) the resistance of a single anchor not influenced by any partial factor is given, (CEN/TS 1992-4-2, 2009). This equation is considering the un-cracked coefficient k_{ucr} but there is an empirical factor for pre-cracked concrete as well.

$$N^{o}_{Rk,c} = k_{ucr} \times \sqrt{f_{ck,cube}} \times h_{ef}^{1,5} \tag{3.4}$$

3.2 Effect of axial spacing and edge distance

In order to reduce the strength of the single anchor which is placed close to an edge or close to another anchor Equation (3.5) is used where the geometry is taken into account (CEN/TS 1992-4-2, 2009). The reference area for one anchor can be seen in Figure 3.1

$$\frac{A_{c,N}}{A^{0}_{c,N}} \tag{3.5}$$

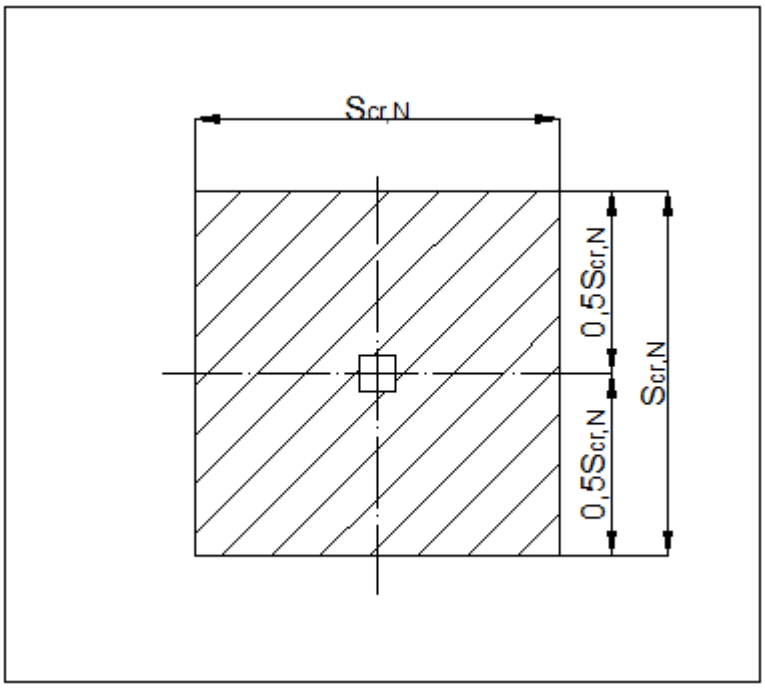

Figure 3.1 -Projected area $A^0_{c,N}$ for one anchor.

3.3 Effect of the disturbance due to edges

The factor $\psi_{s,N}$ takes account for the disturbance due to edge. If there is more than one close edge, the smallest should be used in the Equation (3.6), (CEN/TS 1992-4-2, 2009).

$$\psi_{s,N} = 0{,}7 + 0{,}3 \times \frac{c}{c_{cr,N}} \leq 1 \qquad (3.6)$$

3.4 Effect of shell spalling

This effect takes account for a dense reinforcement for an embedment depth h_{ef}< 100 mm. If the reinforcement is placed with a spacing of 150 mm or more, or if the reinforcement with a diameter of 10 mm or less is provided with a spacing of 100 mm or more then the $\psi_{re,N}$ should be taken as 1, otherwise should Equation (3.7) be used, (CEN/TS 1992-4-2, 2009).

$$\psi_{re,N} = 0{,}5 + \frac{h_{ef}}{200} \leq 1 \qquad (3.7)$$

3.5 Effect of the eccentricity of the load

When more than one anchor is used and the anchors interrupt on each other's cone with different tension loads on each anchor, then the factor $\psi_{ec,N}$ should be considered. This is when an anchor is placed closer than half of $S_{cr,N}$. The factor $\psi_{ec,N}$ should be calculated separately if there is an eccentricity in two directions and inserted in Equation (3.3). $\psi_{ec,N}$ is given in Equation (3.8), (CEN/TS 1992-4-2, 2009).

$$\psi_{ec,N} = \frac{1}{1+2\times\frac{e_n}{S_{cr,N}}} \leq 1 \qquad (3.8)$$

3.6 Spitting failure

Splitting failure is a possible failure mode if the element is not stiff enough for a concrete cone failure to break out. This can be checked by using the bending moment capacity.

The point load that can be applied on a single anchor in centre for a circular slab based on bending capacity is given by Equation (3.9).

$$P_{Rd} = \frac{2 \times \pi \times M_{Rd}}{b} \tag{3.9}$$

For a group of anchor simple linear FE analysis can be made to determine a relation between the point load and the moment, see Equation (3.10)

$$M = K \times P \tag{3.10}$$

When the relation between point load and moment is known, a point load for the group can be calculated using the bending capacity, see Equation (3.11)

$$P_{Rd} = \frac{M_{Rd}}{K} \tag{3.11}$$

3.6.1 Un-reinforced cross-section

For an un-reinforced cross-section the bending capacity can be calculated using Equation (3.12).

$$M_{Rdu} = f_{ctm} \times \frac{b \times H^2}{6} \tag{3.12}$$

3.6.2 Reinforced cross-section

For a reinforced cross-section the bending capacity can be calculated using Equation (3.13).

$$M_{Rd} = F'_S \times \left(d - d'\right) + F_C \times (d - \beta \times x) \tag{3.13}$$

Where $F'_S = E_S \times \varepsilon'_S \times A'_S$

$F_C = \alpha \times f_{cm} \times b \times x$

$\alpha = 0.81$

$\beta = 0.416$

4 Physical Tests at Luleå University of Technology

Tests concerning the impact of surface reinforcement on concrete cone failure have been made by (Elfgren & Nilsson, 2009) where it was shown to give more capacity for the concrete cone failure.

In 2009, 66 tests were carried out by (Elfgren & Nilsson, 2009) to study the capacity of concrete cone failure of cast in headed studs and to check the influence of surface reinforcement as well as other boundary conditions. The check of capacity was done against the capacity given by (CEN/TS 1992-4-2, 2009), these equations can also be seen in Chapter 3.

In the beginning 12 pilot tests were performed where different amount of reinforcement, un-cracked- and pre-cracked concrete conditions were tested. Tests were performed on slabs that rested on four supports. The support conditions did however make the slab get splitting failure instead of concrete cone failure. The support condition was therefore changed to a ring support on top of the slab while the slab rested on a flat surface, see Figure 4.1. For the cross section with reinforcement layout, see Figure 4.2 (Elfgren & Nilsson, 2009).

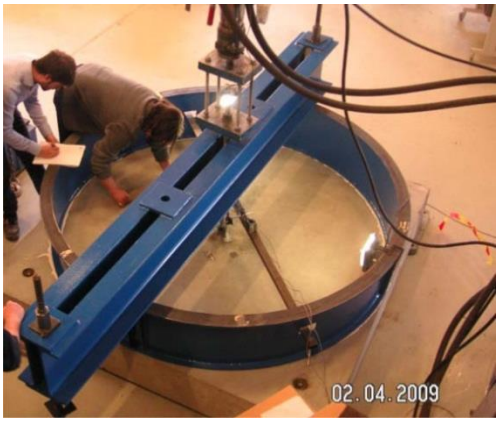

Figure 4.1-Demonstration of anchor test (Elfgren & Nilsson, 2009).

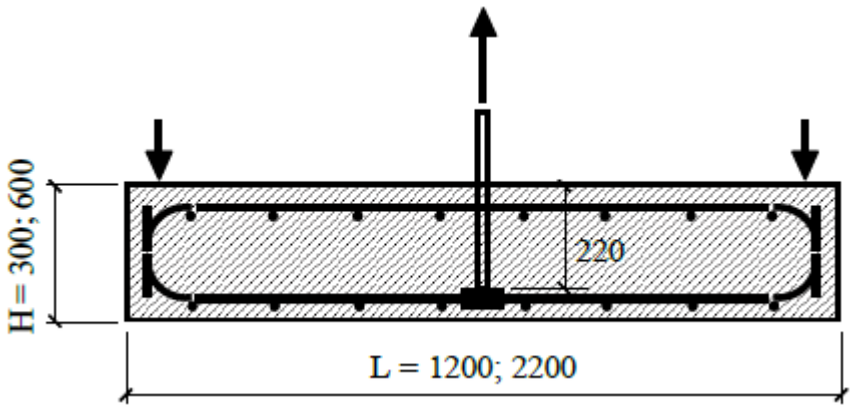

Figure 4.2-Forces acting on slab with ring support (Elfgren & Nilsson, 2009).

The main 66 tests were then carried out on a single anchor in a concrete of class C25/30. For all tests the anchor had a stud diameter of 30 mm and a head diameter of 45mm and the effective length was 220 mm. The slabs were squared with two different sizes of the width (*L)*, 1.2 m and 2.2 m. The slabs were also tested for two different thicknesses (*H*), 0.3 m and 0.6 m. The tests were carried out for un-cracked- and pre-cracked concrete conditions. For pre-cracked condition the crack was 0.8 mm.

The tests also considered the spacing of the reinforcement around the bolt and the thickness of the concrete cover for the reinforcement. Finally the reinforcement was then varied between 0% to 1.2% for the different slabs, where the diameter was of size ϕ12 or ϕ16 and the spacing varied between 100mm to 300mm. The loading of the tests were of static nature. A summary of the tests result for the un-cracked tests can be seen in Table 4.1 (Elfgren & Nilsson, 2009).

Table 4.1- Summary of results from un-cracked tests.

No.	*L* [m]	*H* [m]	*Top reinforcement*	P_{Test} [kN]	*Deformation* $_{Test}$ [mm]
1	1,2	0,3	-	193	10,4
2	1,2	0,3	Φ12cc300	280	9,2
3	1,2	0,3	Φ16cc150	319	7,6
4	1,2	0,3	Φ16cc100	302	1,9
5	1,2	0,6	Φ12cc300	357	9,6
6	2,2	0,3	Φ12cc400	241	8,8
7	2,2	0,3	Φ12cc150	262	8,0
8	2,2	0,6	Φ12cc150	327	8,7

From the tests it was seen that the surface reinforcement had an impact on the capacity of the slab. For the thin slab without surface reinforcement a splitting failure occurred while for the reinforced and for the thicker slabs cone failure occurred.

The observation was that if the global stiffness was increased an increase in capacity was also achieved and for too low stiffness the concrete cone failure cannot be reached before splitting failure happened. The increase of the capacity given by the reinforcement depends on the geometry, amount and placement of the reinforcement (Elfgren & Nilsson, 2009).

In the report it was also mentioned that more research is needed in the form of numerical evaluations looking at different boundary conditions, such as loading in tension of a group of anchors (Elfgren & Nilsson, 2009).

5 Finite Element Modelling

The modelling was done in both DIANA and ABAQUS to compare the software and how well they explain the behaviour of concrete for concrete cone failure in both maximum strength and displacement. In this chapter it is explained what modelling assumptions that were made, what material models that were used for the software and which improvements and simplifications that had to be made for the models.

5.1 Modelling assumptions

In order to model the anchorage failure in concrete a non-linear analysis with 3D solid elements were needed. A comparison between the FE-model given from DIANA and the experimental tests needed to be done to verify that the model was giving credible outputs. When the DIANA model was calibrated against these tests further investigation could be continued on single anchor and on group of anchors. The calibration was done by comparing three slabs with different dimensions and reinforcement amounts. The aim was to get the right failure mode and similar capacity and displacement for the model as it in tests performed for the three slabs.

Based on the DIANA model a model in ABAQUS was created that was first verified against some results from single anchors given by the DIANA-model to determine that credible results were given for the ABAQUS model as well. The ABAQUS model was then used for analyses on group of anchors and the results were compared with the results given by the analyses performed in DIANA.

The different models for the different slabs have the same interactions between anchor and concrete and between reinforcement and concrete. The boundary conditions, mesh size, number of steps and tolerance for the models were also the same once the calibration was performed. The only things that did differ were the slab thickness (H), reinforcement amount and some small changes of the material parameters for the concrete of the calibrations slabs since these slabs are cast from different concrete batches for the tests performed by (Elfgren & Nilsson, 2009). Principle sketches over the slabs to be model for a single anchor can be seen in Figure 5.1 and in Figure 5.2 for a group of anchors.

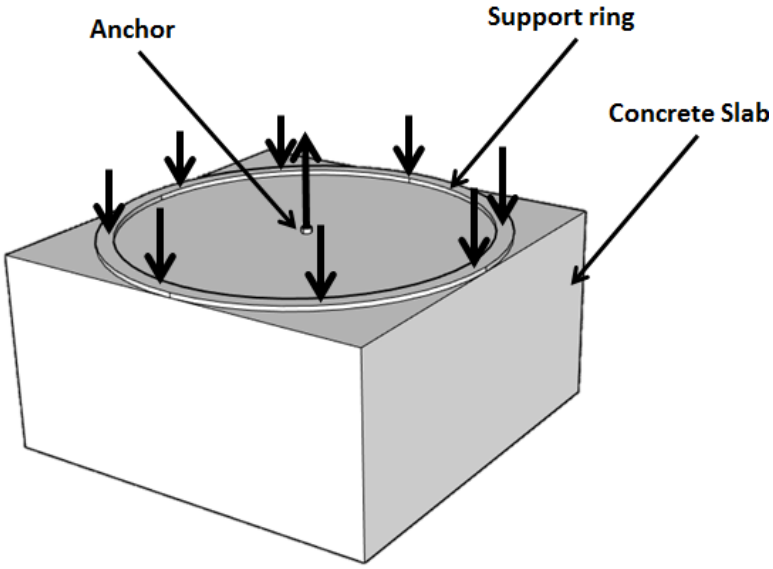

Figure 5.1- Principle sketch over slabs to be model for single anchor.

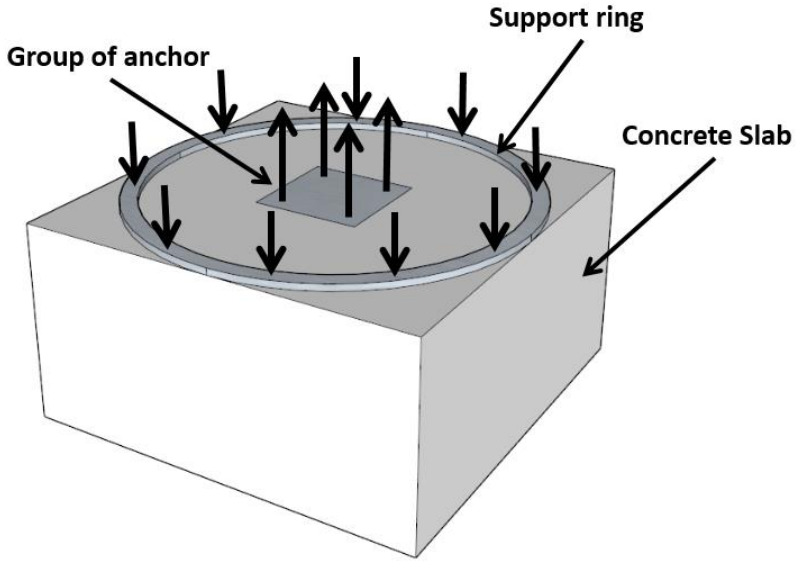

Figure 5.2- Principle sketch over slab to model for group of anchor

The non-linear analysis is more time consuming than linear and therefore some assumptions were made to decrease the computational time. Only a fourth of the slab was modelled and symmetry line was used in both x- and y-axis, see Figure 5.3 for single anchor and Figure 5.4 for group of anchors. The model was prevented from displacement in the z-direction at the top of supporting ring but not in the bottom of the slab, this is done because the concrete slab is free to move upwards in reality and this is decisive for tension strength. Also instead of applying a distributed load on the top of the anchor a prescribed displacement (δ) was applied since this was assumed to be more favourable when doing the non-linear analysis and deformation controlled loading is often more stable analysis than load controlled (Broo, et al., 2008). The reaction force (R) at the anchor was extracted from the results to determine the capacity in the form of a "Load", see Figure 5.3 and Figure 5.4.

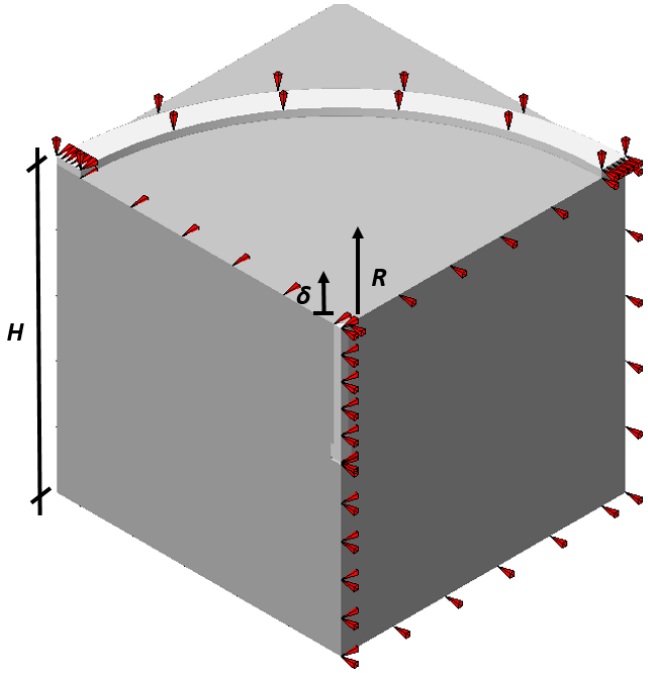

Figure 5.3- Principle sketch of modelling of symmetry boundary on one fourth of the slab for single anchor, prescribed displacement (δ) and reaction force(R).

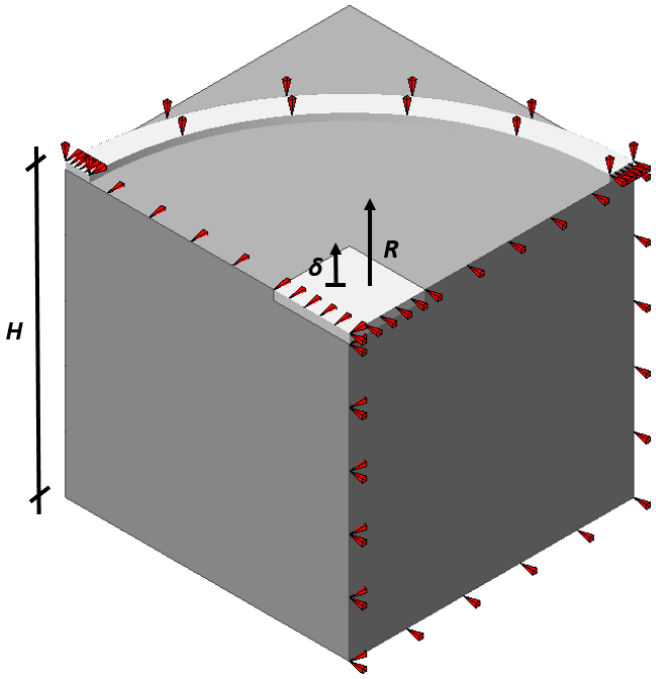

Figure 5.4- Principle sketch of modelling of symmetry boundary on one fourth of the slab for group of anchors, prescribed displacement (δ) and reaction force(R).

The interface between the anchor and the concrete was modelled to have frictionless behaviour in z-direction. The interface at the top of the anchor head was however modelled with stiffness so that the load was able to be transferred from the anchor to the concrete. This was a conservative assumption since in reality there is some friction along the anchor and the concrete but as explained in Section 2.2.1 the main load transfer is through mechanical interlock for cast in headed anchors between the anchor head and the concrete. It is also hard to estimate how much friction that should be applied for the anchor. The interface between the concrete and the bottom of the

anchor head was also hard to describe in a way that represented reality, where the concrete did not move up into the anchor once loading begun. Therefore a gap was created between the concrete and the bottom of the anchor head, see Figure 5.5.

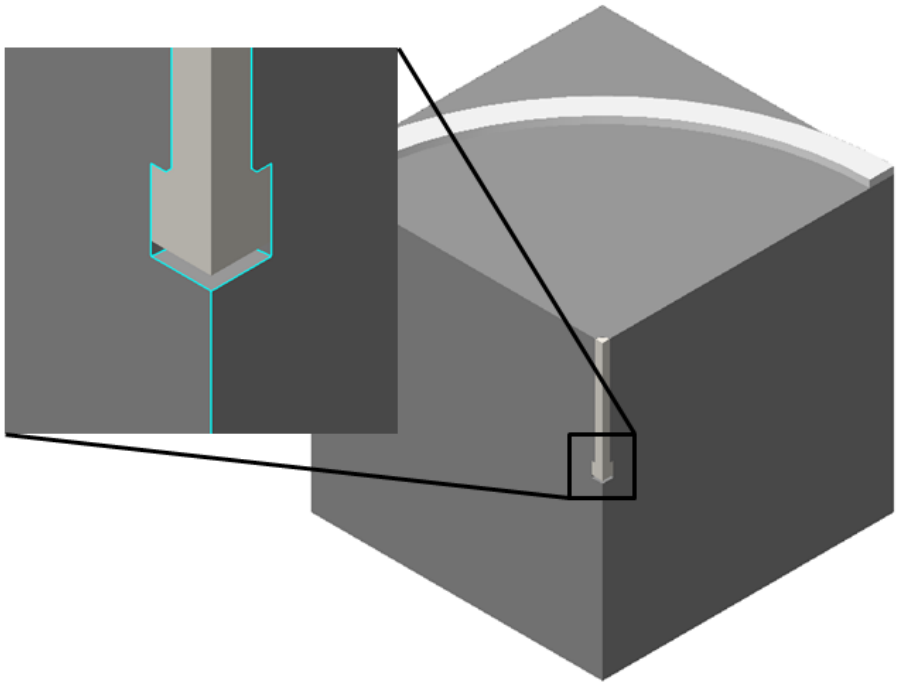

Figure 5.5- Illustration of gap between concrete and bottom of anchor head.

The surface reinforcement is usually modelled either with full interaction between reinforcement and concrete or as 3D-elements where there is bond slip between the reinforcement and concrete. The concrete only gets higher stiffness when full interaction is assumed and no separate elements or degrees of freedom for the reinforcement are created with this method. This means that the strain and forces in the bars are calculated from the surrounding concrete elements. If the reinforcement is modelled as separate 3D-elements there can be a slip between the concrete and the reinforcement when a crack appears. This better resemble the actual interaction between concrete and reinforcement. The reinforcement would carry the tensile stresses while the concrete would be neglected where the crack has appeared.

It takes more computational time to model bond slip with 3D-element bars therefore full interaction bars were the first approach for the model but bond slip was also later implemented to see if it should be used for the calibration.

5.2 Modelling in DIANA

5.2.1 Material model (Total strain crack model)

The material model that was used to describe the non-linear behaviour of concrete in DIANA was the total strain crack model. The total strain crack model describes the tensile and compressive behaviour of concrete with one stress-strain relationship. It was originally proposed by Vecchio and Collins but the three-dimensional extension to the theory is proposed by Selby and Vecchio. The material model is useful for analyses in both Service limit state (SLS) and Ultimate limit state (ULS) that are mainly governed by cracking and crushing (TNO DIANA BV, 2015).

The model is able to describe cracks as fixed or rotating. For rotating crack model the stress- strain relationships are evaluated in the principal direction of the strain vector. For the fixed crack model the stress- strain relationships are evaluated in fixed coordinate system, fixation occurs when cracking starts. Both models work for reinforced concrete structures but the fixed crack model is more suitable when it comes to analysing the physical phenomenon of cracking (TNO DIANA BV, 2015).

The total strain crack model is based on smeared crack approach for modelling of the cracks (tensile behaviour), meaning that deformation of a crack is smeared out over a crack band width. The crack band width is the width of the band of elements that the crack localizes in and is usually chosen to one element length for concrete without reinforcement in perpendicular direction of the cracks. For reinforced concrete where there is full interaction between the concrete and reinforcement the crack band width can be chosen to be the same as the mean crack distance and for reinforcement with bond slip the crack can be assumed to localize in one element length same as for unreinforced concrete (Broo, et al., 2008).

The compressive behaviour of the concrete is described with a stress softening branch which means that when the concrete reaches its peak value for the compression stress the strain can still increase to some extent. The softening branch may however need to be modified if compressive failure is reached but is localized to a small region. The softening branch can then be extended so the behaviour is more realistic.

For this thesis the model that was analysed used the total strain rotating crack model as material model for the concrete. The tensile behaviour for the model was described with nonlinear softening curve according to Hordijk, which takes fracture energy into account when cracks start to develop. This means that the concrete can still carry some load in tension after a crack has developed but with decreasing capacity as the strains increases, see Figure 5.6. The material parameters that needs to be defined for the behaviour according to Hordijk is tensile capacity for the concrete (f_t), fracture energy (G_f) and the crack band width (h). The crack band width can also be given a default value of $\sqrt[3]{V}$ where V is the volume of the element, (TNO DIANA BV, 2015).

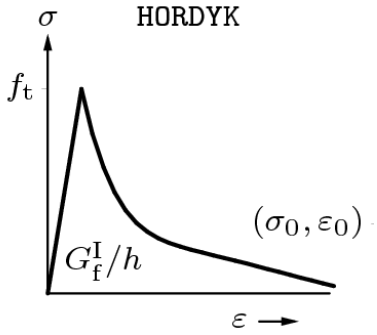

Figure 5.6- Stress-strain relationship in tension for concrete, according to Hordijk, (TNO DIANA BV, 2015).

The relation between the stress and strain for the softening curve according to Hordijk is given in Equation (5.1) (TNO DIANA BV, 2015).

$$\frac{\sigma^{cr} \cdot \varepsilon^{cr}}{f_t} = \begin{cases} \left(1 + \left(c_1 \cdot \frac{\varepsilon^{cr}}{\varepsilon^{cr}{}_{ult}}\right)^3 \cdot exp\left(-c_2 \cdot \frac{\varepsilon^{cr}}{\varepsilon^{cr}{}_{ult}}\right)\right. & if\ 0 < \varepsilon^{cr} < \varepsilon^{cr}{}_{ult} \\ \left. -\frac{\varepsilon^{cr}}{\varepsilon^{cr}{}_{ult}}(1 + {c_1}^3) \cdot exp(-c_2)\right. & \\ 0 & if\ \varepsilon^{cr}{}_{ult} < \varepsilon^{cr} < \infty \end{cases} \qquad (5.1)$$

Where $c_1 = 3$

$c_1 = 6.93$

The ultimate strain can be determined with Equation (5.2), (TNO DIANA BV, 2015).

$$\varepsilon_{ult}^{cr} = 5.136 \cdot \frac{G_f}{h \cdot f_t} \quad (5.2)$$

For the compressive behaviour the material is modelled according to Thorenfeldt which describes the compressive strength as decreasing for strains higher than the peak strain given by maximal compressive strength, see Figure 5.7, (TNO DIANA BV, 2015). The only material parameter that needs to be defined for the behaviour according to Thorenfeldt is compressive capacity for the concrete (f_c). It is however also possible to define lateral confinement and scaling factor (l) to change the behaviour of the Thorenfeldt curve. This is described further in Section 5.2.2.

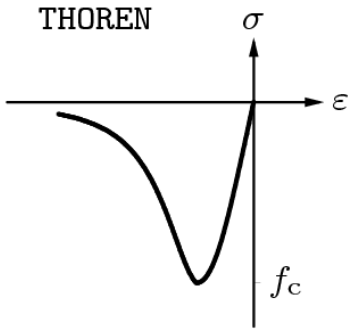

Figure 5.7- Stress-strain relationship in compression for concrete, according to Thorenfeldt, (TNO DIANA BV, 2015).

The relation between the stress and strain for the Thorenfeldt curve is given in Equation (5.3) (TNO DIANA BV, 2015).

$$f = -f_c \cdot \frac{\varepsilon}{\varepsilon_p} \cdot \left(\frac{n}{n - \left(1 - \left(\frac{\varepsilon}{\varepsilon_p}\right)^{nk}\right)}\right) \quad (5.3)$$

Where $n = 0.8 + \frac{f_c}{17}$

$$k = \begin{cases} 1 & if\ \varepsilon_p < \varepsilon < 0 \\ 0.67 + \frac{f_c}{62} & if\ \varepsilon \leq \varepsilon_p \end{cases}$$

5.2.2 Model development

Compressive failure

All loads were transferred from the anchor head to the concrete. The anchor head had relatively small area meaning that there were large compressive stresses in the concrete that was close to the top of the anchor head. These stresses were much larger than the capacity of the concrete in compression which means that there was crushing of the concrete in these areas, which lead to convergence problem in the analyses. The

compressive behaviour could however be modified so that higher compressive strength and longer strain softening branches was achieved.

One way to modify the compressive behaviour is to introduce lateral confinement which can be applied when the concrete is exposed to multiaxial compressive loading. Both strength and ductility of the concrete is increased for compression when lateral confinement is introduced, see Figure 5.8. It was therefore used in the model in order to avoid crushing of the concrete. The influence of lateral confinement in the model was given by Selby and Vecchio.

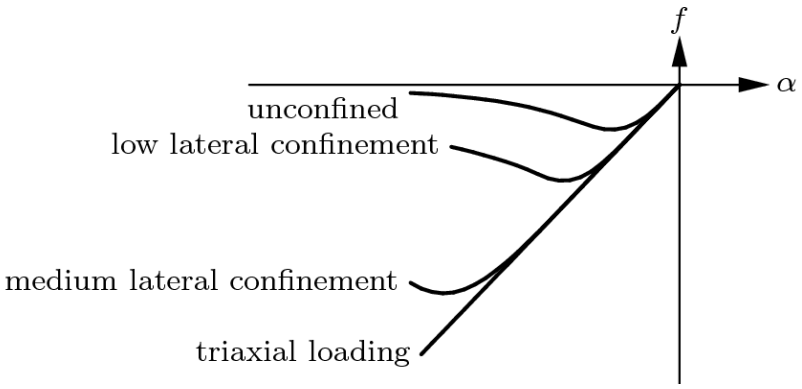

Figure 5.8- Influence of lateral confinement on stress-strain relation, (TNO DIANA BV, 2015).

The compressive stress-strain curve can also be modified by extending the compressive softening branch by considering localization of compressive stresses (Broo, et al., 2008). Since there was a large stress concentration in the concrete close to the top of the anchor head this is a reasonable improvement. The material model for compression softening given by (Thorenfeldt, et al., 1987) has determined the stress-strain relation based on tests performed on samples with the size of 300mm, the softening branch should (based on this) modified for the number of elements where the large compression stresses are assumed to localized in, (Hanjari, et al., 2011), See Figure 5.9. The modification can be problematic since it is not known in advance how many elements the compressive region will localize in (Hanjari, et al., 2011).

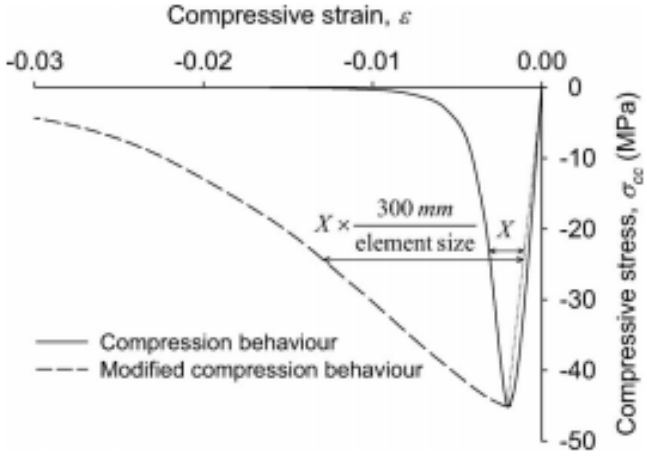

Figure 5.9- Scaling of softening branch, (TNO DIANA BV, 2015).

The equation used to obtain how large the scaling factor (which is defined in DIANA) for the localization of compression should be is given in Equation (5.4).

$$l = h \cdot \frac{300mm}{element\ size(Where\ the\ compression\ localize)} \quad (5.4)$$

The scaling factor was used in Diana to influence the softening part of the Thorenfeldt curve. This is done in Diana by replacing the strain (ε) with the Equation (5.5), (TNO DIANA BV, 2015):

$$\varepsilon_p + \left(\varepsilon - \varepsilon_p\right) \cdot \frac{h}{l} \quad (5.5)$$

Crack pattern/crack band width

The elements in the concrete where the concrete cone is assumed to break out should be of the same size as the element size used for the anchor. This is in order to get a good crack pattern for the concrete cone since the model is based on smeared crack approach and thereby the cracks should localize in the chosen crack band width (*h*). If the elements are of different size where a crack should be localized the crack pattern can be unrealistic or cause convergence problems.

Element types

The model used Solid tetrahedron elements (TE12L) for the concrete, anchor and support ring with three degrees of freedom, translations in x, y and z. For the interface between the anchor and the concrete 2D plane triangle interface elements (T18IF) were used and were modelled without any stiffness for the parts where no friction was wanted and with high stiffness where load was to be transferred. The reinforcement modelled with full interaction had no separate element type but was embedded into the solid concrete elements.

5.3 Modelling in ABAQUS

5.3.1 Material model (Concrete damage plasticity model)

The concrete damage plasticity model is based on models proposed by (Lubliner, et al., 1989) and (Lee & Fenves, 1998). It is intended to provide capability for analyses of concrete under cyclic and/or dynamic loading. The model is intended for reinforced concrete but can be used for plain concrete. The mechanical behaviour is based on plastic damage for the concrete where tensile cracking and compressive crushing are the assumed main failure mechanisms, (Dassault Systèmes , 2013).

The tensile behaviour for the model has a linear elastic relationship for the stress-strain response until the tensile capacity for the concrete is reached. Past the tensile capacity the micro-cracks in the concrete will be represented macroscopically with a softening stress-strain response, which induces strain localization in the concrete, see Figure 5.10, (Dassault Systèmes , 2013).

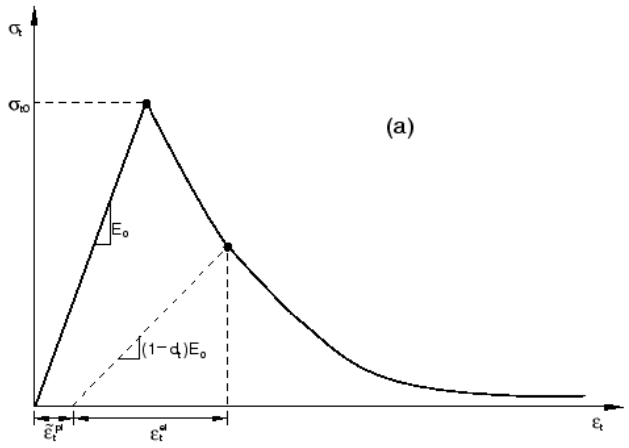

Figure 5.10- Tensile behaviour used for Concrete Damage Plasticity model, (Dassault Systèmes , 2013).

The modelling of the post-failure behaviour in tension is given by tension stiffening which gives the strain softening for cracked concrete and also the interaction effect between the concrete and the reinforcement. The tension stiffening can be specified with stress-strain relation where a cracking strain is defined or by defining the energy that is required to open a unit area of the crack, fracture energy (G_f). By using the fracture energy the relationship is rather stress vs displacement than stress vs strain behaviour and can be given by defining displacement, see Figure 5.11 or by defining the fracture energy, see Figure 5.12, (Dassault Systèmes , 2013).

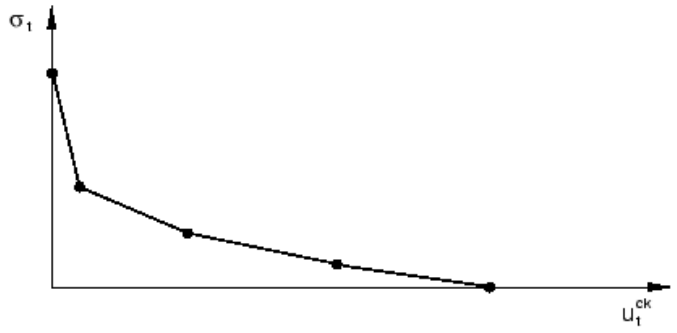

Figure 5.11- Stress- displacement relations defining displacement, (Dassault Systèmes , 2013).

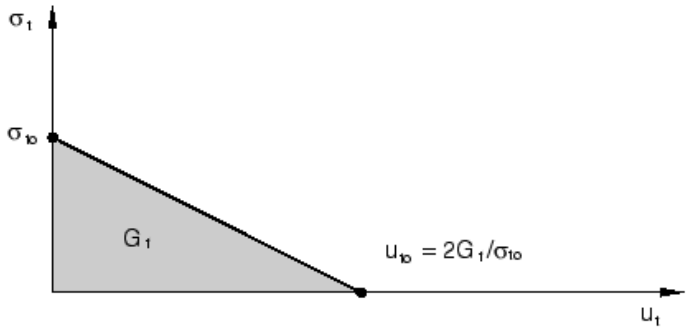

Figure 5.12- Stress- displacement relation defining fracture energy, (Dassault Systèmes , 2013).

The compressive behaviour is also linear until compressive capacity is reached. After this there is stress hardening which is then followed by strain softening for the concrete, see Figure 5.13.

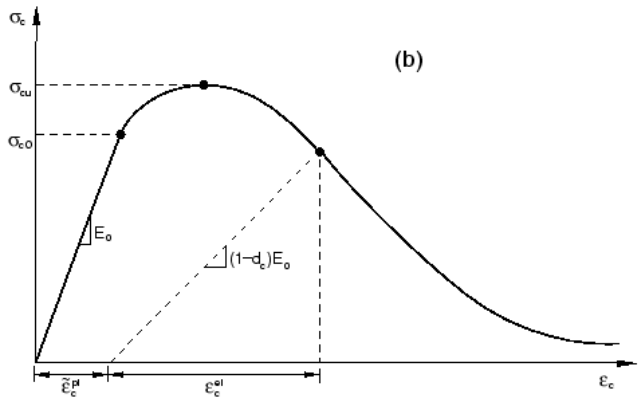

Figure 5.13- Compressive behaviour used for Concrete Damage Plasticity model, (Dassault Systèmes , 2013).

The parameters that needs to be defined for the concrete in concrete damage plasticity model is young's modulus (E_{cm}), compressive capacity (f_{cm}), tensile capacity (f_{ctm}), fracture energy (G_f), poisons ratio (υ) and dilation angle (ψ).

5.3.2 Model development

The model was modelled in the same way as described in Section 5.1. All improvements made for the DIANA model when calibrating the model was also supposed to be used for the ABAQUS model but some alternation had to be made for the ABAQUS model to optimize the computational time for the analyses. This is described further in Section 7.1.7.

Element types

The model used solid tetrahedral element (C3D10) for the concrete and the anchor and solid hexadral elements (C3D8R) for the support ring with three degrees of freedom, translations in x, y and z. The interface between anchor and concrete was modelled with an interaction property called "frictionless". The reinforcement used linear line elements (T3D2) and was modelled with embedded region so that the reinforcement had full interaction with the concrete.

5.4 Material parameters

5.4.1 Calibration

In (Elfgren & Nilsson, 2009) the value for the mean compressive strength (f_{cm}) is given for all the tests. An average mean compressive strength for the slab to be calibrated could therefore be determined and the remaining material parameters needed for the analyses could then be determined from equations given in (1992-1-1:2005, 2008). Equations (5.6) to (5.9) are used to determine strength material parameters of concrete used for calibration.

$$f_{cm,cube} = f_{cm} \cdot 1.2 \qquad (5.6)$$

$$f_{ck} = f_{cm} - 8 \qquad (5.7)$$

$$f_{ctm} = 0.3 \cdot {f_{ck}}^{2/3} \quad (5.8)$$

$$E_{cm} = 22 \cdot (\frac{f_{cm}}{10})^{0.3} \quad (5.9)$$

The material parameters used for the concrete and the amount of reinforcement for the different slabs are shown in Table 5.1-5.3 and were determined from the tests performed by (Elfgren & Nilsson, 2009) and equations above. The material parameters for reinforcement and anchor are shown in Table 5.4 and 5.5 these are also determined from the tests performed by (Elfgren & Nilsson, 2009).

Table 5.1- Material properties for concrete for slab 1.2m×1.2m×0.6m, ϕ12 S300.

Slab 1.2m × 1.2m×0.6m ϕ12 S300		*Comments*
f_{cm}(28days)	36 Mpa	(Elfgren & Nilsson, 2009)
f_{ctm} (28days)	2.8 Mpa	(1992-1-1:2005, 2008)
$f_{cm,cube}$ (28days)	43 Mpa	(1992-1-1:2005, 2008)
E_{cm} (28days)	32 Gpa	(1992-1-1:2005, 2008)
v	0.2	Assumed value
G_f	70 Nm/m^2	Assumed value
h	10 mm	Assumed value

Table 5.2- Material properties for concrete for slab 1.2m×1.2m×0.3m, ϕ12 S300.

Slab 1.2m×1.2m×0.3m ϕ12 S300		*Comments*
f_{cm}(28 days)	33 Mpa	(Elfgren & Nilsson, 2009)
f_{ctm} (28 days)	2.6 Mpa	(1992-1-1:2005, 2008)
$f_{cm,cube}$ (28 days)	40 Mpa	(1992-1-1:2005, 2008)
E_{cm}(28 days)	31 Gpa	(1992-1-1:2005, 2008)
v	0.2	Assumed value
G_f	70 Nm/m^2	Assumed value
h	10 mm	Assumed value

Table 5.3- Material properties for concrete for slab 1.2m×1.2m×0.3m, ϕ16 S100.

Slab 1.2m×1.2m×0.3m ϕ16 S100		*Comments*
f_{cm}(28 days)	36 Mpa	(Elfgren & Nilsson, 2009)
f_{ctm} (28 days)	2.8 Mpa	(1992-1-1:2005, 2008)
$f_{cm,cube}$ (28 days)	43 Mpa	(1992-1-1:2005, 2008)
E_{cm}(28 days)	32 Gpa	(1992-1-1:2005, 2008)
v	0.2	Assumed value
G_f	70 Nm/m^2	Assumed value
h	10 mm	Assumed value

Table 5.4- Material properties for reinforcement.

	f_y [Mpa]	*E-modulus* [GPa]	v
Steel B500B	500	210	0.3

Table 5.5- Material properties for anchor.

	f_y [Mpa]	f_{ub} [Mpa]	*E-modulus* [GPa]	v
Steel bolt 8.8	640	800	210	0.3

5.4.2 Single and group of anchors

Once the model was calibrated it was used to evaluate the influence of surface reinforcement and thickness of slab for both single anchor and group of anchors. Meaning all configurations and assumptions that were achieved when calibrating was still valid for the new analyses.

The material properties were chosen to be the same for all analyses of the single anchors and group of anchors in order to make comparison for different slab thickness, amount of reinforcement and for CEN/TS. They were also the same for both FE-software DIANA and ABAQUS to make comparisons for these as well. The concrete class that was used was C25/30 and the material properties are shown in Table 5.6.

Table 5.6- Material properties used for analyses of single anchors and group of anchors.

Material parameters C25/30		*Comments*
f_{cm}(28 days)	33 Mpa	(1992-1-1:2005, 2008)
f_{ctm} (28 days)	2.6 Mpa	(1992-1-1:2005, 2008)
$f_{cm,cube}$ (28 days)	40 Mpa	(1992-1-1:2005, 2008)
E_{cm} (28 days)	31 Gpa	(1992-1-1:2005, 2008)
v	0.2	From calibrations
G_f	70 Nm/m^2	From Calibrations
h	10 mm	From calibrations
ψ	35°	Only used for Abaqus

6 Numerical Evaluations reported in the literature

By the authors knowledge numerical evaluations have been made by both (Segle, et al., 2013) and (Nilforoush, 2015) that were based on the tests performed by (Elfgren & Nilsson, 2009) where more parameters and boundary conditions were analysed to investigate the impact of surface reinforcement on concrete cone failure.

6.1 Segle, et al.

Numerical evaluations have been done by (Segle, et al., 2013) where they investigated the impact of surface reinforcement on the concrete cone failure. A part of the analysis was to simulate the concrete cone failure for a single anchor and to calibrate the model for both non-reinforced and reinforced concrete. The non-reinforced concrete model is calibrated against tests performed by (Eligehausen, et al., 1992), and for reinforced concrete the model is calibrated against the tests performed by (Elfgren & Nilsson, 2009).

Analyses were also made for a group of anchors for non-reinforced and reinforced concrete. In all analyses with a group of anchors the concrete is un-cracked in the initial state. The analyses were made for tension loading as well as for shear loading.

The analyses were made for one fourth of the actual slab and symmetry boundaries were used, see Figure 6.1 (Segle, et al., 2013). Many different parameters were studied when calibrating the tests do get reliable results.

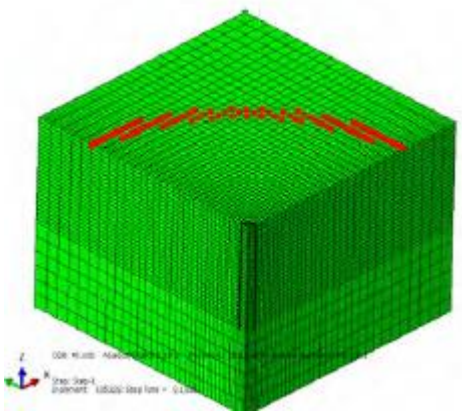

Figure 6.1- Simplification of model (Segle, et al., 2013).

The first simulations were made for single anchor in un-cracked and non-reinforced concrete. The results were then compared with the test performed by (Eligehausen, et al., 1992) as well as the design code (CEN/TS 1992-4-2, 2009). For results see Table 6.1.

Table 6.1- Result for single anchor in non-reinforced concrete (Segle, et al., 2013).

h_{ef} [mm]	N_{norm} [kN]	$N_{simulation}$ [kN]	$N_{CEN/TS}$ [kN]
50	29	30	31
150	157	190	163
450	1084	1190	845

The second simulations were made for single anchors in both un-cracked and pre-cracked reinforced concrete and the results were compared with the test performed by (Elfgren & Nilsson, 2009). For results see Table 6.2.

Table 6.2- Results for single anchor in reinforced concrete (Segle, et al., 2013).

No.	*L* [m]	*H* [m]	*Top reinforcement*	Pre-cracked [mm]	N_{test} [kN]	$N_{simulations}$ [kN]	$N_{simulations}/N_{test}$
1	1,2	0,3	-	0	196	270	1,38
2	1,2	0,3	ϕ12cc300	0	280	284	1,01
3	1,2	0,3	ϕ16cc150	0	319	305	0,96
4	1,2	0,3	ϕ16cc100	0	317	346	1,09
5	1,2	0,6	ϕ12cc300	0	357	349	0,98
6	2,2	0,3	ϕ12cc400	0	241	267	1,11
7	2,2	0,3	ϕ12cc150	0	262	288	1,10
8	2,2	0,6	ϕ12cc150	0	327	354	1,08
9	1,2	0,3	-	0,5	144	212	1,47
10	1,2	0,3	ϕ12cc300	0,5	292	245	0,84
11	1,2	0,3	ϕ16cc150	0,5	303	266	0,88
12	1,2	0,3	ϕ16cc100	0,5	256	325	1,27
13	2,2	0,3	ϕ12cc500	0,5	217	249	1,15

The third simulation was for groups of anchors, with four or six symmetrically placed anchors in un-cracked, non-reinforced concrete. The main parameters studied were spacing between the anchors and the effective length of the anchors and were then compared with the results for single anchors as well as with (CEN/TS 1992-4-2, 2009) see Figure 6.2.

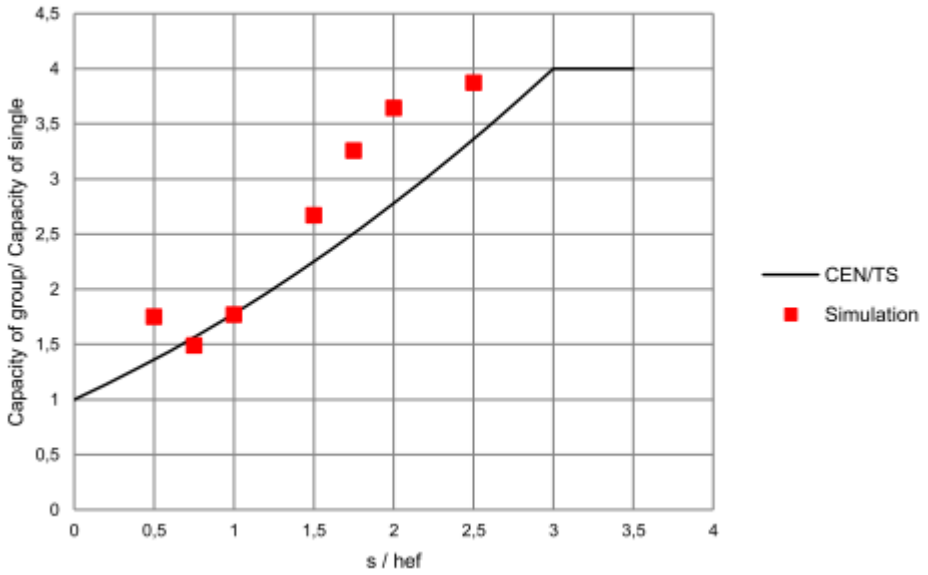

Figure 6.2- Results for group of anchor, non-reinforced (Segle, et al., 2013).

Finally a simulation was made for groups of anchors in reinforced concrete. The geometry of the slab, amount of reinforcement and amount of anchors was analysed and compared against the capacity for single anchors and (CEN/TS 1992-4-2, 2009), see Table 6.3.

Table 6.3- Result for group of anchors with reinforcement (Segle, et al., 2013).

Slab	*Slab dimension* [m]	*Top reinforcement*	*Support*	*Anchor group*	*Cross section of profile* [mm]	N_{group} [kN]
1	2,2×2,2×0,3	ϕ12cc300	Ring	2x2	120x120	314
2	2,2×2,2×0,3	ϕ12cc150	Ring	2x2	120x120	464
3	2,2×2,2×0,3	ϕ12cc100	Ring	2x2	120x120	492
4	2,2×2,2×0,3	ϕ12cc150	Ring	2x2	220x220	461
5	2,2×2,2×0,3	ϕ12cc300	Ring	2x3	120x120	340
6	2,2×2,2×0,3	ϕ12cc150	Ring	2x3	120x120	443
7	2,2×2,2×0,3	ϕ12cc100	Ring	2x3	120x120	502
8	2,2×2,2×0,6	ϕ12cc150	Ring	2x2	120x120	612
9	2,2×2,2×0,6	ϕ12cc150	Ring	2x2	220x220	622
10	3×3×0.6	ϕ12cc300	Simply	2x2	220x220	600
11	3×3×0.6	ϕ12cc300	Clamped	2x2	220x220	618

The conclusions that were drawn from all these results were that:

- The global stiffness has impact on the capacity for the concrete cone failure since low global stiffness will give tendency to splitting failure. This is not considered in (CEN/TS 1992-4-2, 2009) since here is sufficient stiffness for the structure already assumed (Segle, et al., 2013).
- The capacity is increased with the amount of reinforcement but there is no big difference in capacity between four and six number of anchors (Segle, et al., 2013).

6.2 Nilforoush

Numerical analyses were performed by (Nilforoush, 2015) where the model were calibrated against (Elfgren & Nilsson, 2009) test results for verification. The study was to investigate how the member thickness, size of the anchor head and surface reinforcement had an impact on the anchorage capacity for single anchors and the results were compared with (CEN/TS 1992-4-2, 2009).

The model was set for a fourth of the concrete specimen and used symmetry boundaries, see Figure 6.3. Models were made for both un-cracked and pre-cracked concrete (Nilforoush, 2015).

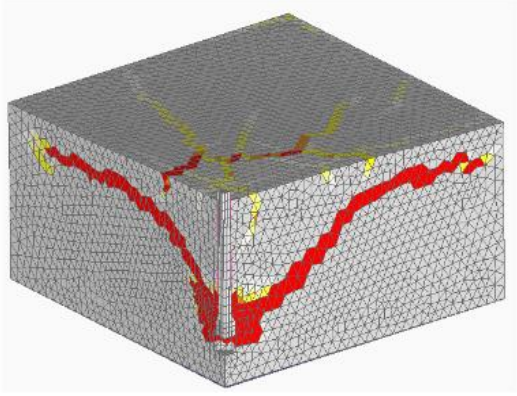

Figure 6.3- Un-cracked concrete, one fourth of the specimen (Nilforoush, 2015).

The results from the analyses where the size of the anchor head was investigated showed that the size of the head had some influence on the capacity and that the largest head had largest capacity. The member thickness was also shown to have increasing effect on the capacity, where thicker members had higher capacity. For the case with surface reinforcement an increase could also be seen. The reinforcement had largest effect on the thinner members. The largest impact was for members where

the total height of the specimen was less than 1.5 times the embedment length of the anchor. The result also showed that the amount of reinforcement used had a small increase on the capacity, instead it was the fact that reinforcement was introduced that increased the capacity (Nilforoush, 2015). Finally analyses showed that if the concrete was pre-cracked the capacity was decreased with 20-30% compared to the un-cracked concrete, (Nilforoush, 2015).

The conclusions for surface reinforcement analyses were that a modification factor could be used to take the increase in capacity into account, see Equation (6.1). An increase capacity for the concrete cone failure could be utilized for members with less than three times the embedment length (Nilforoush, 2015).

$$\psi_{sr} = \begin{cases} 1.25\ for & H \leq 1.5 \times h_{ef} \\ 1.10\ for & 1.5 \times h_{ef} < H < 3 \times h_{ef} \\ 1.00\ for & H \geq 3 \times h_{ef} \end{cases} \quad (6.1)$$

7 Numerical Results in DIANA

In this chapter the results from the calibration, the influence of the thickness and amount of surface reinforcement for both a single anchor and a group of anchors will be presented in load versus displacement graphs and pictures of the crack pattern.

7.1 Parameter studies for modelling

In order to optimize the model a number of different parameter studies have been made where only one parameter has been changed between the analyses such as mesh size, step length etc. The studies were performed on one slab of dimension 1.2m×1.2m×0.6m and with reinforcement amount of ϕ12 S300. The material parameters were not the same as the original values given in Section 5.1. The result from the studies were not analysed for final values used in calibration but only to study some of the parameters in the analyses with the physical tests capacities in mind. The aim was to catch a reasonable behaviour for the load versus displacement curve, that the crack pattern developed in a realistic way and to see if the capacity for the slab was going toward a value once the different parameters were increased or decreased.

The compressive strength was set to elastic to avoid the assumed compressive failure of the concrete and all analyses were displacement controlled.

The studies were performed in the FE software DIANA but the idea was to use the determined parameters for analyses in FE software ABAQUS as well.

7.1.1 Step length

A step study was performed for four different step lengths (0.02, 0.01, 0.00625 and 0.004) mm per step. This was done to ensure that the step lengths were sufficient for the model. In the study it could be seen that for too big steps such as 0.02 mm, the curve for the model deviates from the rest of the curves for the load versus displacement. For the smaller steps 0.004-0.01 mm the behaviour was similar to each other, see Figure 7.1. The peak value got a small decrease the smaller the steps were.

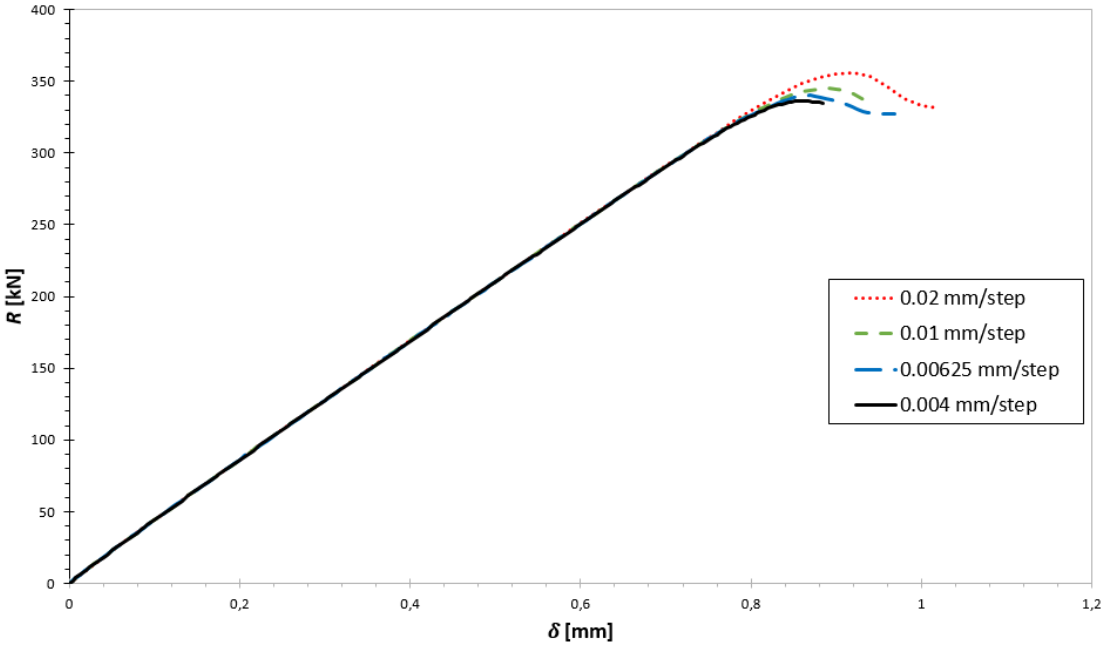

Figure 7.1- Load (R) versus displacement (δ) for different step lengths, cf. Figure 5.3.

For further studies it was believed to be sufficient to use 0.01 mm per step to decrease computational time and still capture a realistic behaviour for the load versus displacement. However when more accurate values for the failure load is needed, smaller steps might be required such as 0.00625 mm.

7.1.2 Tolerance

A tolerance of the energy variation study was performed for four different tolerances (0.005, 0.001, 0.0005 and 0.0001) to determine accurate values. The mesh size was chosen to 10 mm for the more fine mesh part and the step length was set to 0.01 mm.

The study shows similar behaviour for all the curves representing different tolerances for the energy variation. The failure load was seen decreasing for smaller value of the tolerance which was expected. The tolerance of 0.005 does however show a much larger "failure load" than the other tolerances, see Figure 7.2.

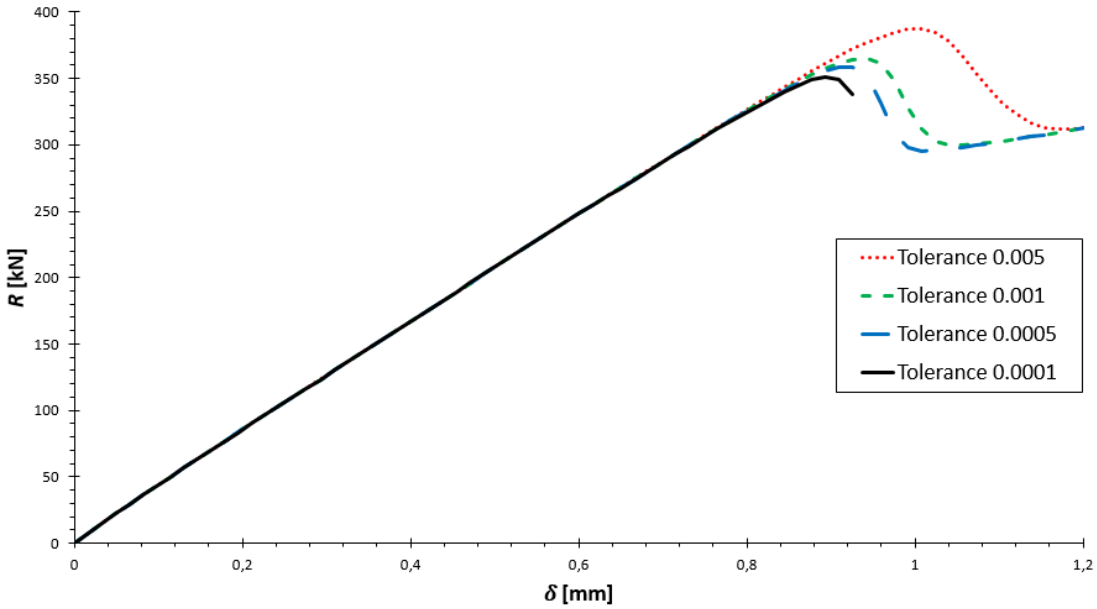

Figure 7.2- Load (R) versus displacement (δ) for different tolerance in energy variation, cf. Figure 5.3.

The tolerance chosen for further analyses was 0.001 since it was believed to capture a similar behaviour for the load versus displacement curve as for the smaller tolerance. The failure load might though be too high but the run time for analysis was decreased with higher value on the tolerance which is an important aspect.

7.1.3 Mesh geometry

In order to optimize the analyses for the models the slabs were modelled with a more dense mesh at the region where the crack pattern was assumed to develop, see Figure 7.3. The crack pattern and the capacity for the concrete cone failure were depending on how this dense part of the mesh was formed and therefore a number of different mesh geometries were analysed in order to determine the best suitable mesh for the dense part. The studies were based on how the crack pattern developed and which capacities the analyses showed. The analyses were performed with a tolerance for the energy variation of 0.001, step length was 0.01 mm per step and the mesh was 15 mm for the more dense part.

Three different types of mesh geometries were analysed. Two types of meshes followed the assumed crack angle (α_{cr}) of 35° between the crack and the concrete, see Figure 7.4. One of the mesh geometries was like a cone, see Figure 7.3a, one with straight lines, Figure 7.3b. The third mesh geometry was like a cylinder and no angle between the crack and the concrete had to be defined, Figure 7.3c.

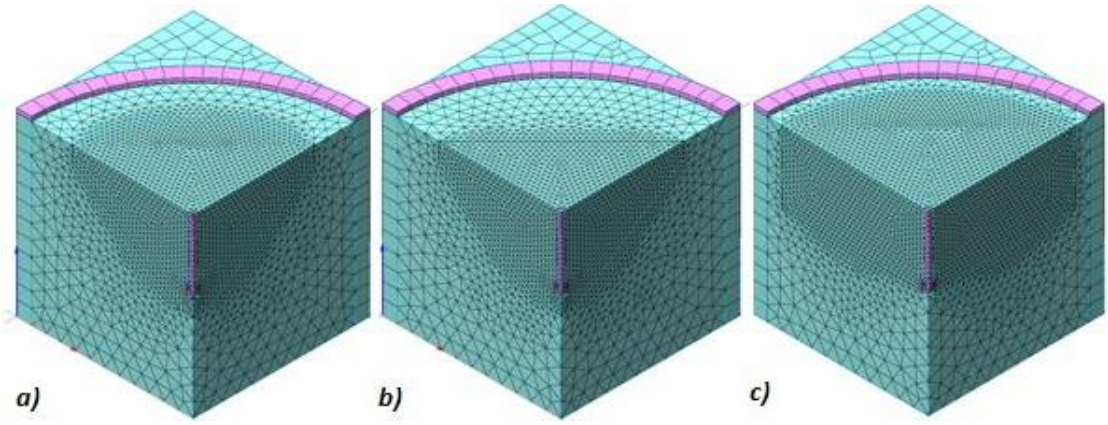

Figure 7.3-Different mesh geometries for dense part a) cone b) Straight lines c) Cylinder

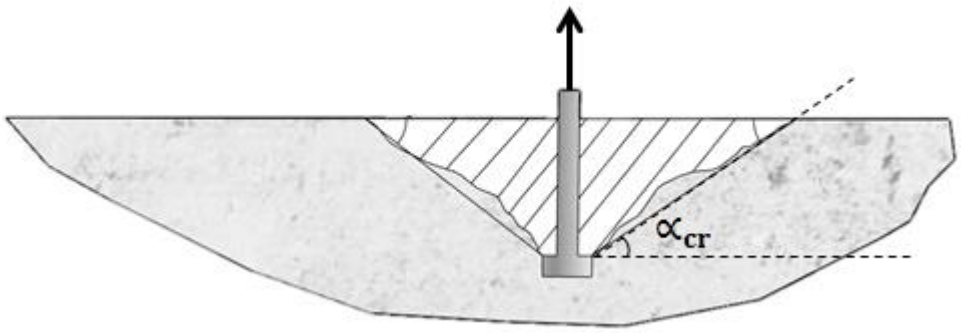

Figure 7.4- Angle between the crack and the concrete.

First the crack pattern were analysed for the different meshes. Similar behaviour for the cracks were achieved for the different mesh geometries and for all mesh geometries the cracks seemed to be localized in one element row as assumed with the crack band width, see Figure 7.5.

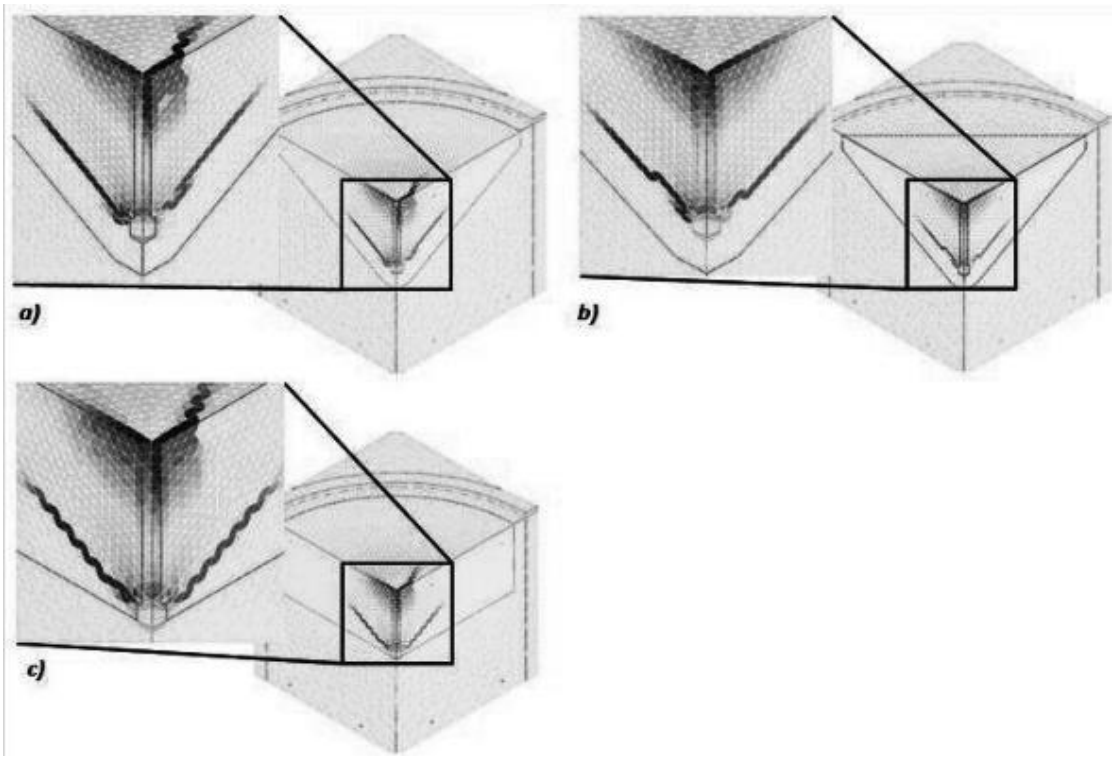

Figure 7.5- Crack pattern for different mesh geometries with same scale a) Cone b) Straight lines c) Cylinder.

The slab was also cut to see how the cracks developed further in to the slab. When analysing these cracks the mesh with straight lines and cylinder shape still localized in one element row see Figure 7.6b and Figure 7.6c. The elements for the cone mesh did however seem to get bigger further into the slabs and the crack pattern did therefore not correspond quite to what was assumed, see Figure 7.6a.

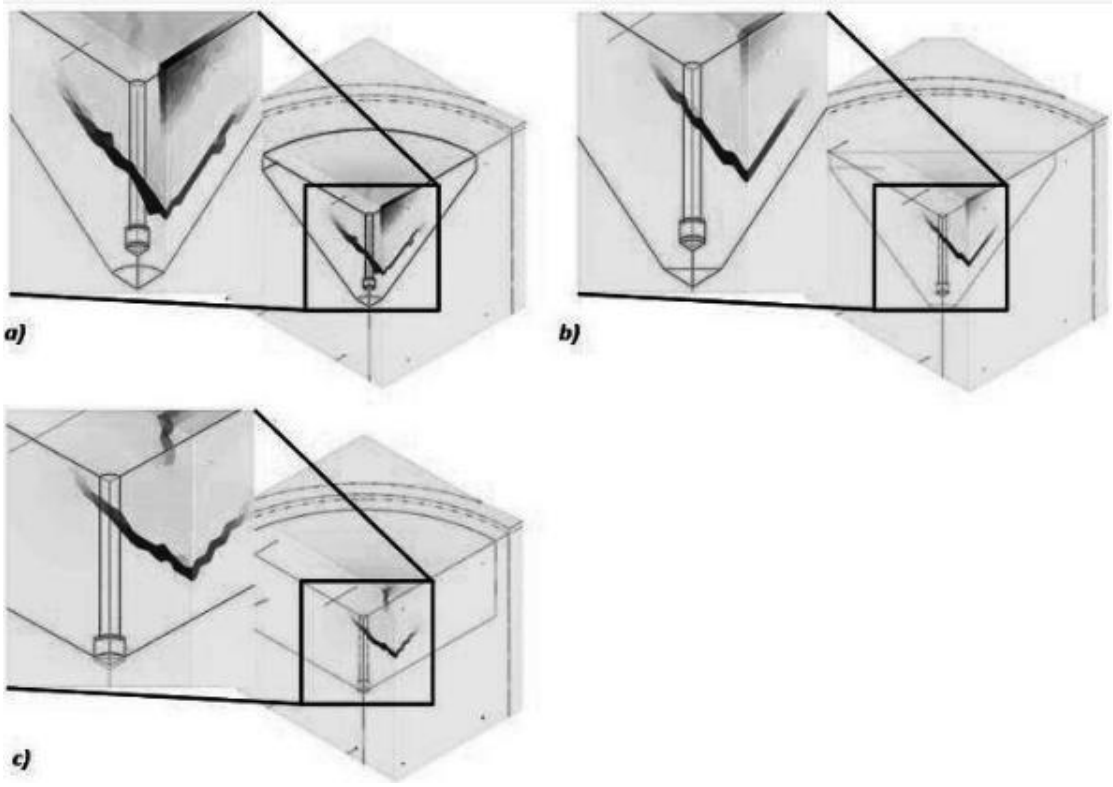

Figure 7.6- Crack pattern further into the slab for different geometries a) Cone b) Straight lines c) Cylinder.

The cone and the cylinder mesh gave similar capacities while the straight lines mesh gave decreased capacity, see Figure 7.7. Both cone and the straight lines mesh had an angle of 35°.

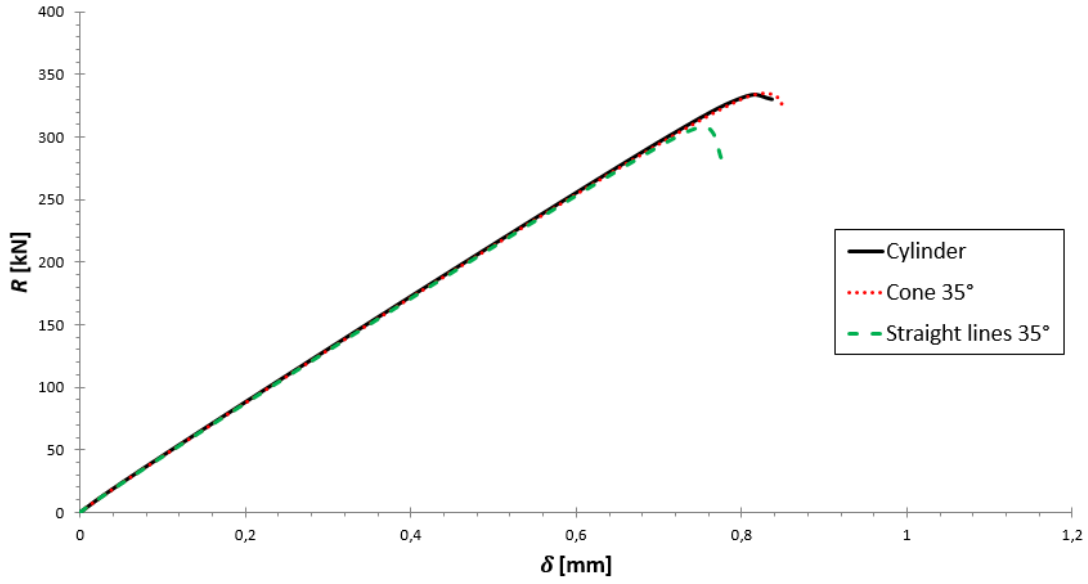

Figure 7.7- Load (R) versus displacement (δ) for different mesh geometries, cf. Figure 5.3.

Based on the crack pattern the straight lines and cylinder mesh was believed to be appropriate mesh geometries for further studies but the cone mesh was not. All the meshes gave however the behaviour of cone failure. For the capacity in the load (*R)*

versus displacement (δ) the straight lines mesh gave smaller capacity compared to the other mesh geometries and higher capacity might be wanted when later continuing the calibrations. The cylinder mesh geometry was believed to be the most reliable mesh geometry and was therefore used for further analyses.

7.1.4 Mesh size

A mesh study was performed for four different mesh sizes (8 mm, 10 mm, 12 mm, and 15 mm) to determine an appropriate mesh size for the more fine part of the mesh. Length of the steps was chosen to 0.01 mm and the tolerance for the energy variation was set to 0.001.

In the mesh study it was seen that, the smaller mesh used the higher the capacity was for the load versus displacement and the curves seems to be converging toward a value, see Figure 7.8. However for the smallest mesh of 8 mm the curve deviates from the rest of the curves and the model seems to have more stiffness than the other meshes.

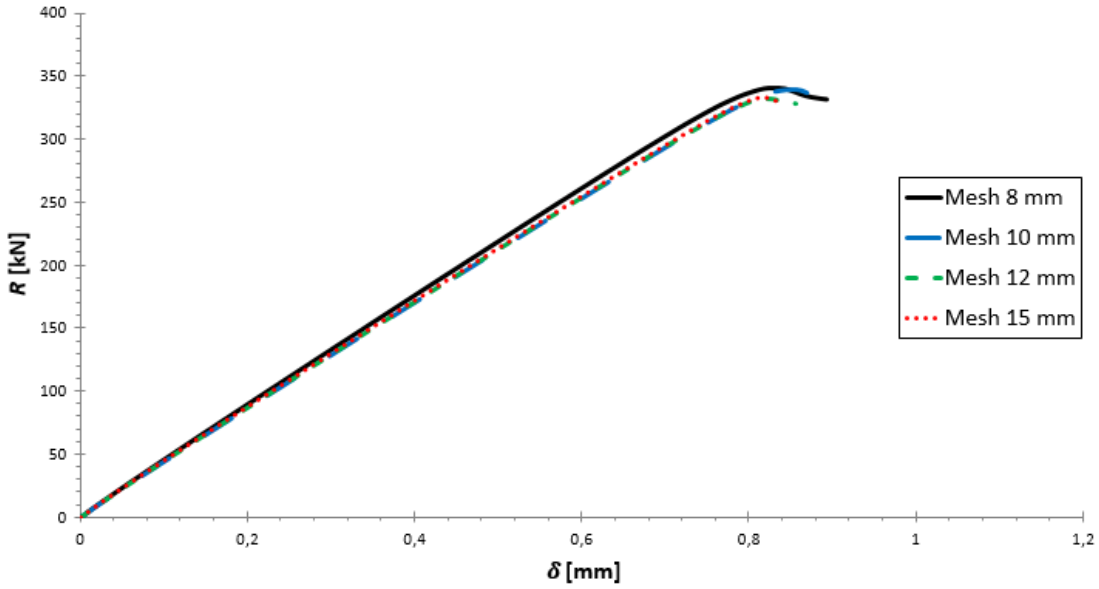

Figure 7.8-Load (R) versus displacement (δ) for different mesh sizes, cf. Figure 5.3.

The crack pattern for the all the different meshes seems appropriate and seems to be localizing in one element row, see Figure 7.9a-d.

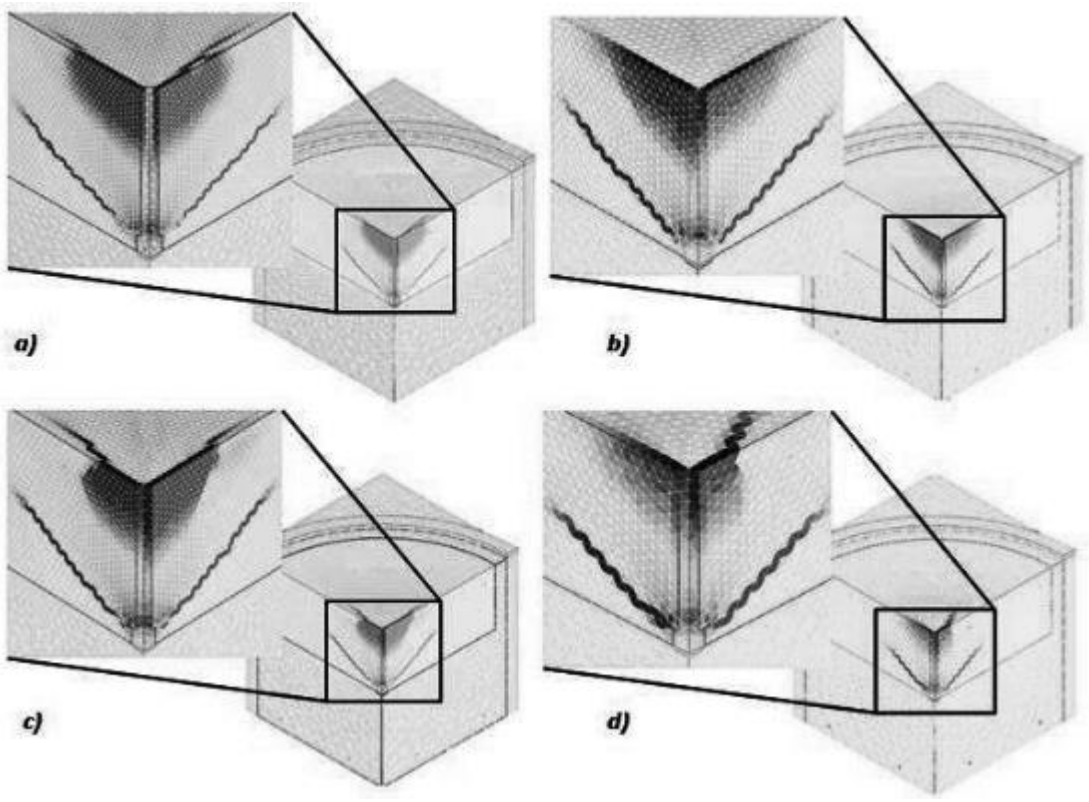

Figure 7.9- Crack pattern for different mesh sizes a) 8 mm *b) 10* mm c) 12 mm *d) 15* mm.

For additional analyses a mesh size of 10 mm for the finer mesh part of the model was used since this mesh size was able to give a good crack pattern and capacity for the model.

7.1.5 Stress distribution

The cylinder mesh was also checked for how the stresses were developed in the model. It was seen that stresses developed in parts where the element was of larger size compared to the fine part of the mesh, see Figure 7.10a. Therefore an analysis where the entire upper part of the slab were meshed with smaller elements and analysed to see if the stresses in the larger elements had an impact on the behaviour and/or the capacity of the model, see Figure 7.10b.

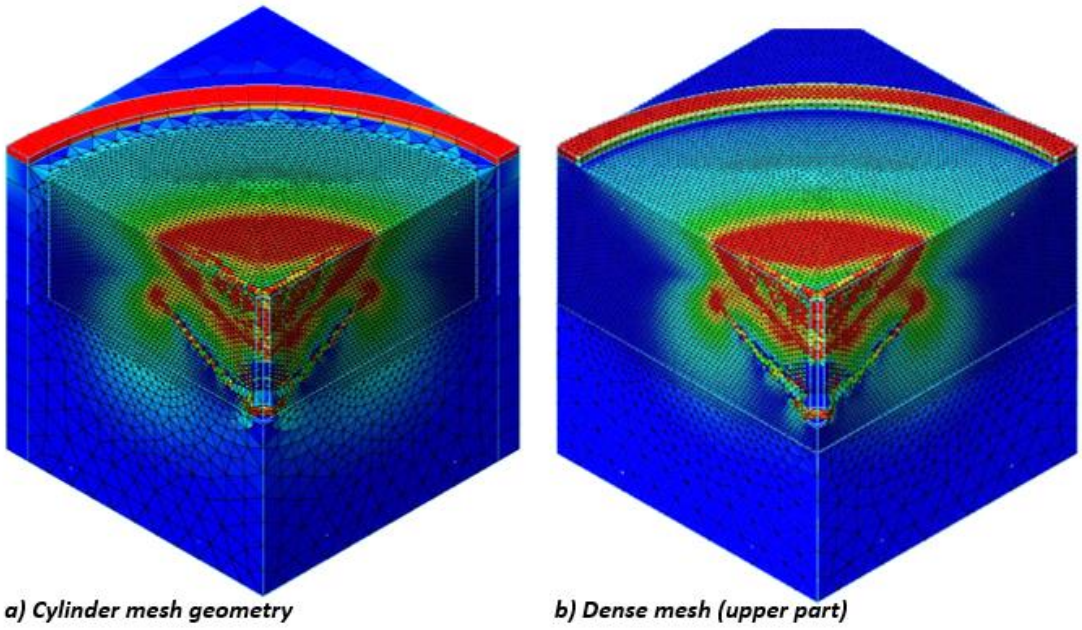

Figure 7.10- Stress distribution for different meshes.

The behaviour for the load versus displacement and the capacity was similar for the two models, see Figure 7.11. A study was also conducted on a smaller slab with dimensions 1.2m×1.2m×0.3m and reinforcement amount of ϕ12 S300 to see that the stresses in the larger elements did not affect this type of slab either. The result was that the model with the cylinder mesh had lower capacity, see Figure 7.12. The stress distribution into the larger elements is believed to be the reason for this and the model with the entire upper part of the slab with small mesh size is believed to reflect the reality more accurate and is therefore used in further analyses.

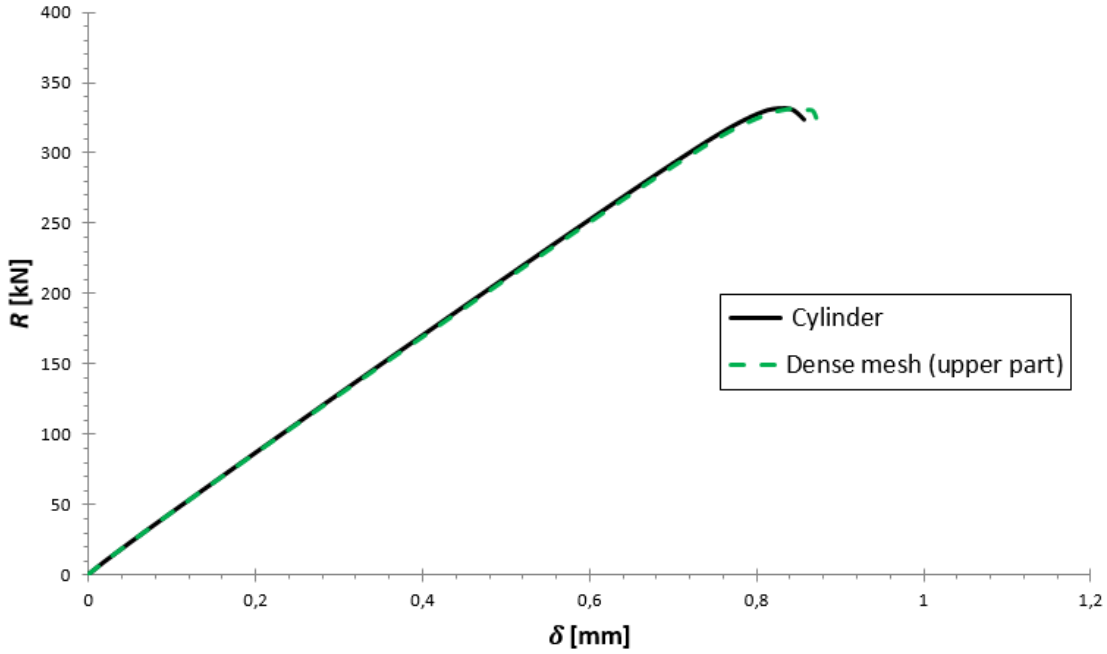

Figure 7.11-Load (R) versus displacement (δ) for different dense meshes for slab 1.2m×1.2m×0.6m φ12 S300, cf. Figure 5.3.

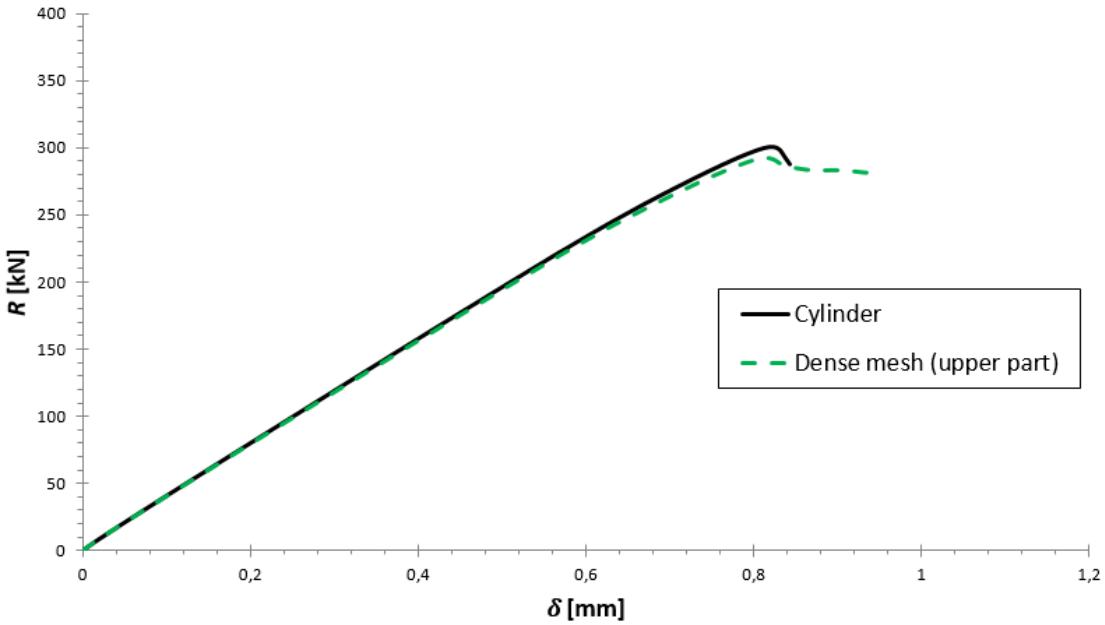

Figure 7.12- Load (R) versus displacement (δ) for different dense meshes for slab 1.2m×1.2m×0.3m φ12 S300, cf. Figure 5.3.

7.1.6 Interaction between reinforcement and concrete

A study is performed where full interaction between reinforcement and concrete was compared to when there was bond slip between concrete and reinforcement. The difference in modeling reinforcement with full interaction and with bond slip was explained in Section 5.1.

The rebars were modelled with solid elements of type C3D8R to represent the reinforcement and the bond slip was modeled using 2D interface elements around the reinforcement. The solid elements for reinforcement were modeled with quadratic cross section but with the same area as for circular cross section Φ12. This was due to better fit the elements around it.

In order to model the reinforcement with bond slip a new mesh was created which was adapted to the rebars, see Figure 7.13.

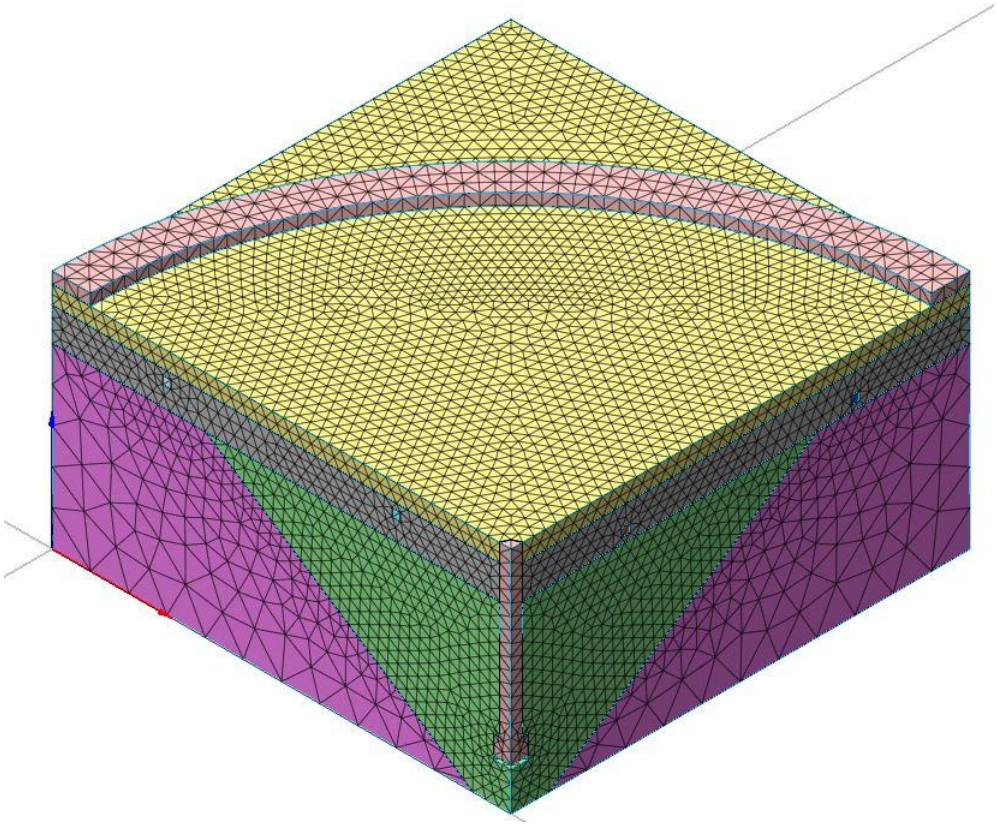

Figure 7.13-Illustration of the new mesh for introduced bond slip interaction.

To make a correct comparison between the two different ways of modeling the reinforcement, the mesh used for modelling bond slip was also used when modelling with embedded reinforcement. This was because different mesh geometries have an impact on the capacity of the anchor as shown in the mesh geometry study.

The bond slip which was introduced was of cubic law by (Dörr, 1980). The input parameters are the stiffness in normal and tangential direction, a constant *C* and Shear slip. The stiffness was set to an average of steel and concrete as suggested in (TNO DIANA BV, 2015) the constant *C* is recommended to be equal to the mean tensile capacity for the concrete (TNO DIANA BV, 2015) and the shear slip was also given as a recommended value from (TNO DIANA BV, 2015). For all values see Table 7.1.

Table 7.1-Parameters for bond slip by (Dörr, 1980).

	Normal stiffness [Mpa]	Tagential Stiffness [Mpa]	Constant *C*	Shear slip [m]
Bond slip Dörr	1,2E+08	1,2E+07	2,6E+06	6,0E-05

Three graphs are shown in Figure 7.14 for three different analyses. One represent bond slip, another represent embedded reinforcement but with the same mesh as for bond slip and the third represent embedded reinforcement with the regular mesh. The capacity was decreased when bond slip was introduced and the graph was also slightly more non-linear compared to the analyses with embedded reinforcement, see Figure 7.14.

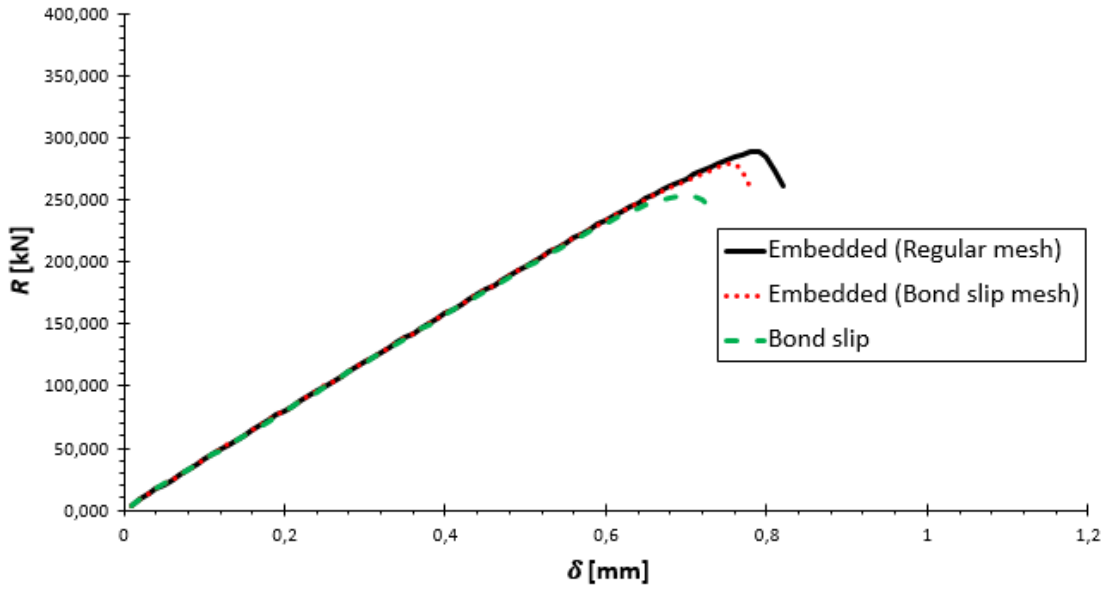

Figure 7.14- Load (R) vs Displacement (δ) for different interaction between reinforcement and concrete cf. Figure 5.3.

Interaction with embedded reinforcement was used for further analyses due to small changes in the behavior, more computational time and more complex mesh that were required for the model with bond slip interaction.

7.1.7 Summary of parameter studies

When continuing with the analyses in DIANA for the calibration and also further analyses of all different slabs, the step length, tolerance of energy variation, mesh size and chosen interaction between concrete and reinforcement is given in Table 7.2.

Table 7.2- Parameters later used for analyses in DIANA.

Step Length	Tolerance (Energy Variation)	Mesh Geometry	Mesh Size	Interaction Reinforcement-Concrete
0.00625 mm	0.001	Dense mesh (Upper part)	10 mm	Embedded

7.2 Model calibration

The calibration against the tests performed by (Elfgren & Nilsson, 2009) has been carried out in DIANA. The slab type, reinforcement amount etc. for the test which was calibrated against is described in Section 5.1.

All the models were able to get behaviour for the cracks (strains) which agreed well with what is expected for a concrete cone failure. However as assumed and discussed in Section 5.2.2 the models did not converge since there was compression failure before a fully developed concrete cone was able to grow.

The compression failure was highly dependent on which element size that was used, see Figure 7.15. For this reason localization of compression was considered to gain strength for the compressive behaviour. Lateral confinement was also introduced to gain strength.

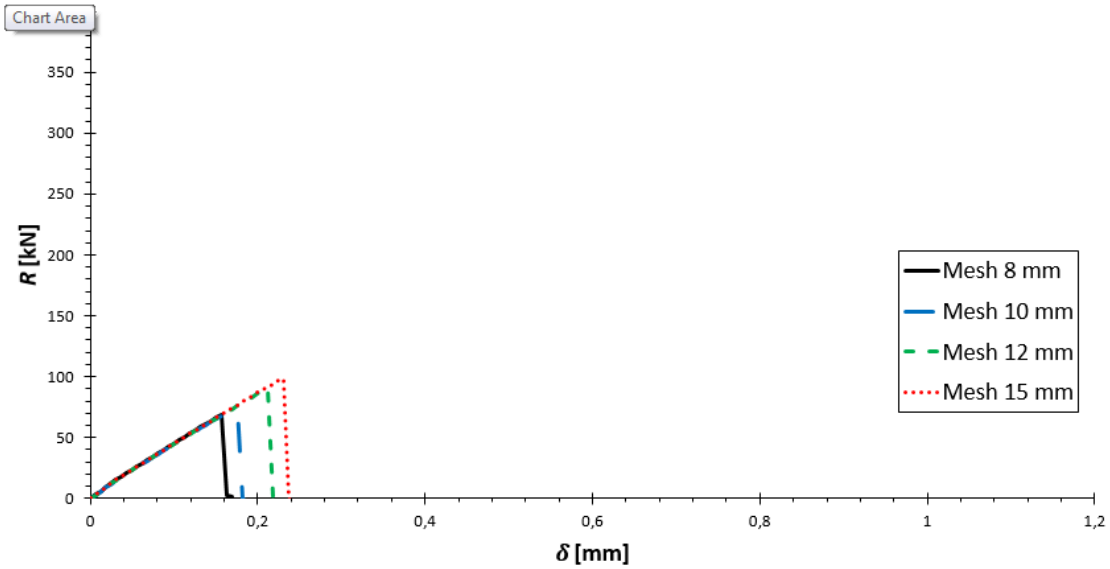

Figure 7.15- Compressive failure for different element size, given by slab 1.2m×1.2m×0.6m ϕ12 S300, cf. Figure 5.3.

Localisation of compression was considered by introducing a scaling factor of 0.4 m. This corresponds to that the compressive failure is localized in the elements right above the head of the anchor given by Equation (5.4). This gave an increase in capacity but not sufficient. The introducing of lateral confinement also gave increased capacity but also not enough, this was also the case for a combination of them both, see Figure 7.16.

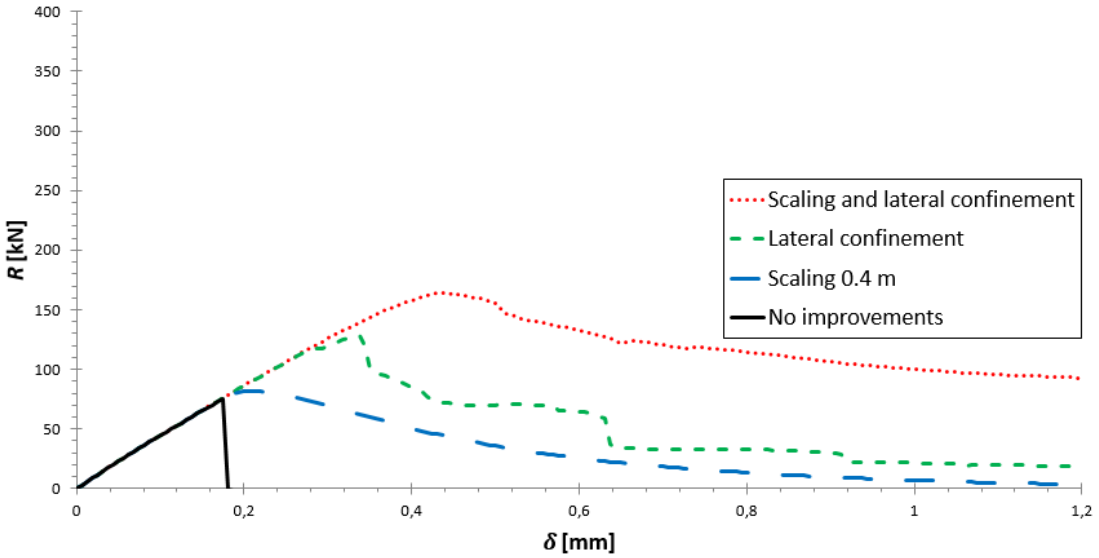

Figure 7.16- Compressive failure with different improvements for the compressive strength given by slab 1.2m×1.2m×0.6m ϕ12 S300, cf. Figure 5.3.

A model was created where the elements around the head was set to elastic in compression to work around this problem. This was however the same result as setting all elements to elastic in compression and the compressive failure was thereby ignored. This made the concrete cone fully develop, and the failure was then governed by the tensile strength and fracture energy of the concrete, see Figure 7.17.

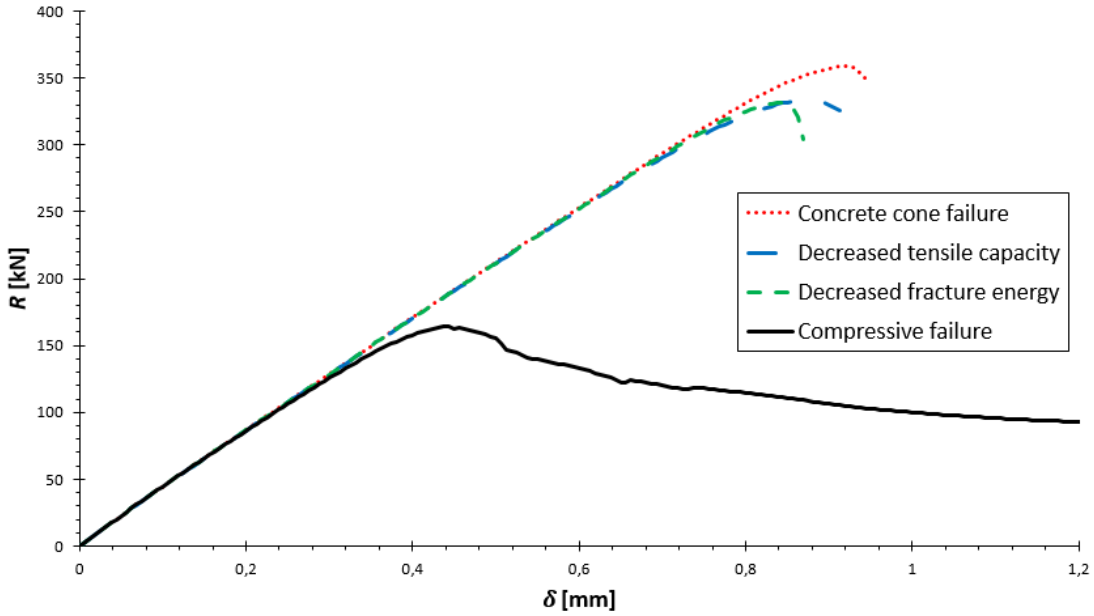

Figure 7.17-Curves indicating compressive failure and tensile failure, given by slab 1.2m×1.2m×0.6m ϕ12 S300, cf. Figure 5.3.

The calibration was then performed for the slabs that were presented in Section 5.1 to see that the analyses had similar failure load and linear behaviour for the curves as the performed tests by (Elfgren & Nilsson, 2009).

The load versus displacement curves for the analyses and all the tests used for the calibrations for each slab is presented in Figure 7.18-7.20. The load versus displacement curves given by the analyses has similar behaviour as the test at low values. However at failure load the displacement was much larger for the tests compared to the analyses. This was equivalent for all the slabs that calibrations have been carried out for.

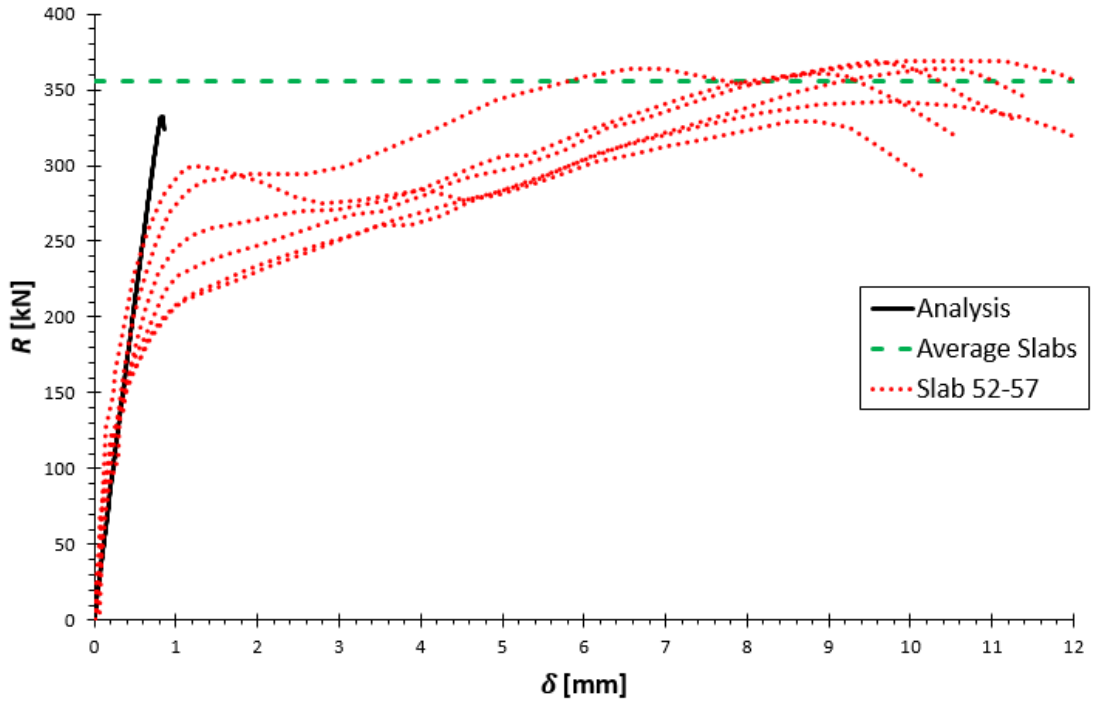

Figure 7.18- Load (R) vs Displacement (δ) calibration for slab 1.2m×1.2m×0.6m ϕ12 S300, cf. Figure 5.3.

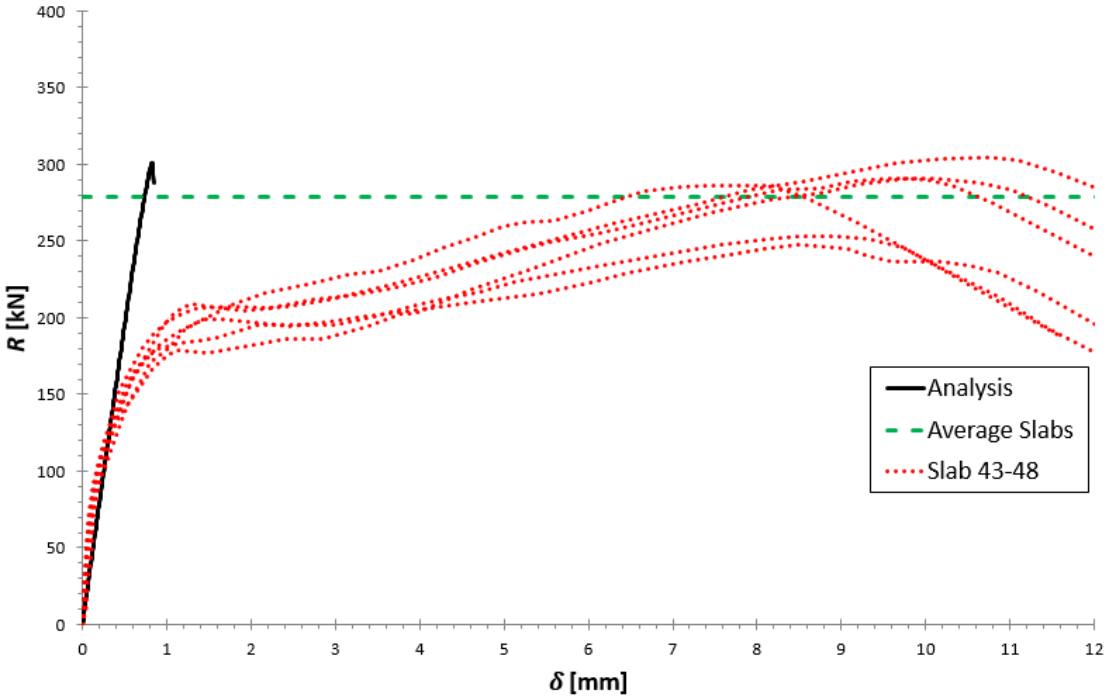

Figure 7.19- Load (R) vs Displacement (δ) calibration for slab 1.2m×1.2m×0.3m ϕ12 S300, cf. Figure 5.3.

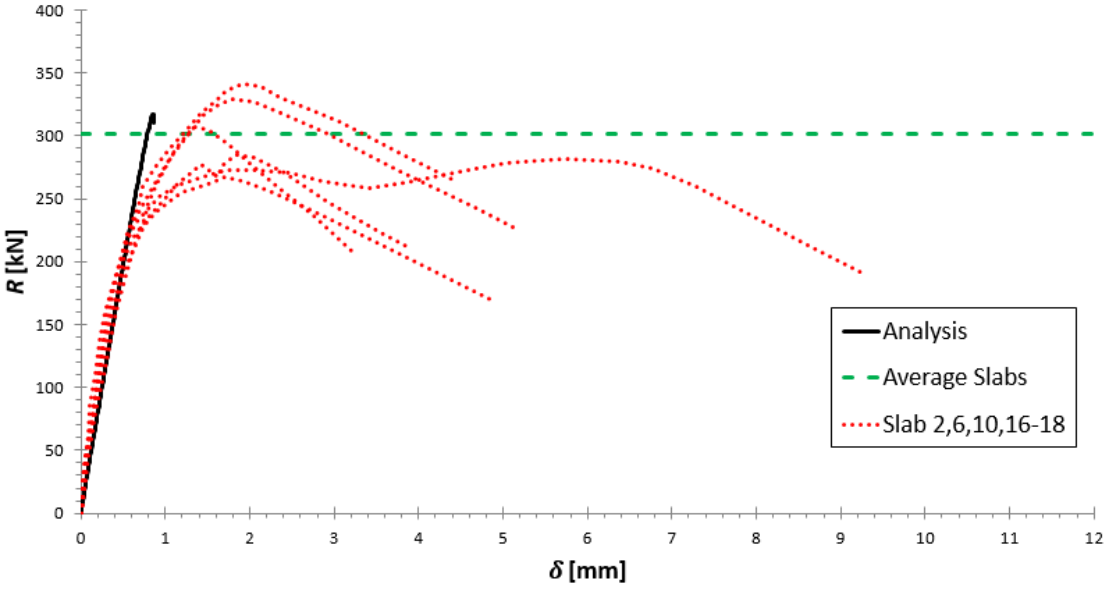

Figure 7.20- Load (R) vs Displacement (δ) calibration for slab 1.2m×1.2m×0.3m ϕ16 S100, cf. Figure 5.3.

For all the different slabs that were used for calibration the capacity does not coincided completely with the average values given from the tests but they were still within the range that the tests by (Elfgren & Nilsson, 2009) had shown, see Table 7.3.

Table 7.3- Capacity for calibration of the different slabs.

No.	*H* [m]	Top reinforcement	$N_{Test\ Range}$ [kN]	$N_{Test\ Average}$ [kN]	$N_{Analysis}$ [kN]	$N_{Analysis}/N_{Test\ Average}$
1	0,6	ϕ12 S300	331-371	357	332	0,930
2	0,3	ϕ12 S300	249-306	280	292	1,043
3	0,3	φ16 S100	268-341	302	317	1,050

7.3 Single anchor in tension

7.3.1 CEN/TS

There is code of praxis that takes concrete cone failure into account as mentioned in Section 3. The only factor that needed to be considered in Equation (3.3) for calculations on single anchors was $N^{o}_{Rk,c}$, the other factor could be set to one. The values which are calculated are characteristic and are on the safe side which makes it hard to compare against the results from the analyses therefore a mean value for this code was better suited to have as a comparison. To get a mean capacity for the failure mode the k_{ucr}-parameter was changed from 11.9 to 15.5 according to (Eligehausen, et al., 2006). The Equation (7.1) for the mean capacity was higher and probably closer to the results presented by the analyses.

$$N_{Rk,c} = k_{ucr} \times \sqrt{f_{ck,cube}} \times h_{ef}^{1,5} =$$

$$= 15.5 \frac{N^{0.5}}{mm^{0.5}} \times \sqrt{30MPa} \times (220mm)^{1,5} = 277kN \qquad (7.1)$$

7.3.2 Numerical analyses

The results for the analyses performed in DIANA are presented in five different diagrams where the capacity of the concrete cone failure was compared for different slab thickness and with different amount of reinforcement, see Figure 7.21-7.25. The diagrams are also complimented with figures of the crack pattern which is given by the first principle strain for the different analyses, see Figure 7.26-7.29. These figures were taken the step before failure where δ was around 0.8-0.9 mm. Number of element and computational time for the analyses of different thicknesses of the slab is presented in Table 7.4.

Table 7.4- No. of elements and computational time for the analyses performed on different thicknesses for a single anchor in DIANA.

Anchor	*H* [m]	No. Of Elements	Computational Time
Single	0.3	424419	5-7 hours
Single	0.6	477269	6-8 hours

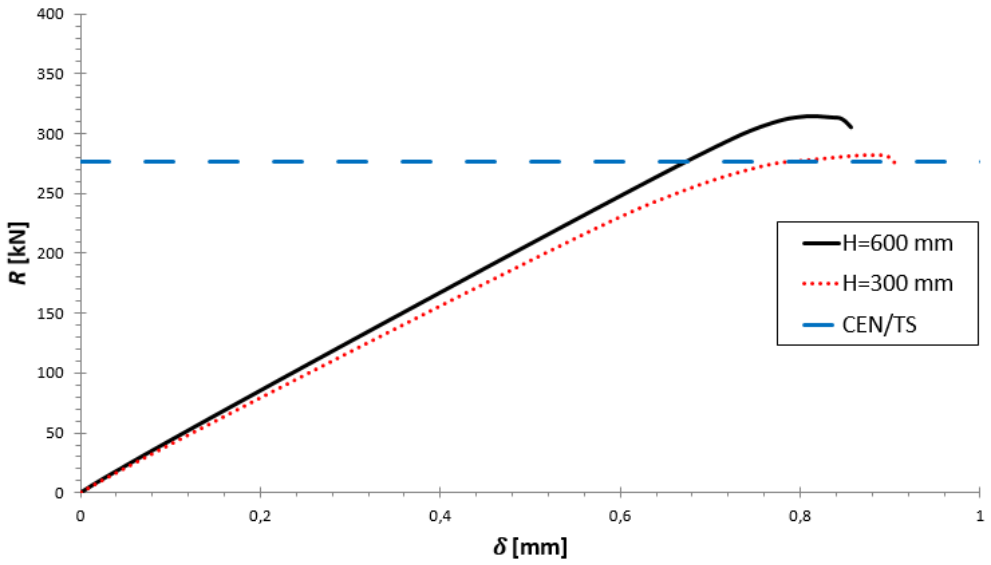

Figure 7.21- Load (R) vs Displacement (δ) for un-reinforced slabs, cf. Figure 5.3.

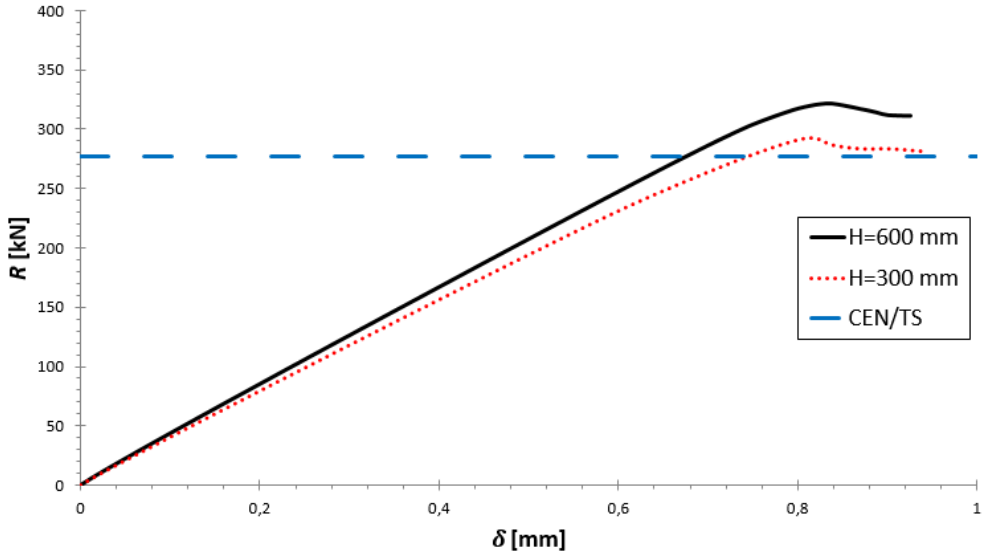

Figure 7.22- Load (R) vs Displacement (δ) for slabs with φ12 S300, cf. Figure 5.3.

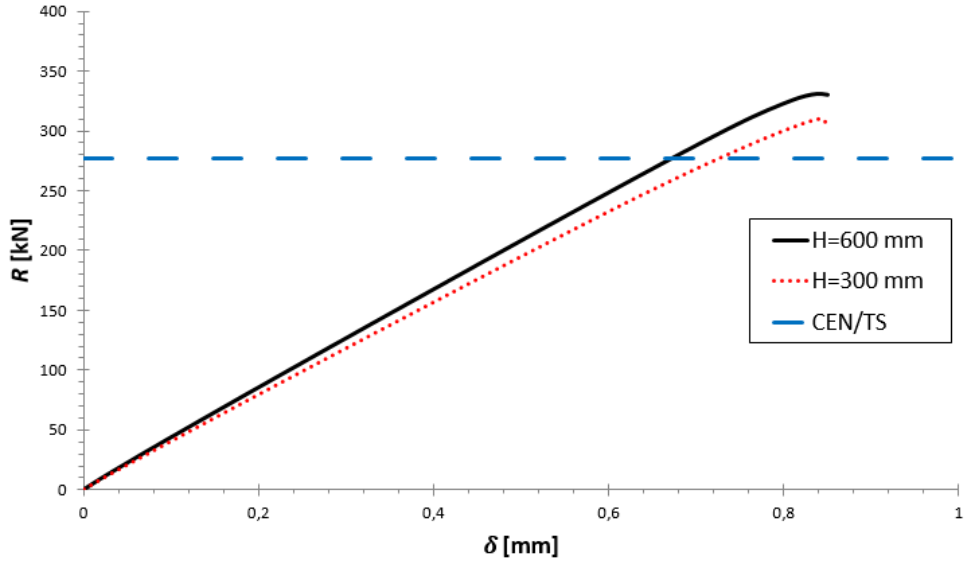

Figure 7.23- Load (R) vs Displacement (δ) for slabs with φ16 S100, cf. Figure 5.3.

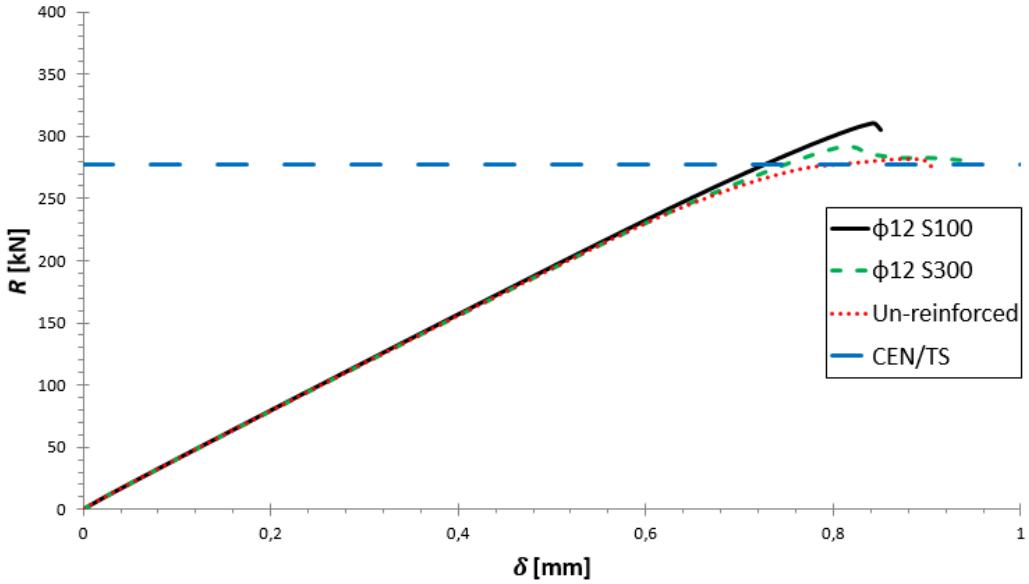

Figure 7.24- Load (R) vs Displacement (δ) for slabs with thickness H=300 mm, cf. Figure 5.3.

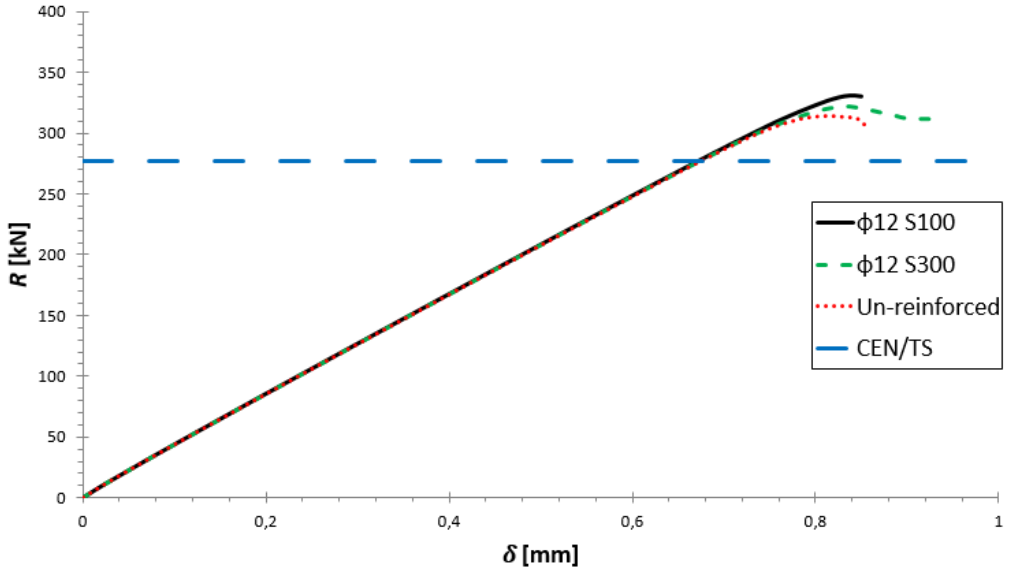

Figure 7.25- Load (R) vs Displacement (δ) for slabs with thickness H=600 mm, cf. Figure 5.3.

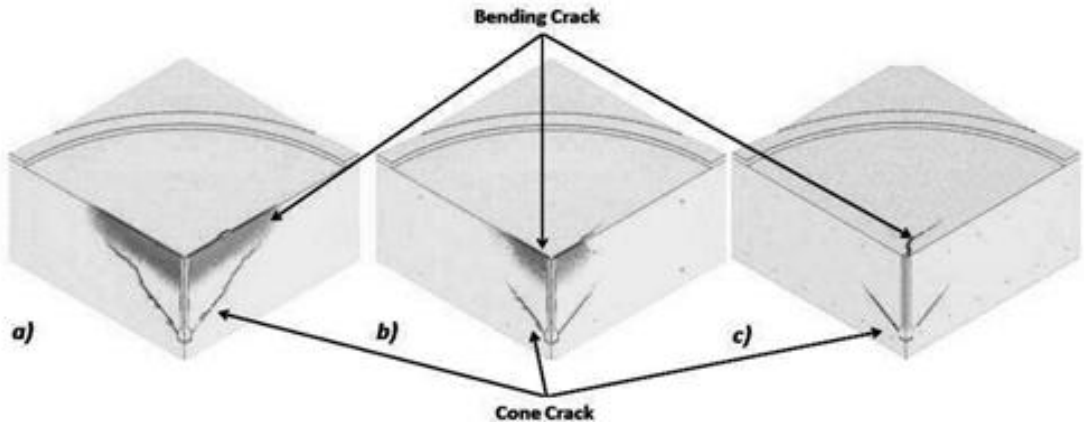

Figure 7.26- Crack pattern for single anchor, H=300 mm

a) Un-reinforced at δ=0.875 mm, see *Figure 7.24 b) φ12 S300 at δ=0.813* mm, see *Figure 7.24 c) φ16 S100 at δ=0.844* mm, see *Figure 7.24*

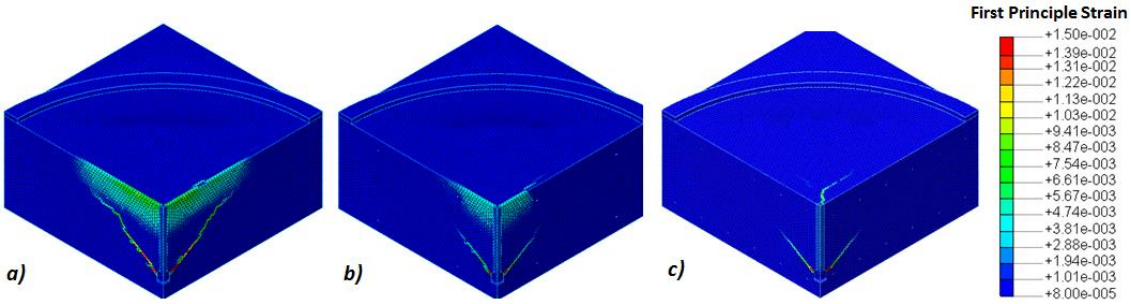

Figure 7.27- Crack pattern for single anchor with indication of size of strains, H=300 mm a) Un-reinforced at δ=0.875 mm, see *Figure 7.24 b) φ12 S300 at δ=0.813* mm, see *Figure 7.24 c) φ16 S100 at δ=0.844* mm, see *Figure 7.24.*

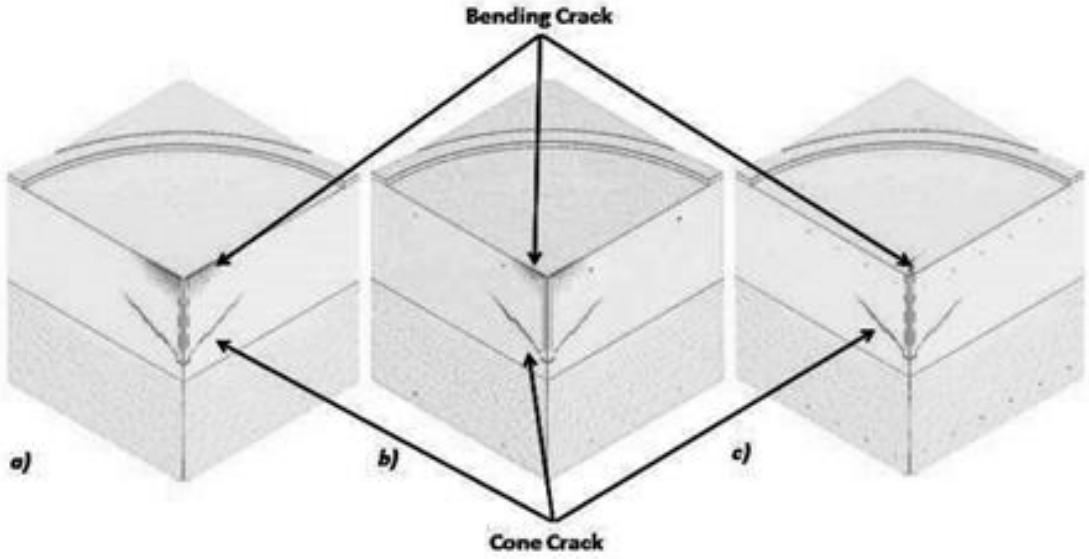

Figure 7.28- Crack pattern for single anchor, H=600 mm a) Un-reinforced at δ=0.813 mm, see Figure 7.25 b) φ12 S300 at δ=0.831 mm, see Figure 7.25 c) φ16 S100 at δ=0.838 mm, see Figure 7.25

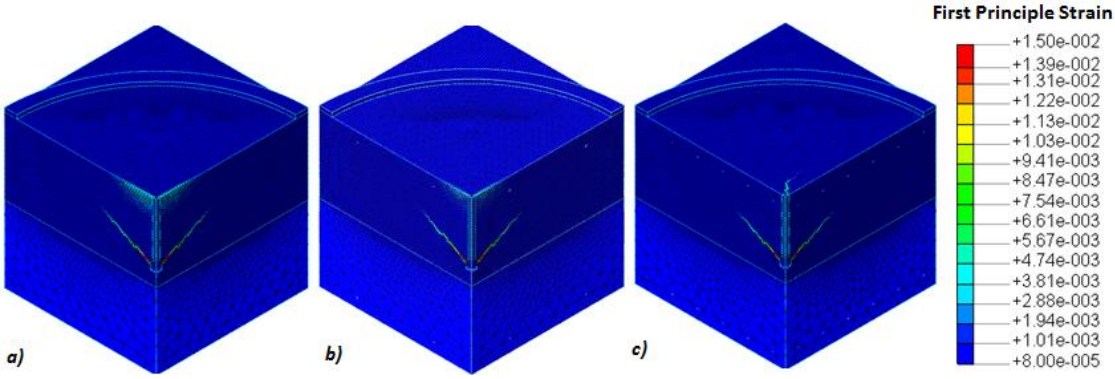

Figure 7.29- Crack pattern for single anchor with indication of size of strains for H=600 mm a) Un-reinforced at δ=0.813 mm, *see Figure 7.25 b) φ12 S300 at δ=0.831* mm, *see Figure 7.25 c) φ16 S100 at δ=0.838* mm, see *Figure 7.25*.

The maximal capacity for the different analyses and comparison with the code of praxis are presented in Table 7.5.

Table 7.5- Capacity for single anchor analyses and comparison with (CEN/TS 1992-4-2, 2009).

No.	H [m]	Top reinforcement	N_{Single}[kN]	$N_{Single}/N_{CEN/TS}$
1	0,6	-	314	1,134
2	0,6	ϕ12 S300	322	1,162
3	0,6	φ16 S100	331	1,195
4	0,3	-	282	1,018
5	0,3	ϕ12 S300	292	1,054
6	0,3	ϕ16 S100	310	1,119

7.3.3 Splitting failure

The test from Luleå University showed that un-reinforced slabs with 300 mm in thickness had a brittle failure caused by splitting. The capacity showed in the test was around 200 kN.

Checks were made to see that the analyses should not have gotten splitting failure instead of concrete cone failure. This was done by using equations presented in Section 3.6. Checks were first made on un-reinforced slabs calculating the resisting bending moment (M_{Rd}) using Equation (3.12) and a resisting force (P_{Rd}) was then calculated from Equation (3.9). For the thinner slab with dimensions (1.2m×1.2m×0.3m) without reinforcement the splitting capacity was 246 kN according to Equation (7.2). For the thicker slab with dimensions (1.2m×1.2m×0.6m) without reinforcement the splitting capacity was 980 kN according to Equation (7.3).

$$P_{Rd300} = \frac{2\times\pi\times M_{Rdu300}}{b} = \frac{2\times\pi\times 45\ kNm}{1.15\ m} = 246\ kN \qquad (7.2)$$

$$P_{Rd600} = \frac{2\times\pi\times M_{Rdu600}}{b} = \frac{2\times\pi\times 179\ kNm}{1.15\ m} = 980\ kN \qquad (7.3)$$

The splitting failure for the thinner slab was lower than the determined cone failure from analysis given in Equation (7.4), does further checks were needed for the analysis of same thickness but with reinforcement. The splitting capacity for the thicker slabs was however higher than the determined cone break out failure given from analysis given in Equation (7.5), no further checks were needed for this slab thickness.

$$P_{Rd300} = 246\ kN < N_{single}(4) = 282\ kN \qquad (7.4)$$

$$P_{Rd600} = 980\ kN > N_{single}(1) = 314\ kN \qquad (7.5)$$

To determine the bending moment capacity for a reinforced slab Equation (3.13) was used and the resisting force (P_{Rd}) was calculated to 350kN for the thinner slab with dimensions (1.2m×1.2m×0.3m) and reinforcement φ12 S300 in Equation (7.6).

$$P_{Rd300} = \frac{2\times\pi\times M_{Rd300}}{b} = \frac{2\times\pi\times 64\ kNm}{1.15\ m} = 350\ kN \qquad (7.6)$$

This capacity is larger than the cone break out failure determined in the analysis, see Equation (7.7), does no further checks were needed for slabs of 300 mm.

$$P_{Rd300} = 350\ kN > N_{single}(5) = 292\ kN \qquad (7.7)$$

Calculations for M_{Rdu} for un-reinforced and M_{Rd} for reinforced slabs are presented in Appendix A.

7.4 Group of anchors in tension

The same material parameters, configurations and assumptions were used for a group of anchors as for a single anchor to clearly see the difference between these anchor arrangements. The dimensions for the group of anchors are shown in Figure 7.30. Where there are 4 anchors with the same embedment depth and diameter as the single anchor. The embedment depth for a group of anchors is counted from the top of the steel plate to the anchor head.

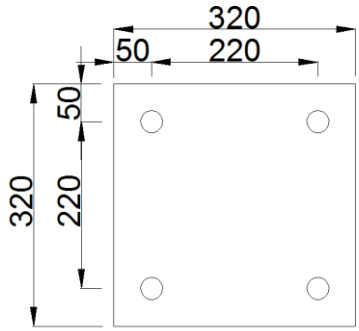

Figure 7.30- Geometry for anchor plate and spacing between anchors.

7.4.1 CEN/TS

The code of praxis that takes concrete cone failure into account as explained in Section 3 was used for group of anchors in the same way as single anchor but the term $A_{c,N}/A^0_{c,N}$ was introduced in Equation (3.3) to consider the anchors interference on each other's cones. The other factors were kept equal to one. Same as for single anchor the values which are calculated are characteristic and are on the safe side which makes it hard to compare against the results from the analyses therefore a mean value for this code was also used for group of anchors and the k_{ucr}-parameter was set to 15.5 according to (Eligehausen, et al., 2006). The Equation (7.8) gives the mean capacity according code of praxis for a group of anchors.

$$N_{Rk,c} = k_{ucr} \cdot \sqrt{f_{ck,cube}} \cdot h_{ef}^{1,5} \cdot \frac{A_{c,N}}{A^0_{c,N}} =$$

$$= 15.5 \frac{N^{0.5}}{mm^{0.5}} \cdot \sqrt{30MPa} \cdot 220mm^{1,5} \cdot \frac{0.77m^2}{0.44m^2} = 493kN \qquad (7.8)$$

For calculations see Appendix B.

7.4.2 Numerical analyses

The results for a group of anchor performed in DIANA are presented in five different diagrams, same as for single anchor, where the capacity of the concrete cone failure was compared for different slab thickness and with different amount of reinforcement, see Figure 7.31-7.35. The diagrams are also complimented with figures of the crack pattern which is given by the first principle strain for the different analyses, see Figure 7.36-7.39. These figures were taken at the end of simulation where δ was around 0.3-

0.6 mm. Number of element and computational time for the analyses of different thicknesses of the slab is presented in Table 7.6.

Table 7.6- No. of elements and computational time for the analyses performed on different thicknesses for a group of anchors in DIANA.

Anchor	*H* [m]	No. Of Elements	Computational Time
Group	0.3	408184	6-11 hours
Group	0.6	470946	5-6 hours

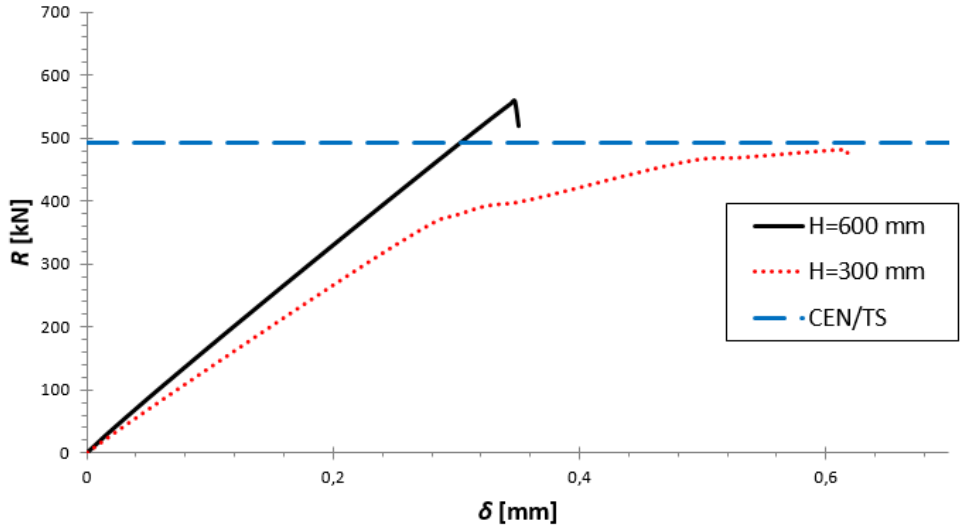

Figure 7.31- Load (R) vs Displacement (δ) for un-reinforced slabs and group of anchors, cf. Figure 5.4.

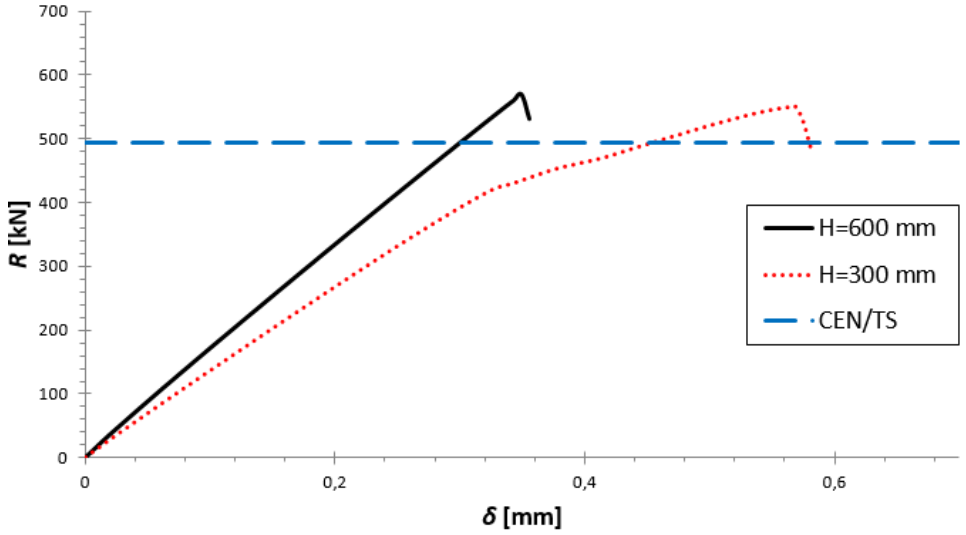

Figure 7.32- Load (R) vs Displacement (δ) for slabs with reinforcement amount φ12 S300 and group of anchors, cf. Figure 5.4.

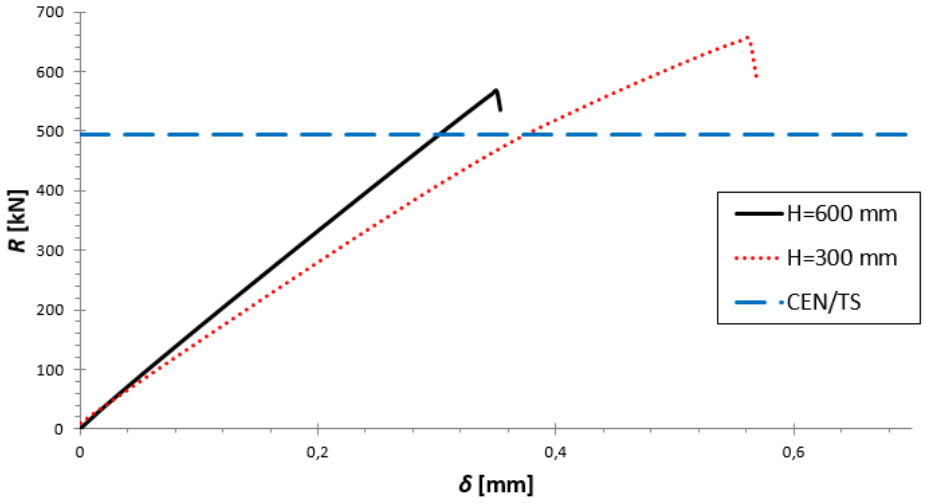

Figure 7.33- Load (R) vs Displacement (δ) for slabs with reinforcement amount φ16 S100 and group of anchors, cf. Figure 5.4.

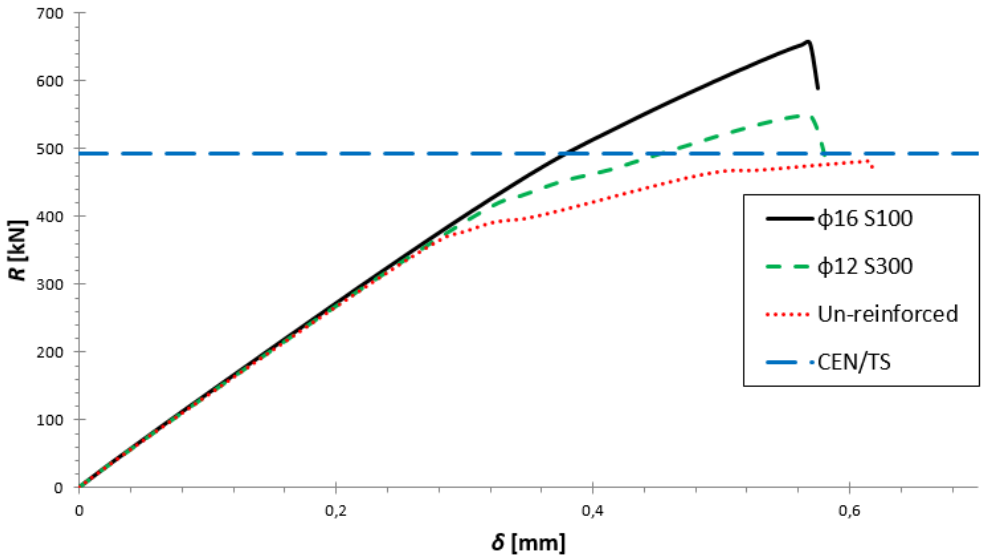

Figure 7.34- Load (R) vs Displacement (δ) for slabs with thickness H=300 mm and group of anchors, cf. Figure 5.4.

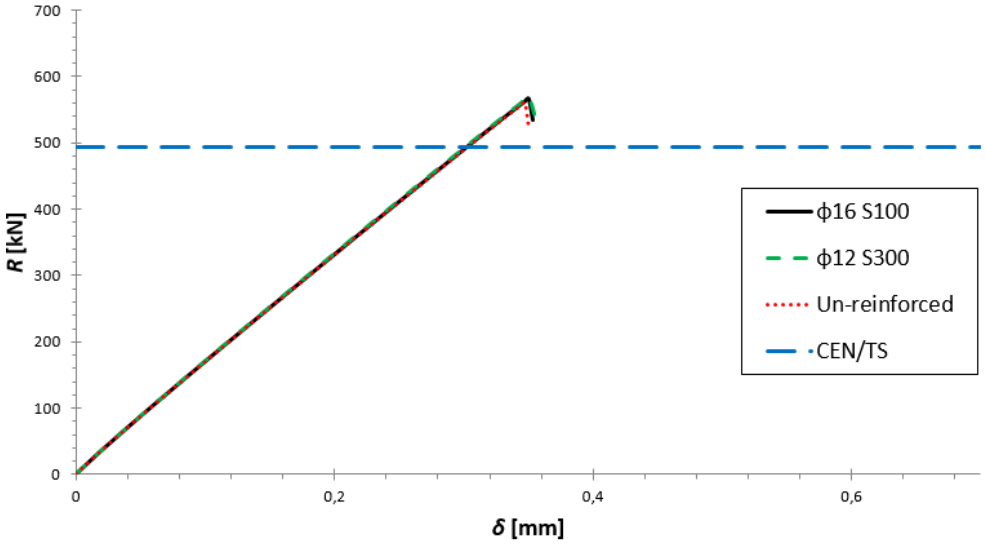

Figure 7.35- Load (R) vs Displacement (δ) for slabs with thickness H=600 mm and group of anchors, cf. Figure 5.4.

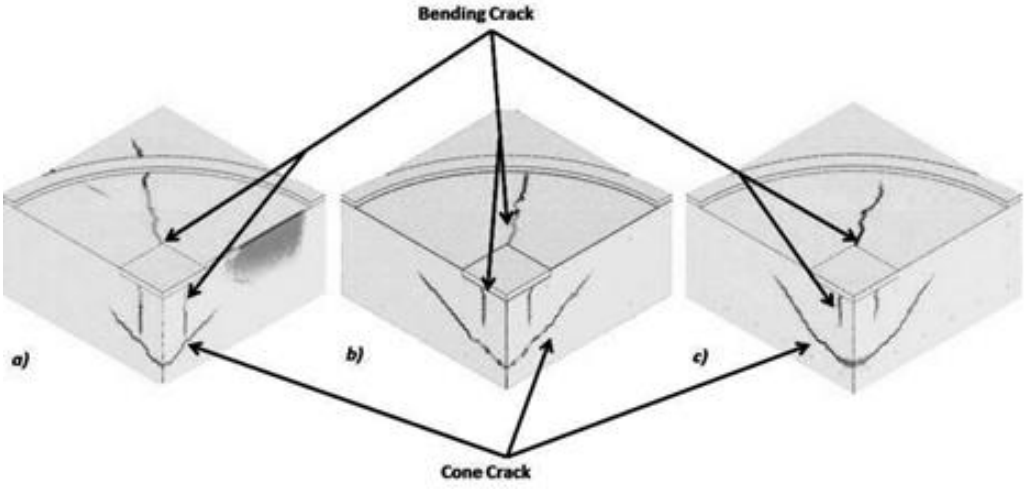

Figure 7.36- Crack pattern for group of anchors, H=300 mm a)

Un-reinforced at δ=0.619 mm, see Figure 7.34 b) φ12 S300 at δ=0.581 mm, see Figure 7.34 c) φ16 S100 at δ=0.575 mm, see Figure 7.34

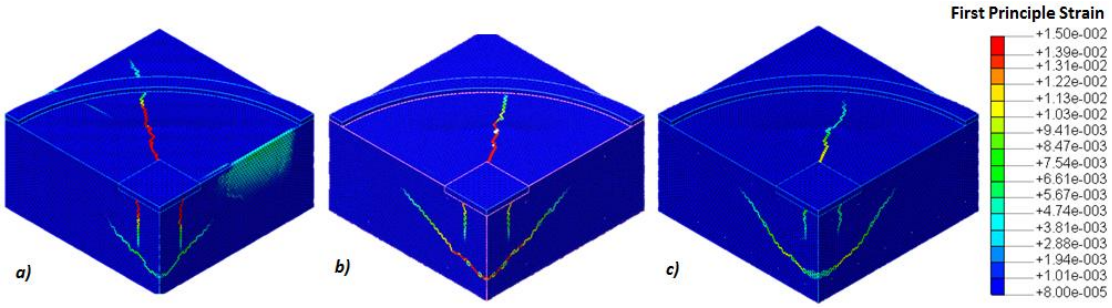

Figure 7.37- Crack pattern indicating size of strains for group of anchors, H=300 mm a) Un-reinforced at δ=0.619 mm, see Figure 7.34 b) φ12 S300 at δ=0.581 mm, see Figure 7.34 c) φ16 S100 at δ=0.575 mm, see Figure 7.34

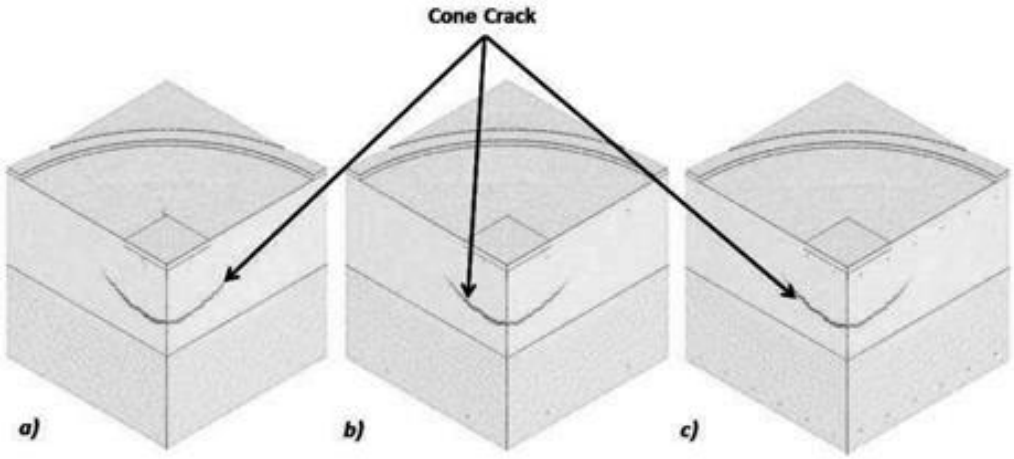

Figure 7.38- Crack pattern for group of anchors, H=600 mm a) Un-reinforced at δ=0.350 mm, see Figure 7.35 b) φ12 S300 at δ=0.356 mm, see Figure 7.35 c) φ16 S100 at δ=0.353 mm, see Figure 7.35

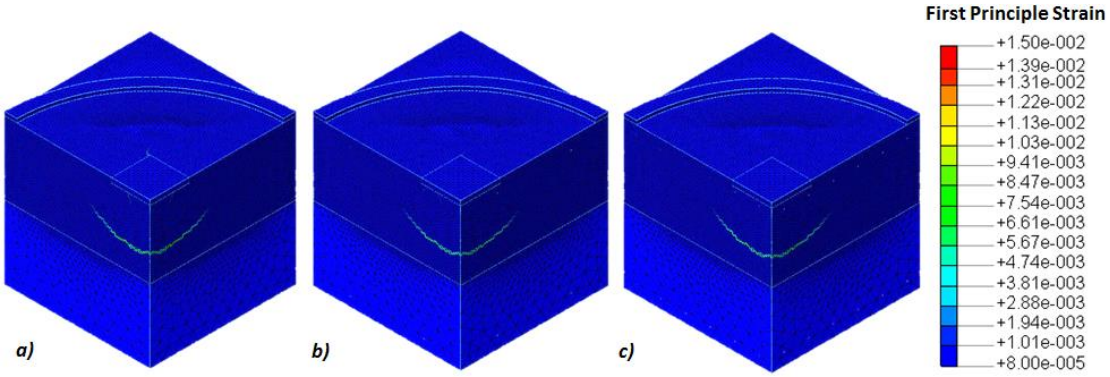

Figure 7.39- Crack pattern indicating size of strains for group of anchors, H= 600 mm a) Un-reinforced at δ=0.350 mm, see Figure 7.35 b) φ12 S300 at δ=0.356 mm, see Figure 7.35 c) φ16 S100 at δ=0.353 mm, see Figure 7.35

The maximal capacity for the different analyses for a group of anchors and comparison with the code of praxis is presented in Table 7.7.

Table 7.7- Capacity for group of anchors analyses and comparison with (CEN/TS 1992-4-2, 2009).

No.	*H* [m]	Top reinforcement	N_{Group}[kN]	$N_{Group}/N_{CEN/TS}$
7	0,6	-	560	1,136
8	0,6	ϕ12 S300	570	1,156
9	0,6	φ16 S100	567	1,150
10	0,3	-	481	0,976
11	0,3	ϕ12 S300	550	1,116
12	0,3	ϕ16 S100	656	1,331

7.4.3 Splitting failure

To check the slabs against splitting failure calculations for the bending capacity were calculated. For a group of anchors the force P_{Rd} was calculated using a linear analysis in ABAQUS with shell elements, where a slab with a group of anchors was loaded and a bending moment was determined in the middle of the slab see Figure 7.40 for a principle sketch of the model and see Figure 7.41 for a deformed given by the analysis in ABAQUS.

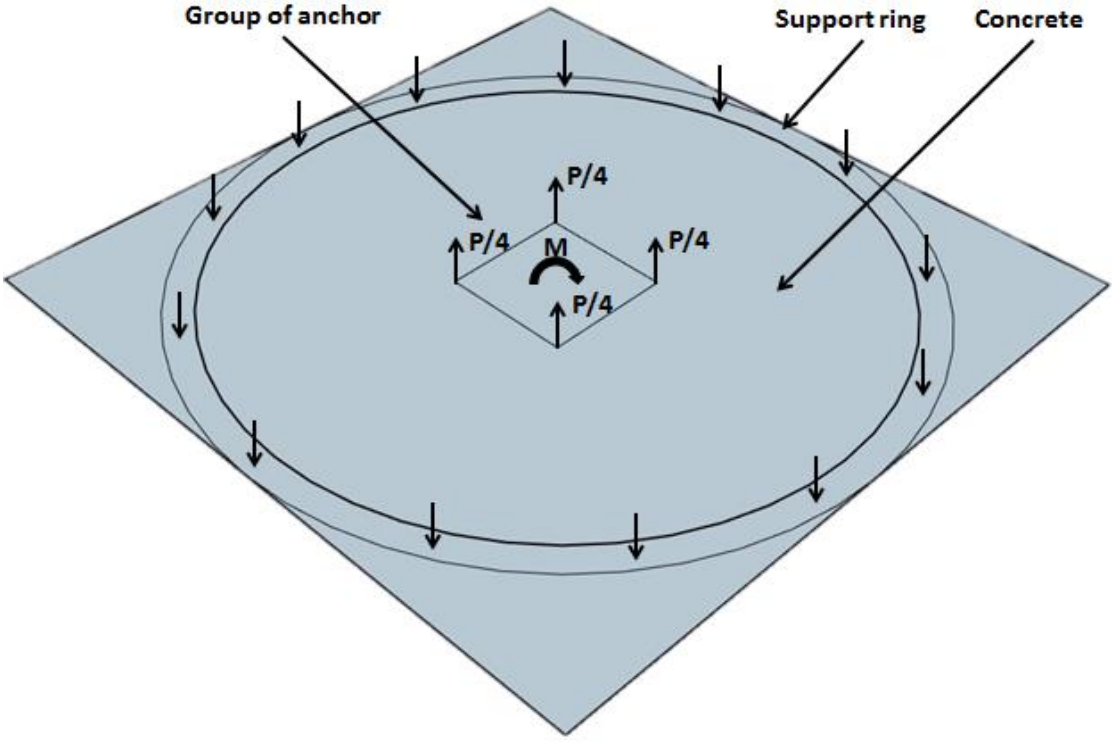

Figure 7.40- Principle sketch for splitting model of group of anchors

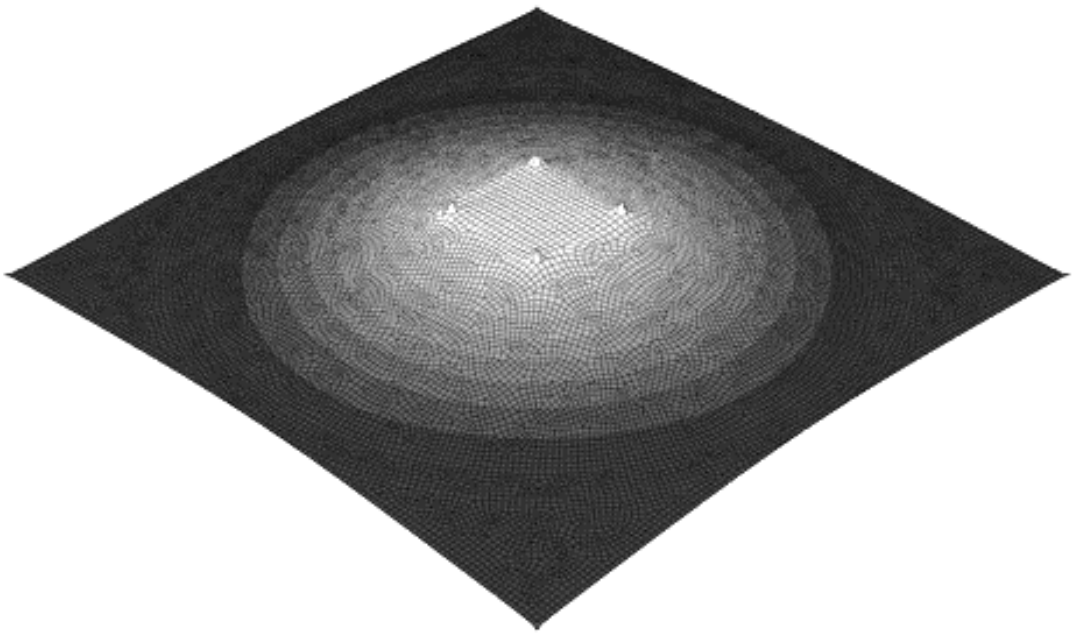

Figure 7.41 – Deformation when the force was applied on four spots on the slab which was represented by shell elements in ABAQUS. A simplification of a group of anchors loaded in tension.

From this analysis a ratio *K* was calculated between four anchors and the maximum bending moment in the middle of the slab, see Appendix A. The relation between the applied force and the moment is linear and a maximum force P_{Rd} could be identified due to known moment capacity given from Equation (3.12). For the thinner slab with dimensions (1.2m×1.2m×0.3m) without reinforcement the splitting capacity was 333 kN according to Equation (7.9). For the thicker slab with dimensions (1.2m×1.2m×0.6m) without reinforcement the splitting capacity was 1329 kN according to Equation (7.10).

$$P_{Rd300} = \frac{M_{Rdu300}}{K} = \frac{45\ kNm}{0.135\ m} = 333\ kN \qquad (7.9)$$

$$P_{Rd600} = \frac{M_{Rdu600}}{K} = \frac{179\ kNm}{0.135\ m} = 1329\ kN \qquad (7.10)$$

The splitting failure capacity for the thinner slab was lower than the determined cone failure (333kN<481kN), and a check was needed for the analysis of same thickness but with reinforcement. The splitting capacity for the thicker slabs was however higher than the determined cone break out failure given from analysis, no further checks were needed for this slab thickness.

To determine the bending moment capacity for the thinner slab with reinforcement φ12 S300 Equation (7.11) was used and the resisting force (P_{Rd}) was calculated to 474kN.

$$P_{Rd300} = \frac{M_{Rd300}}{K} = \frac{64\ kNm}{0.135\ m} = 474\ kN \qquad (7.11)$$

This capacity was still smaller than the cone break out failure determined in the analysis (474kN<550kN), see Equation (7.11) and Table (7.8), and a check was also needed for slabs of 300 mm thickness and reinforcement amount φ16 S100. The capacity was 2008kN according to Equation (7.12). This capacity was sufficient and no further checks were needed (2008kN>656kN).

$$P_{Rd300} = \frac{M_{RdS100}}{K} = \frac{271\ kNm}{0.135\ m} = 2008\ kN \qquad (7.12)$$

7.5 Single and group compared to CEN/TS

A comparison between single anchor and group of anchors were also made for the DIANA-model. The comparison was made with the ratio between the capacities for the two, for the same slab dimension and reinforcement amount, see Table 7.8. The ratio was also compared with the ratio between the capacities given from (CEN/TS 1992-4-2, 2009) which were calculated above in Section 7.3.1, Equation (7.1) and Section 7.4.1, Equation (7.8). The ratio from (CEN/TS 1992-4-2, 2009) is calculated in Equation (7.13).

$$\frac{N_{Rd,c}(Group)}{N_{Rd,c}(Single)} = \frac{493kN}{277kN} = 1.78 \qquad (7.13)$$

Table 7.8- Comparison in capacity between group of anchors and single anchors.

H [m]	Top reinforcement	N_{Single}[kN]	N_{Group}[kN]	N_{Group}/N_{Single}
0,6	-	314	560	1,783
0,6	ϕ12 S300	322	570	1,770
0,6	φ16 S100	331	567	1,713
0,3	-	282	481	1,706
0,3	ϕ12 S300	292	550	1,884
0,3	ϕ16 S100	310	656	2,116

8 Numerical Results in ABAQUS

8.1 Parameter studies for modelling

For ABAQUS the same parameters determined and used for DIANA were supposed to be used so that simple comparison could be made but the analyses were time consuming and alterations were made to decrease the computational time. The step length was automatic with start value of 0.01 m, the tolerance was residual force based equilibrium instead of energy variation and the mesh geometry of the dense part was made smaller, see Figure 8.1.

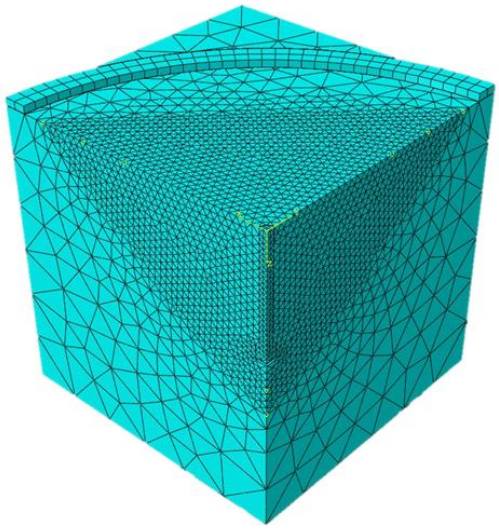

Figure 8.1- Mesh geometry used for ABAQUS model.

Analyses with mesh size of 10 mm and 15 mm were also performed to determine which mesh was most appropriate. The capacity, crack pattern and also the computational time for the two analyses were compared, see Figure 8.2, Figure 8.3 and Table 8.1 .

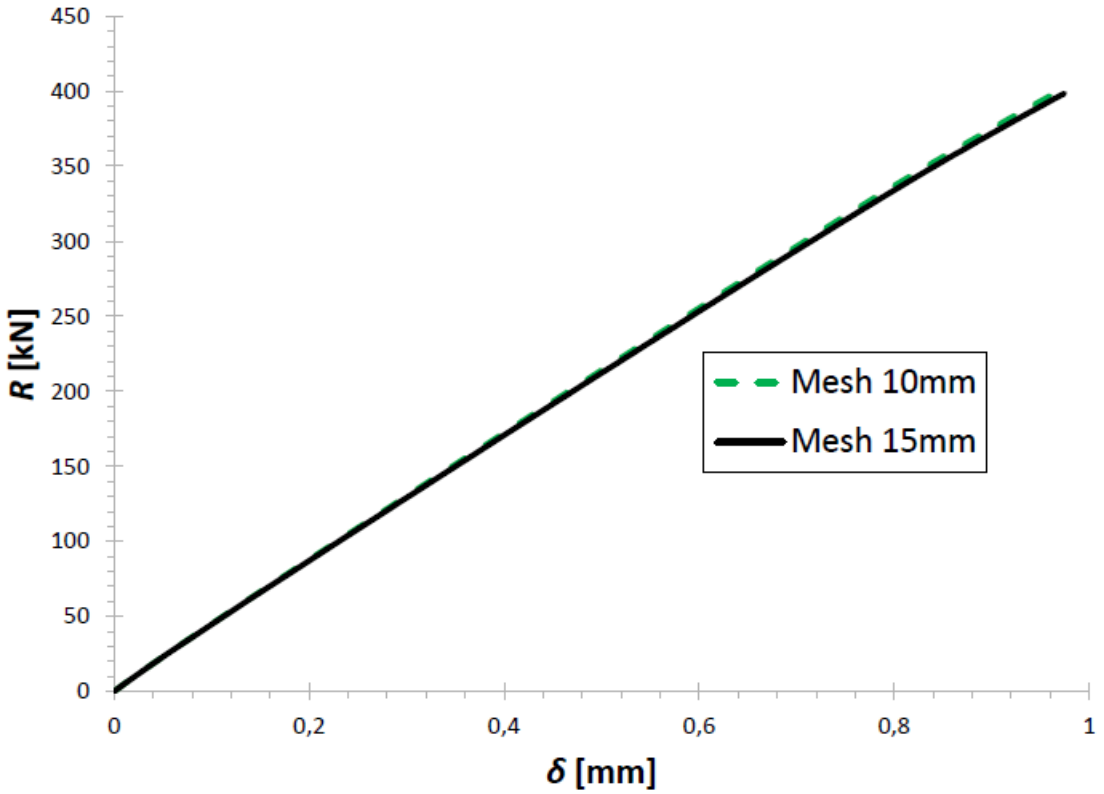

Figure 8.2- Load (R) vs Displacement (δ) for different mesh sizes in ABAQUS, cf. Figure 5.3.

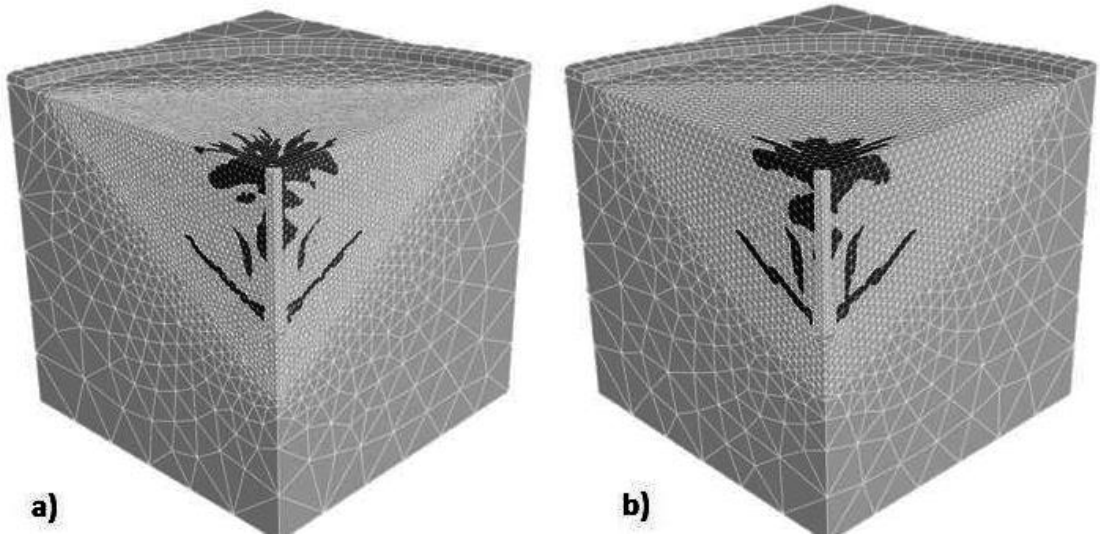

Figure 8.3- Crack pattern for different mesh size in ABAQUS a) 10 mm *b) 15* mm.

Table 8.1- Computational time for different mesh sizes in ABAQUS.

Mesh size [mm]	No. Of Elements	Computational Time
10	114037	~240 hours
15	47876	35-40 hours

The capacity for the two analyses did not differ much and the crack patterns were similar, where both showed that cone cracks had developed. The computational time was however much larger for a mesh of 10mm. Therefore the mesh of 15mm was

chosen for further analyses. The parameters that were used for ABAQUS are presented in Table 8.2.

Table 8.2- Parameters later used for analyses in ABAQUS

Step length	Tolerance (Residual force)	Mesh geometry	Mesh size	Interaction Reinforcement- Concrete
0.01	0.005	Straight lines	15 mm	Embedded

8.2 Numerical analyses on single anchor in tension

The results for single anchor analyses performed in ABAQUS are presented in one diagram, where the capacity of the concrete cone failure was compared for two different thicknesses of the slab, both slabs with reinforcement amount of φ12 S300, see Figure 8.4. The diagram is also complimented with figures of the crack pattern which is given by the first principle strain for the two different analyses, see Figure 8.5 and Figure 8.6. These figures were taken at the end of the simulation and where δ was around 0.9-1.0 mm. Number of element and computational time for the analyses is also presented in Table 8.3.

Table 8.3- No. of elements and computational time for the analyses performed on different thicknesses for a single anchor in ABAQUS.

Anchor	*H* [m]	No. Of Elements	Computational Time
Single	0.3	56213	45-50 hours
Single	0.6	47876	35-40 hours

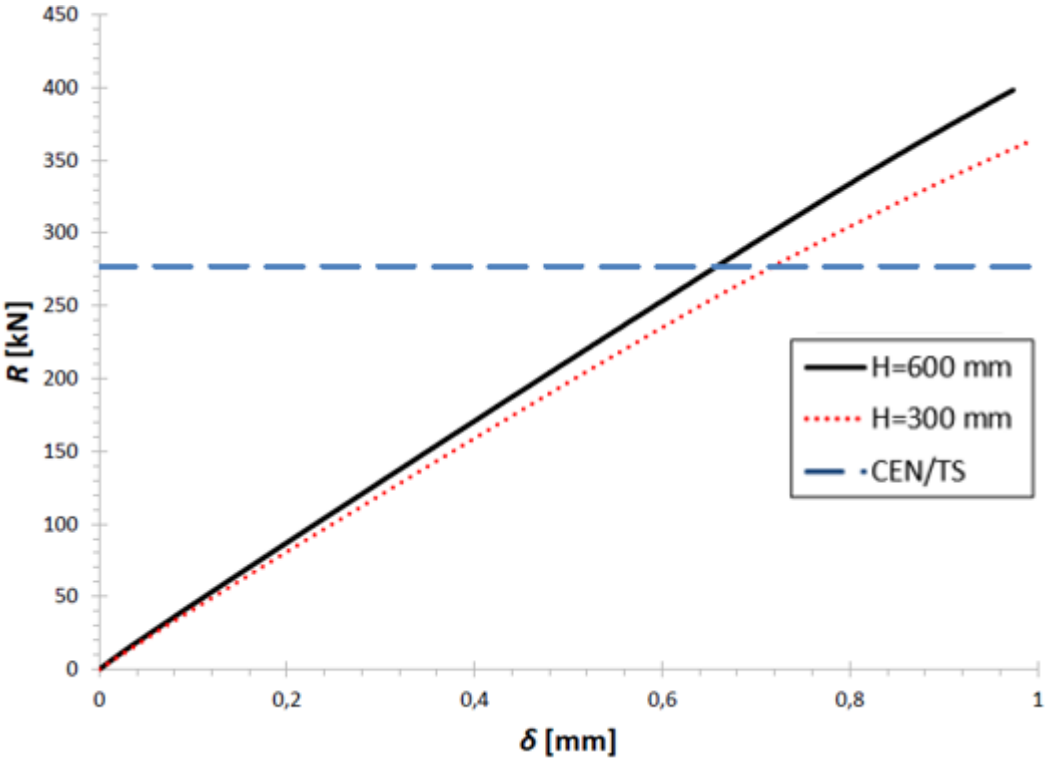

Figure 8.4- Load (R) vs Displacement (δ) for slabs with φ12 S300, cf. Figure 5.3.

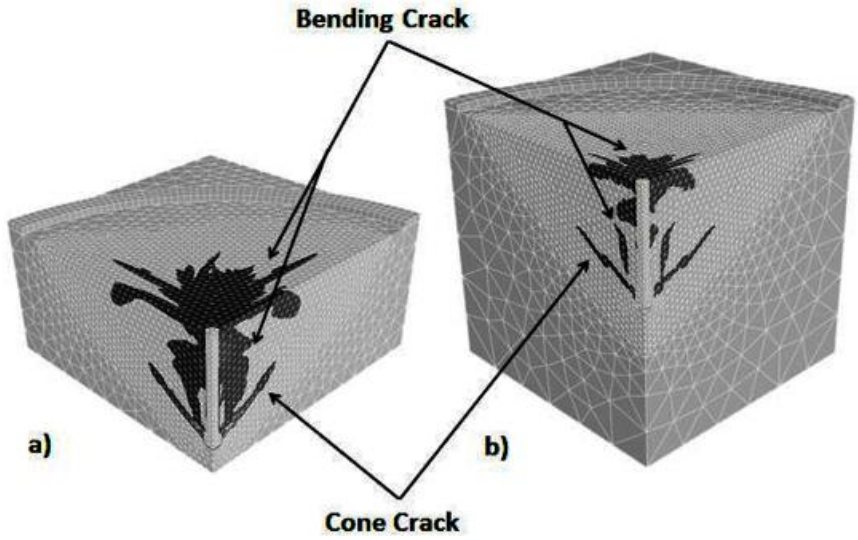

Figure 8.5- Crack pattern for single anchor with reinforcement amount of φ12 S300 a) H=300 mm at δ= 0.989 mm, see Figure 8.4 b) H=600 mm at δ=0.975 mm, see Figure 8.4

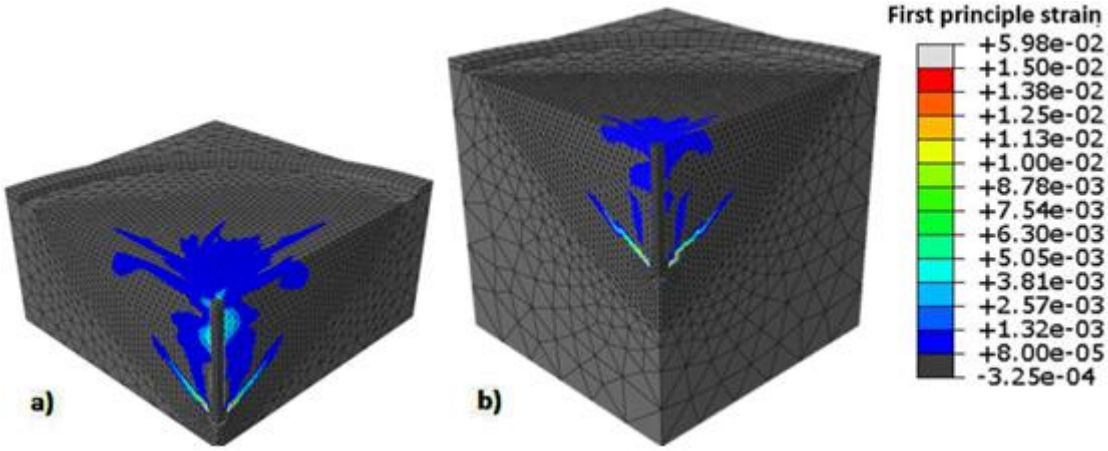

Figure 8.6- Crack pattern with indication of strains for single anchor with reinforcement amount of φ12 S300 a) H=300 mm at δ=0.989 mm, see Figure 8.4 b) H=600 mm at δ=0.975 mm, see Figure 8.4

In Table 8.4 capacities given by analyses in ABAQUS were compared with capacities given by analyses in DIANA.

Table 8.4- Comparison between capacities for analyses performed in ABAQUS and DIANA.

H [m]	Top reinforcement	N_{single}[kN] (ABAQUS)	N_{Single}[kN] (DIANA)	ABAQUS/DIANA
0,6	ϕ12 S300	399	322	1,239
0,3	ϕ12 S300	362	292	1,240

8.3 Numerical analyses on group of anchors in tension

The results for group of anchor analyses performed in ABAQUS are presented in five different diagrams, same as for DIANA, where the capacity of the concrete cone failure was compared for different slab thickness and with different amount of

reinforcement, see Figure 8.7-8.11. The diagrams are also complimented with figures of the crack pattern which is given by the first principle strain for the different analyses, see Figure 8.12- 8.15. These figures were taken at the end of simulation where δ was around 0.4-0.7 mm. Number of element and computational time for the analyses of different thicknesses of the slab is presented in Table 8.5.

Table 8.5- *No. of elements and computational time for the analyses performed on different thicknesses for a group of anchors in ABAQUS.*

Anchor	H [m]	No. Of Elements	Computational Time
Group	0.3	42580	13-16 hours
Group	0.6	63269	14-17 hours

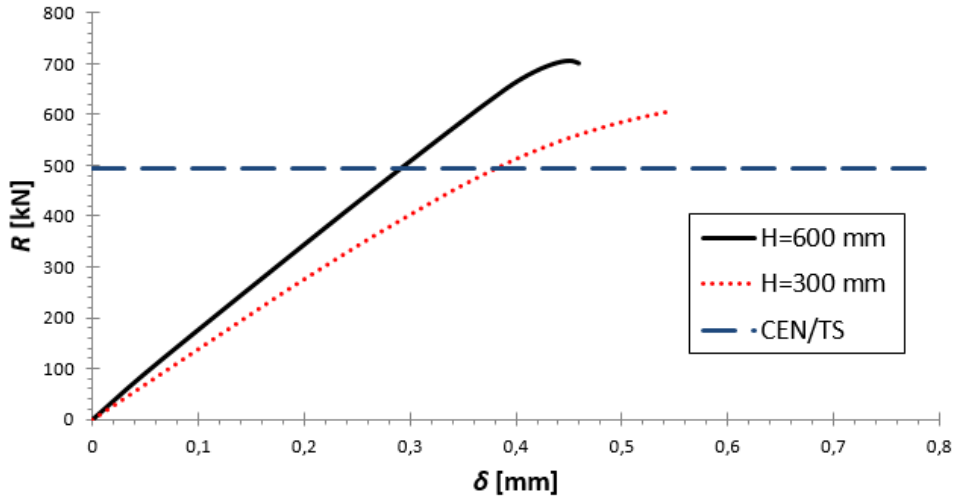

Figure 8.7- Load (R) vs Displacement (δ) for un-reinforced slabs and group of anchors, cf. Figure 5.4.

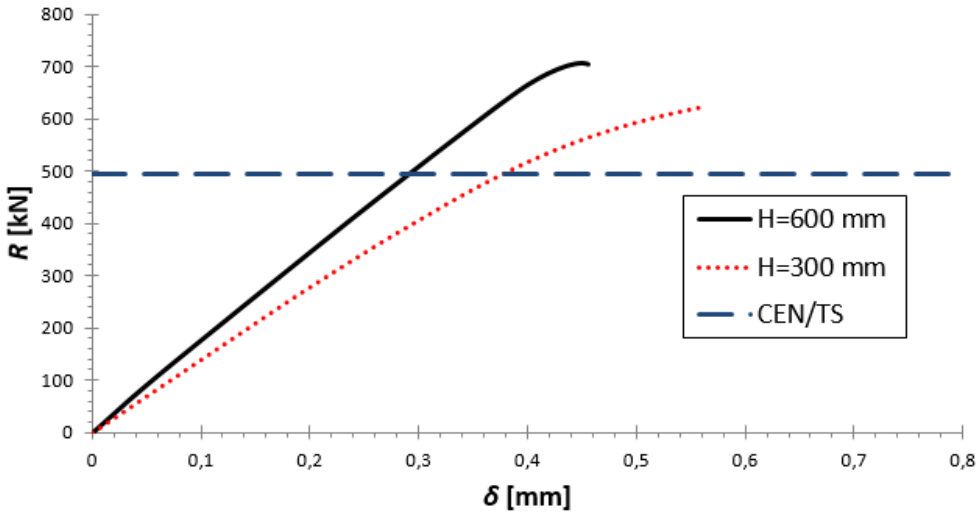

Figure 8.8- Load (R) vs Displacement (δ) for slabs with φ12 S300 and group of anchors, cf. Figure 5.4.

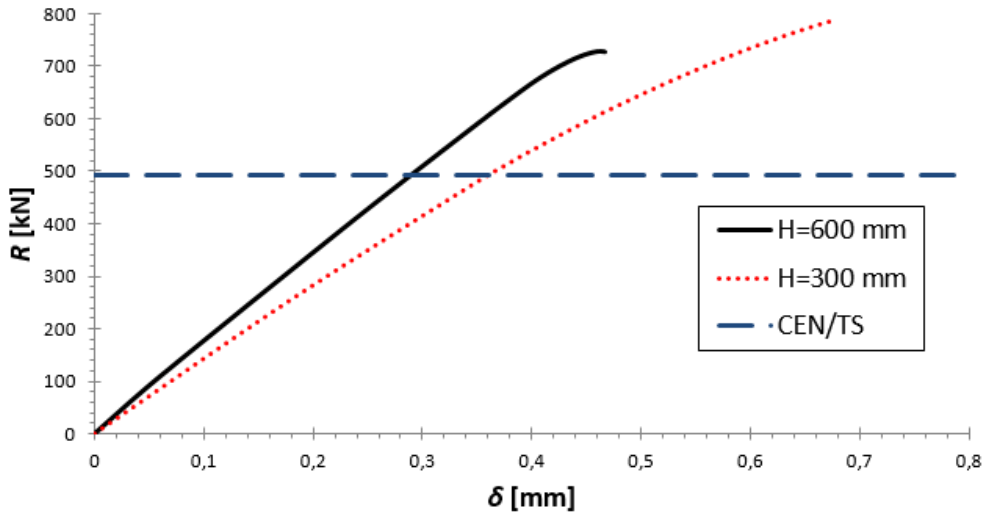

Figure 8.9- Load (R) vs Displacement (δ) for slabs with φ16 S100 and group of anchors, cf. Figure 5.4.

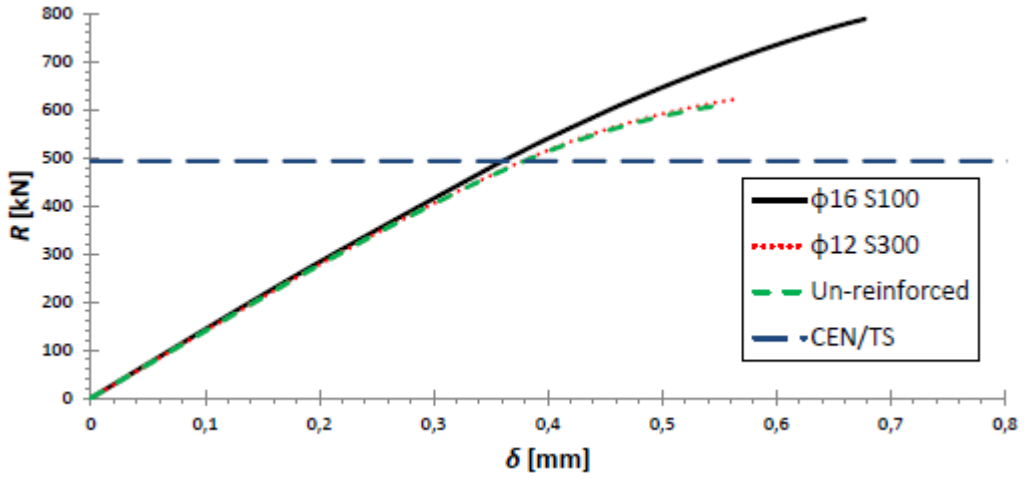

Figure 8.10- Load (R) vs Displacement (δ) for slabs with thickness H=300 mm and group of anchors, cf. Figure 5.4.

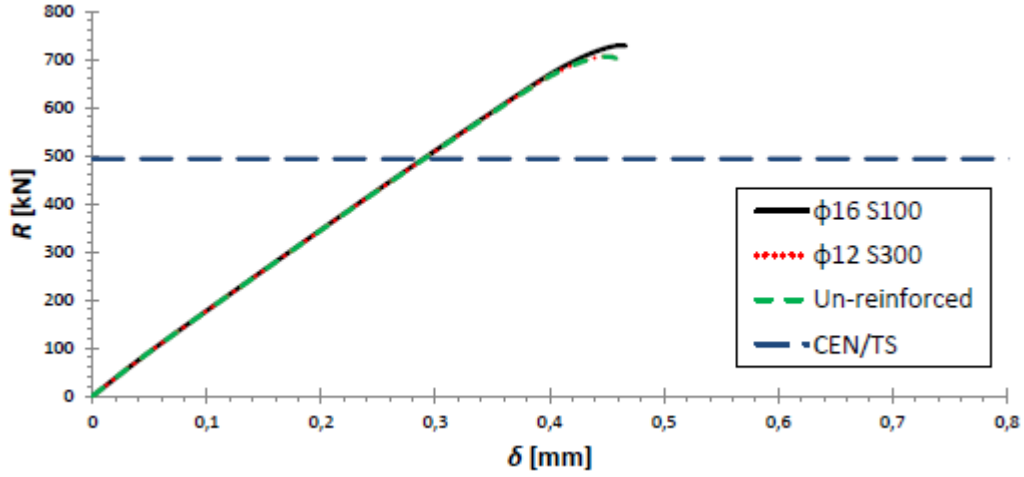

Figure 8.11- Load (R) vs Displacement (δ) for slabs with thickness H=600 mm and group of anchors, cf. Figure 5.4.

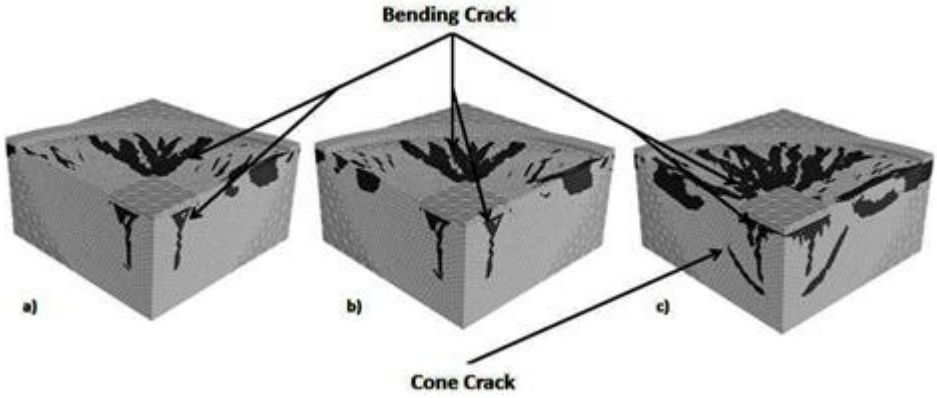

Figure 8.12- Crack pattern for group of anchors, H=300 mm a) Un-reinforced at δ=0.548 mm, see Figure 8.10 b) φ12 S300 at δ=0.562 mm, see Figure 8.10 c) φ16 S100 at δ=0.678 mm, see Figure 8.10

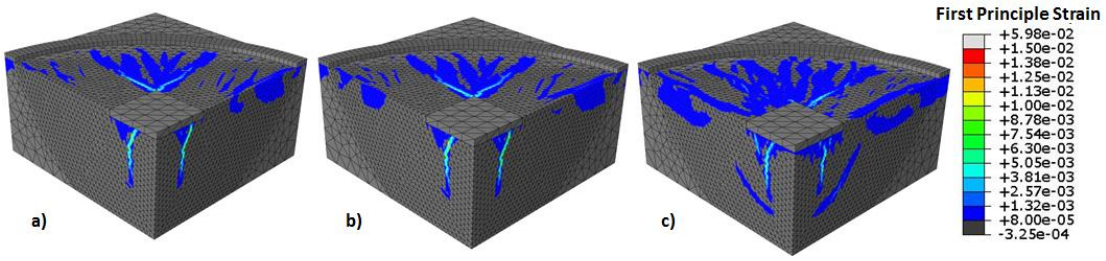

Figure 8.13- Crack pattern with indication of size of strains for group of anchors, H=300 mm a) Un-reinforced at δ=0.548 mm, see Figure 8.10 b) φ12 S300 at δ=0.562 mm, see Figure 8.10c) φ16 S100 at δ=0.678 mm, see Figure 8.10

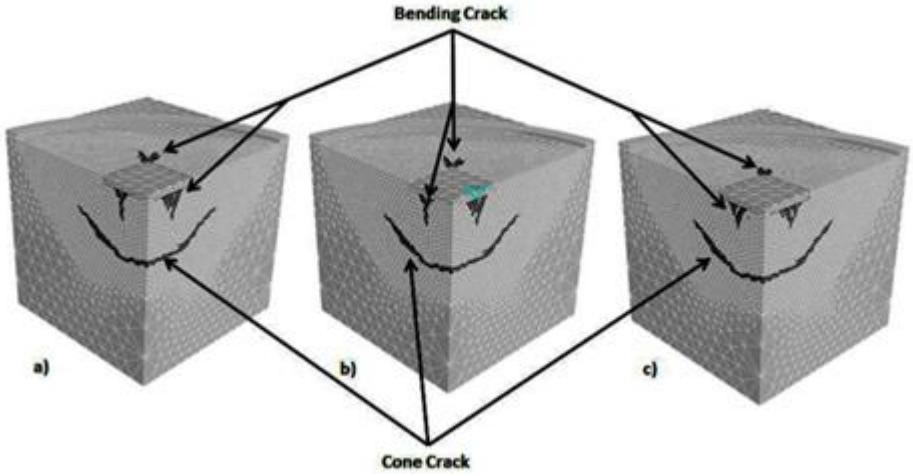

Figure 8.14- Crack pattern for group of anchors H=600 mm a) Un-reinforced at δ=0.449 mm, see Figure 8.11 b) φ12 S300 at δ=0.450 mm, see Figure 8.11 c) φ16 S100 at δ=0.462 mm, see Figure 8.11.

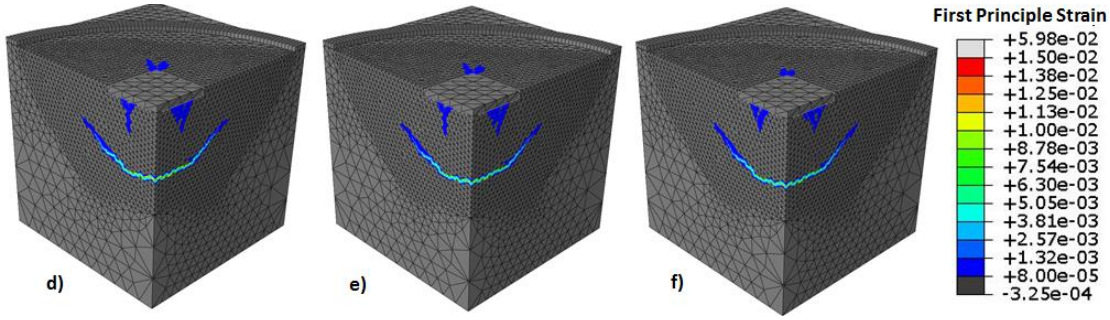

Figure 8.15- Crack pattern with indication of size of strains for group of anchors H=600 mm a) Un-reinforced at δ=0.449 mm, see Figure 8.11 b) φ12 S300 at δ=0.450 mm, see Figure 8.11 c) φ16 S100 at δ=0.462 mm, see Figure 8.11.

In Table 8.6 capacities given by analyses in ABAQUS are compared with capacities given by analyses in DIANA.

Table 8.6- Comparison between capacities for analyses performed in ABAQUS and DIANA for group of anchors.

H [m]	Top reinforcement	N_{Group}[kN] (ABAQUS)	N_{Group}[kN] (DIANA)	ABAQUS/DIANA
0,6	-	706	560	1,261
0,6	ϕ12 S300	706	570	1,239
0,6	ϕ16 S100	729	567	1,286
0,3	-	608	481	1,264
0,3	ϕ12 S300	621	550	1,129
0,3	ϕ16 S100	789	656	1,203

9 Discussion

9.1 Modelling studies

The data from the studies shows that there are many parameters (step length, tolerance, mesh geometry, mesh size, stress distribution and interaction) affecting the load (*R)* vs displacement (δ) curve for the DIANA-model.

The step length and the tolerance of the energy variation goes hand in hand and the values were carefully considered so that the behavior was captured but within reasonable computational time.

The mesh was of great importance when it came to the crack pattern and the analyses was based on cracks in one element row it was important to see that there were no disturbances in the crack pattern anywhere in the model. It was seen that small changes in the mesh geometry or in the mesh size had impact on how the cracks developed in the model. This meant that the capacity for the model was also affected since the crack could develop more or less easy when the mesh formed differently.

When considering the stress distribution through the slab it was noticed that more accurate results were given when the mesh was dense throughout the whole upper part of the slab. In this way the stress distributions were smooth and disturbed areas were avoided and this was assumed to affect the capacity in a more accurate way. It is however believed that the elements "behind" the ring support, furthest from the anchor, does not have to be dense since these elements does not affect the capacity and this could decrease the computational time.

For all the studies the reinforcement was modeled as embedded because of the decreased capacity and more complex mesh when modeled with bond slip interaction by (Dörr, 1980).

9.2 Model calibration

The capacity obtained in the analyses when calibrating were within the range of the achieved capacities for the tests results and the behaviour of the crack pattern indicated that a cone failure was achieved, see Section 7.2. The compression strength around the anchor head was however a problem because the analyses did not converge when the stresses became higher than the concrete strength and therefore no cone failure could develop. Adjustments on the concrete model in compression were made and lateral confinement was added which led to higher capacity but still not enough. When the compression was set to elastic behaviour it could develop concrete cone failure which was approximately twice as high as the compression failure. The displacements gained by the analyses did however not coincide with the tests. The curves from the analyses and the curves from the tests used for calibration diverge in displacement in the region were compressive failure was reached for the analyses. The concrete cone failure is also believed to be a relatively non-ductile failure, see Section 2.3.2 but this is not the case for most of the performed tests. Therefore the compressive failure was believed to be the cause for the large deformations for the tests and these deformations were ignored once the compressive strength was set to elastic for the analyses. The models were however assumed to be accurate enough to continue the analyses to investigate the influence of surface reinforcement on the cone

failure, since like mentioned before the capacity was similar to the tests and the correct mode of failure was achieved for the model.

9.3 Single anchor in tension

The results for the impact of the surface reinforcement and thickness of the slab given from single anchors with the DIANA-model, see Section 7.3.2 show that both thickness and reinforcement, influenced both the crack pattern and the capacity of the slabs. All the analyses also indicated from their crack patterns that a concrete cone failure had been achieved.

The slabs with larger thickness clearly gets a higher global stiffness compared to the thinner slabs, where the curves have different inclinations, which is seen in Figure 7.21-7.23. This increase in global stiffness is believed to be the reason why a higher capacity for the concrete cone failure was achieved for the thicker slabs compared to the less thick slabs. These coincides well with what (Elfgren & Nilsson, 2009), (Nilforoush, 2015) and (Segle, et al., 2013) had concluded from there tests and numerical analyses, see Chapter 4 and Chapter 6.

The results from the calculations on splitting failure of single anchors indicated that the slab with dimension 1.2m×1.2m×0.3m without any reinforcement should have had splitting failure before a cone failure. This was however not the case for the analysis, instead a concrete cone was able to fully developed. In Figure 7.24 there was not much indicating that a splitting failure should have occurred for the unreinforced slab. The analysis did however get more non-linear behaviour around the calculated capacity for splitting failure for the slab. In Figure 7.27 large bending cracks could also be seen for the un-reinforced slab, this could have been an indication that a splitting failure should have occurred. The model did however seem to ignore splitting failure and only focus on cone failure, this might be because some assumptions and simplifications were made for the model that might have affected the ability to develop splitting failure. The results for this analysis was not used and evaluated as a result in capacity for the cone failure since splitting failure should have occurred for the analysis. It was however interesting to see from the splitting failure calculations that once surface reinforcement was introduced, a concrete cone failure was achieved for the slab.

The increase in capacity due to surface reinforcement was clear when studying Table 7.5. Where the capacities from the analyses compared to the code of praxis were higher for all analyses and increasing the amount of surface reinforcement also increased the difference. Increasing the surface amount was most effective for the thinner slab. The difference in capacity for the analyses compared to code of praxis was between 1.8%- 11.9% meaning an increase with 10.1% units from un-reinforced slab to slab with reinforcement amount of φ16 S100. The thin unreinforced slab should however have obtained splitting failure and the capacity was perhaps not trustworthy. The difference for the thicker slab was between 13.4%- 19.5% meaning the increase was higher to begin with compared to code of praxis but the difference between un-reinforced to reinforcement amount φ16 S100 was only 6.1% units.

It is also interesting to study the difference in capacity between reinforcement amount φ12 S300 and φ16 S100, see Table 9.1. From this it was seen that increasing the amount of surface reinforcement in the slab do have an effect for the concrete cone capacity. Interesting was that this was not what (Nilforoush, 2015) had concluded

from their performed analyses. They did however conclude that the surface reinforcement had more impact on thinner slabs than on thicker same as the results for this thesis, see Section 6.2. The reason for the increase in capacity when introducing more reinforcement could however depend on many reasons. One could be the spacing between the reinforcement bars another could simply be the amount of reinforcement. These are studies that could be performed in further investigations for the surface reinforcement's impact on the concrete cone failure.

Table 9.1- Increase in capacity when adding more surface reinforcement.

	Φ12 S300	
Top reinforcement	H=300 mm	H=600 mm
Φ16 S100	6.2 %	2.8 %

In what way the amount of surface reinforcement is impacting the capacity cannot be seen with any difference in inclination for the curves linear parts as it could for the difference in thickness, see Figure 7.24 and 7.25. A more non-linear behaviour does however occur when the slabs have less amount of reinforcement. It is known that introducing reinforcement into concrete will increase the global stiffness for the slab. Therefore the reason for the increased capacity with increased amount of surface reinforcement is also believed to be because of the increased global stiffness same as for the difference in thickness. The reinforcement can also be seen to affect the crack pattern of the bending cracks. When more reinforcement was introduced less bending cracks were appearing which was reasonable. This can also be a reason for why more capacity was achieved, that the bending cracks were affecting the cone break out and with less bending cracks more capacity was reached. This was also observed when comparing Figure 7.24 and 7.25 where the thinner slabs capacity was increased more with the introduction of reinforcement compared to the thicker slabs, since the smaller slabs show more pronounced bending cracks compared to the thicker slabs, see Figure 7.26- 7.29.

Since calibration has been made for the DIANA-model against physical test the results given for single anchor is believed to be rather accurate apart from the displacement.

9.4 Group of anchor in tension

The results for the impact of the surface reinforcement and thickness of the slab given from group of anchors with the DIANA-model, see Section 7.4.2 showed that the amount of surface reinforcement in the slab had a large impact on the capacity for the thinner slab. For the thicker slab the surface reinforcement had almost no impact on the capacity.

For the thin slabs both the un-reinforced slab and the slab with reinforcement amount of φ12 S300 where calculated to fail due to splitting. This was however not the case for these analyses since like discussed for single anchor the model did not seem to be able to get splitting failure only cone failure. Non-linear behaviour was developed early for the analyses when studying the capacity in Figure 7.34 this is however not a sign that splitting failure have occurred but it can be an indication. When studying the crack patterns in Figure 7.36 and Figure 7.37 there were clear that cone cracks had appeared as well as large bending cracks. That also indicated that splitting failure

should have occurred for the two analyses that were calculated to get splitting failure. These analyses were nevertheless ignored when it came to their capacity for concrete cone failure.

For the thin slab with reinforcement amount of φ16 S100 there was however no risk for splitting failure. The crack pattern for this analysis, see Figure 7.36c and Figure 7.37c indicated that a cone failure had developed and that the bending cracks were of smaller size compared to the other two thin slabs. The capacity did however seem large for the analysis since it was 33.1% larger than the value given from code of praxis, see Table 7.7. The capacity was also larger than the capacity for all the analyses for group of anchors with the thicker slab. This did not correspond to the results for single anchor. It was however observed in Figure 7.34 that the analysis had large part of its behaviour that was non-linear and the failure was believed to be ductile. This was not the case for the thicker slab, see Figure 7.35 where the failure seemed to be brittle. If the capacity for the thin slab with reinforcement amount of φ16 S100 resembles reality is however not clear.

For the thicker slabs there were also no risks for splitting failure for any of the analyses. The capacity for cone failure for the different analyses was almost identical, which can be seen in both Figure 7.35 and Table 7.7. Analysing the crack patterns for the different slabs in Figure 7.38 and Figure 7.39 showed similar behaviour for the analyses and for all three analyses there were only cone cracks and no indication of bending cracks. The lack of bending cracks might be the reason why the analyses showed similar capacity for the thicker slab. Since like discussed before in Section 9.3, less bending cracks that might affect the cone cracks could be a reason for increased concrete cone capacity. It can also be noticed in Figure 7.35 that all the analyses for the thicker slab did get brittle failure as mentioned before. This could also be a reason why the analyses for the thick slab had similar capacity. Once a certain load was reached a brittle failure occurred and the introduction of surface reinforcement did not make the slabs more ductile and therefore no more capacity was achieved. If this is a correct assumption this would mean that a ductile behaviour is needed for the slab in order to get an impact from the surface reinforcement for the concrete cone failure.

A reason that the analyses had more brittle failure for group of anchors compared to single anchor could be that the load was distributed on four anchors instead of one and the increase in load distribution also increased the stiffness for the slabs. It could have been favourable if the stiffness could have been keep the same for all the analyses. This could perhaps have been done by increasing the width of the slabs for the analyses on group of anchors.

Since there is no physical performed test for concrete cone failure on group of anchors, the results for the analyses that have been performed cannot be assumed to be completely accurate. If physical tests were to be performed a comparison with the result presented in this thesis could be done to determine their accuracy and perhaps improve the DIANA- model.

9.5 Single and group compared to CEN/TS

A comparison was made between difference in capacity for single and group of anchors given by code of praxis and difference in capacity given the analyses made in DIANA. Since one of the analyses for single anchor and two the analyses for group of

anchors was believed to have had splitting failure only four comparisons where made instead of six. The difference in capacity given by code of praxis was set to 1.78 according to Equation (7.13).

For the thicker slab the ratio was 1.78 when no surface reinforcement was present. However as the capacities for slabs with single anchors increased and the capacities for slabs with group of anchors was kept almost the same when surface reinforcement was introduced and increased the ratio was decreasing down to 1.71, see Table 7.8.

For the thin slab only one comparison was possible, which were for the slab with reinforcement amount of φ16 S100. For this slab the ratio was almost 2.12, see Table 7.8, meaning that for this slab there is more capacity to be achieved for group of anchors than for a single anchor. Still since this was the only comparison made for the thin slabs it was hard to discuss the reason for this. It was also not known if the results from group of anchors were completely reliable since there are no physical tests to compare with.

9.6 ABAQUS

For the ABAQUS-model alterations were made from the DIANA-model to reduce the computational time for the analyses, see Section 7.1.7. These alternations did reduce the computational time but might also have affected the results for the analyses. However even with decreased computational time it was almost increased with a factor of 10 compared to the DIANA-model, which meant less time for adjustments. More proper improvements might have been made if the ABAQUS-model would have been calibrated against the test in the same way as the DIANA-model instead of just making the same assumptions as the DIANA-model. The analyses did however seem to get good behavior for the cracks where clear cone cracks could be seen to have developed, see Figure 8.3. The large computational time was believed to depend on the fact that the two different FE-software used different material models and that the material model used for DIANA was more efficient. Another reason for the difference in computational time could simple be that the solver for DIANA is faster than ABAQUS for this type of analyses.

Since the analyses for a single anchor performed with the DIANA-model was believed to be rather accurate and the values for the ABAQUS-model did not correspond completely with those results the ABAQUS-model was not believed to be precise regarding the capacity. The ABAQUS- model would have required more calibration time in order to get reliable results. However the crack pattern and the load vs displacement graphs were similar, see Figure 8.4- 8.6 which indicated that with some more calibration more alike capacities could have been reached. A difference was however spotted were cracks appeared between the bending cracks and cone cracks. The reason for these cracks is not known but one simple explanation is that there was small differences in the material models used for DIANA and ABAQUS.

In Table 8.4 there could be seen an increase in capacity compared to DIANA with 24 % for both thicknesses indicating that the model in ABAQUS was too stiff. Comparison against CEN/TS was therefore not needed.

The simulations made in ABAQUS had also for group of anchors increased capacity compared to DIANA same as for single anchor. The increment was similar to the one with single anchor around 24%, see Table 8.6. For the thinner slab without reinforcement and with reinforcement amount φ12 S300 there could be seen bending

cracks and no cone cracks, see Figure 8.12 and Figure 8.13. As the calculated capacity for splitting failure in Section 7.4.3 was lower than for cone failure for these two slabs this seemed reasonable. However for the slab with reinforcement amount φ16 S100 there were cone cracks and therefore the capacity was increased. Even though there could not be seen any cone failure for the first two slabs the failure should have come earlier same as for the DIANA analyses. This indicated that ABAQUS could not catch the splitting failure as well.

Even if the analyses for group of anchors ware not evaluated for its capacities it was interesting to see that the load displacement curves got similar behavior as they did for DIANA. The four analyses that were not believed to get splitting failure all got similar increase in capacity compared to DIANA, between 20%- 29% increase, see Table 8.6. The thicker slabs all got similar capacities, same as analyses in DIANA and they all seemed to get brittle failures, see Figure 8.11. While the thinner slab with reinforcement amount of φ16 S100 got higher capacity than all analyses and more ductile failure, same as analyses in DIANA, see Figure 8.10. This supports the hypothesis that a ductile behaviour is required for the slab in order for the surface reinforcement to have an impact on concrete cone failure. The ABAQUS-model did of course use many of the same assumptions as the DIANA-model but they are still different FE-software and they also use slightly different material models.

The difference in computational time for group of anchors was not as big as it was for single anchor. It was decreased to only twice the time for ABAQUS compared to DIANA for this configuration, but keep in mind that the elements were bigger and that the mesh was different compared to DIANA.

10 Conclusions

The aim of the thesis was to investigate the impact from surface reinforcement on concrete cone failure by doing numerical analyses and comparing with code of praxis. The numerical model was created by calibrating against physical tests performed on single anchors in tension. The calibration was successful in terms of capacity and achievement of concrete cone failure but not in displacement. The results showed for the cases studied that surface reinforcement had more impact on thinner slabs than on thicker slabs when a single anchor was loaded. It had no or small impact on thicker slabs and large impact on thinner slabs when a group of anchors were loaded.

The following conclusions could be drawn from the results:

- The small displacements in the analyses compared to the physical tests were believed to be caused by the exclusion of the crushing failure because the crushing failure was localized on top of the anchor head. This would lead to larger displacements in practice instead of diverging in the analyses.
- The surface reinforcement had influence on the capacity for single anchors. It could be seen that the increment was larger in percentage for the thinner slabs than for the thicker. The thinner slabs that were loaded by the group of anchors had also a big influence from the surface reinforcement. However it had no or small influences for the thicker slabs that were loaded with group of anchors.
- Comparing results for single anchor with the code of praxis showed an increase for all slabs. Higher capacity for the thicker slabs with reinforcement compared to thinner slabs with the same amount of reinforcement. For the thicker slabs the increase was as much as 19.5% and for the thinner 11.9% compared to CEN/TS. This is probably due to the increase of global stiffness.
- Comparing results for group of anchors with the code of praxis showed that the thicker slabs had an increased capacity that was almost the same no matter the amount of reinforcement and an incredibly high increment for the thinner slab, as much as 33.1%. This is believed to be because of brittle behavior for the thick slabs and more ductile behavior for the thin slab.
- The capacity for single anchors was well described in DIANA for both the thick and the thin slab and was thereafter used for the configuration of four anchors. This was assumed to be possible in ABAQUS as well if the same studies would have been made for that software. ABAQUS had longer computational time than DIANA, this was believed to be caused by the different material model and/or different solver that were used in ABAQUS, more time consuming model for concrete when it was cracked.
- Splitting failure was prevented with a certain amount of reinforcement for the thinner slabs. The increase in global stiffness was believed to prevent that failure mode. The models did however not seem to be able to catch a splitting failure.

10.1 Suggestions for further studies

This thesis has only studied a small part of how the surface reinforcement is impacting the concrete cone failure when loaded in tension. There are still more to be

analyzed in order to determine a more general conclusion. Some suggestions on further studies for this investigation is presented below.

- Simulations regarding the concrete crushing failure would be of great interest. To check if the assumptions regarding the displacement truly was affected by the crushing failure on top of the anchor head.
- Further studies on the thickness of the slab with reinforcement would be of interest, in order to determine when the capacity stops increasing for more amount of reinforcement for both single and group of anchors. It was clearly seen that in this thesis it stopped earlier for a group of anchors compared to single anchors.
- Different sets of group anchors could be checked to see if these conclusions are valid for other sets as well. Different effective depth, number of anchors and distance between them.
- Perform physical tests for group of anchors to verify these and future numerical results regarding concrete cone failure.

11 References

1992-1-1:2005, S.-E., 2008. *Eurocode 2:Design of concrete structures- Part1-1: General rules and rules for buildings,* Stockholm: Swedish Standards Institute.

Broo, H., Lundgren, K. & Plos, M., 2008. *A Guide to non-linear finite element modelling of shear and torsion in concrete bridges,* Göteborg: Chalmers University of Technology.

CEN/TS 1992-4-1, 2009. *Design of fastenings for use in concrete-Part 4-1: General.* Brussel: European Commitee for Standardization.

CEN/TS 1992-4-2, 2009. *Design of fastenings for use in concrete-Part 4-2:Headed Fasteners.* Brussel: European Committee for Standardization.

Dassault Systèmes , 2013. *Abaqus 6.13 Documentation.* [Online] Available at: http://bobcat.nus.edu.sg:2080/v6.13/books/usb/default.htm [Accessed 4 April 2016].

Dörr, K., 1980. *Ein Beitrag zur Berechnung von Stahlbetonscheiben unter besonderer Berücksichtigung des Verbundverhaltens,* Darmstadt: University of Darmstadt.

Elfgren, L. & Nilsson, M., 2009. *Load-Carrying Capacity of Cast-in Headed Studs in Concrete Structures,* Luleå: Luleå University of Technology.

Eligehausen, R., Bouska, P., Cervenka, V. & Pukl, R., 1992. *Size effect of the concrete cone failure load of anchor bolts,* s.l.: s.n.

Eligehausen, R., Mallée, R. & John F, S., 2006. *Anchorage in Concrete Construction.* 1:a ed. Berlin: Ernst & Sohn.

Engström, B., 2013. Betongbyggnad. In: *Bärande konstruktioner Del1.* Göteborg: Chalmers Tekniska Högskola.

Hanjari, K. Z., Kettil, P. & Lundgren, K., 2011. Modelling the structural behaviour of frost-damaged reinforce concrete structures. *Structure and Infrastructure Engineering,* IX(5), pp. 416-431.

Lee, J. & Fenves, G. L., 1998. Plastic- Damage Model for Cyclic Loading of Concrete Structures. *Jornal of Engineering Mechanics,* CXXIV(8), pp. 892-900.

Lubliner, J., Oliver, J., Oller, S. & Onate, E., 1989. A Plastic- Damage Model for Concrete. *International Jornal of Solids and Structures,* XXV(3), pp. 299-326.

Nilforoush, R., 2015. *Influence of Slab Thickness , Head Size and Surface Reinforcements on the Tensile Capacity of Anchor Bolts.* Stockholm: s.n.

Segle, P. et al., 2013. *Numerical simulations of headed anchors break in reinforced and non-reinforced concrete structures,* Stockholm: Strålsäkerhetsmyndigheten Swedish Radiation Safety Authority.

Thorenfeldt, E., Tomaszewicz, A. & Jensen, J., 1987. *Mechanical properties of high-strength concrete and applications in designed..* Norway, s.n.

TNO DIANA BV, 2015. *DIANA-9.6 User's Manual- Material Library.* First ed ed. The Netherlands: TNO DIANA BV.

Appendix A: Hand calculation splitting failure

Splitting failure

INDATA

Concrete slab

$b := 1.15\ m$ "Effective width for slab"

$h_{300} := 0.3\ m$ "Thickness of slab 300 mm"

$h_{600} := 0.6\ m$ "Thickness of slab 600 mm"

$E_s := 210\ GPa$ "Young's modulus for concrete"

$f_{ck} := 25\ MPa$ "Compressive strength for concrete"

$f_{ctm} := 2.6\ MPa$ "Tensile strength for concrete"

$\varepsilon_{cu} := 3.5 \cdot 10^{-3}$ "Crusing failure for concrete"

$\alpha := 0.81$

$\beta := 0.416$

Reinforcement

$d_{rein.12} := 12\ mm$ "Diameter for reinforcement 12mm"

$d_{rein.16} := 16\ mm$ "Diameter for reinforcement 16mm"

$c := 30\ mm$ "Cover thickness concrete"

$d_{12} := h_{300} - c - \frac{3\ d_{rein.12}}{2} = 0.252\ m$ "Effective hight top reinforcement 12 mm"

$d'_{12} := h_{300} - d_{12} = 0.048\ m$ "Effective hight bottom reinforcement 12 mm"

$d_{16} := h_{300} - c - \frac{3\ d_{rein.16}}{2} = 0.246\ m$ "Effective hight top reinforcement 16 mm"

$d'_{16} := h_{300} - d_{16} = 0.054\ m$ "Effective hight bottom reinforcement 16 mm"

$A_{si.12} := \frac{\pi \cdot d_{rein.12}^{\ 2}}{4}$ "Reinforcement area 12 mm"

$A_{si.16} := \frac{\pi \cdot d_{rein.16}^{\ 2}}{4}$ "Reinforcement area 16 mm"

$n_{12} := 4$ "Number of reinforcement bars for S300"

$n_{16} := 12$ "Number of reinforcement bars for S100"

$f_{yd} := 500\ MPa$ "Yield strength for reinforcement"

$\varepsilon_{sy} := \frac{f_{yd}}{E_s} = 0.002$ "Yield strain for reinforcement"

Bending moment capacity

300 mm slab with reinforcement S300

Assume all reinforcement is in tension and is yielding

$$x := \frac{2 \cdot f_{yd} \cdot A_{si.12} \cdot n_{12}}{\alpha \cdot f_{ck} \cdot b} = 0.019\ m$$

Check assumption

$$\varepsilon_s := \frac{d_{12} - x}{x} \cdot \varepsilon_{cu} = 0.042 \qquad \varepsilon_s > \varepsilon_{sy} = 1 \qquad OK!$$

$$\varepsilon_{s'} := \frac{d'_{12} - x}{x} \cdot \varepsilon_{cu} = 0.005 \qquad \varepsilon_{s'} > \varepsilon_{sy} = 1 \qquad OK!$$

Calculate moment capacity for S300 reinforcement

$$M_{RdS300} := -A_{si.12} \cdot n_{12} \cdot f_{yd} \cdot \left(d_{12} - d'_{12}\right) + \alpha \cdot f_{ck} \cdot b \cdot x \cdot \left(d_{12} - \beta \cdot x\right) = 64.202\ kN \cdot m$$

300 mm slab with S100

Assume top reinforcement in tension and yielding and bottom in tension and not yielding

$$x_c \cdot \alpha \cdot f_{ck} \cdot b = f_{yd} \cdot A_{si.16} \cdot n_{16} - n_{16} \cdot A_{si.16} \cdot E_s \cdot \frac{x_c - d'_{16}}{x_c} \cdot \varepsilon_{cu}$$

$$a(x) := f_{yd} \cdot A_{si.16} \cdot n_{16} + n_{16} \cdot A_{si.16} \cdot E_s \cdot \frac{d'_{16} - x}{x} \cdot \varepsilon_{cu} - x \cdot \alpha \cdot f_{ck} \cdot b$$

$x := 0.1\ m$

$x := \mathbf{root}(a(x), x) = 0.053\ m$

Check assumption

$$\varepsilon_s := \frac{d_{16} - x}{x} \cdot \varepsilon_{cu} = 0.013 \qquad \varepsilon_s > \varepsilon_{sy} = 1 \qquad OK!$$

$$\varepsilon_{s'} := \frac{d'_{16} - x}{x} \cdot \varepsilon_{cu} = 5.948 \cdot 10^{-5} \qquad \varepsilon_{s'} < \varepsilon_{sy} = 1 \qquad OK!$$

Calculate moment capacity for S100 reinforcement

$M_{RdS100} := -A_{si.16} \cdot n_{16} \cdot E_s \cdot \varepsilon_{s'} \cdot \left(d_{16} - d'_{16}\right) + \alpha \cdot f_{ck} \cdot b \cdot x \cdot \left(d_{16} - \beta \cdot x\right) = 271.082\ kN \cdot m$

300 mm slab, un-reinforced

$M_{Rdu} := f_{ctm} \cdot \frac{h_{300}^{\ 2} \cdot b}{6} = 44.85\ m \cdot kN$ "Moment capacity for 300 mm"

600 mm slab, un-reinforced

$M_{Rdu.600mm} := f_{ctm} \cdot \frac{b \cdot h_{600}^{\ 2}}{6} = 179.4\ m \cdot kN$ "Moment capacity for 600 mm"

Splitting capacity single anchor

300 mm slab, un-reinforced

$P_{rundu} := \frac{M_{Rdu} \cdot 2\ \pi}{b} = 245.044\ kN$ "Force needed for a 300 mm cicular slab"

600 mm slab, un-reinforced

$P_{rundu.600mm} := \frac{M_{Rdu.600mm} \cdot 2\ \pi}{b} = 980.177\ kN$ "Force needed for a 600 mm cicular slab"

300 mm slab with reinforcement S300

$P_{rund} := \frac{M_{RdS300} \cdot 2\ \pi}{b} = 350.779\ kN$ "Force needed for a 300 mm reinforced cicular slab"

Splitting capacity group of anchors

$M_{Abaqus} := 27\ kN \cdot m$ "Moment from Abaqus analysis"

$P_{Abaqus} := 200\ kN$ "Force applied in Abaqus"

$K_{group} := \frac{M_{Abaqus}}{P_{Abaqus}} = 0.135\ m$ "Ratio between the force and the moment for four anchors"

300 mm slab, un-reinforced

$\frac{M_{Rdu}}{K_{group}} = 332.222\ kN$ "Slab 300 mm without reinforcement"

300 mm slab with reinforcement S300

$\frac{M_{RdS300}}{K_{group}} = 475.574\ kN$ "Slab 300 mm with reinforcement S300"

300 mm slab with S100

$\frac{M_{RdS100}}{K_{group}} = 2.008\ MN$ "Slab 300 mm with reinforcement S100"

600 mm slab, un-reinforced

$\frac{M_{Rdu.600mm}}{K_{group}} = 1.329\ MN$ "Slab 600 mm without reinforcement"

Appendix B: Hand calculation CEN/TS (Matlab)

```
%Indata
h_ef=220;                % Effective length anchor
d_head=0.045;            % Diameter anchor head
d=0.03;                  % Diameter anchor
f_ck_cube=30;            % Compressive cube strength
k_ucr=15.5;              % Mean uncracked

% psi
psi_sN=1;
psi_reN=1;
psi_ecN=1;

% Force
N_Rk0=k_ucr*sqrt(f_ck_cube)*h_ef^1.5;

% Single anchor
fprintf('Capacity for concrete cone for\nsingle anchor is %0.2f [kN]\n\n',N_Rk0*10^-3)
Capacity for concrete cone for
single anchor is 277.03 [kN]

% Group of anchors
Scrn=3*h_ef;             % Reference width
A_0=Scrn^2;              % Reference area if no intruction on each others cones
A_1=(220+Scrn)^2;        % Effective area for group of anchors
A_ref=A_1/A_0            % Increase due to group of anchors

A_ref = 1.7778

% Force (Group of anchors)
N_RkG=N_Rk0*A_ref;
fprintf('Capacity for concrete cone for\ngroup of anchors is %0.2f [kN]\n\n',N_RkG*10^-3)
Capacity for concrete cone for
group of anchors is 492.50 [kN]
```